

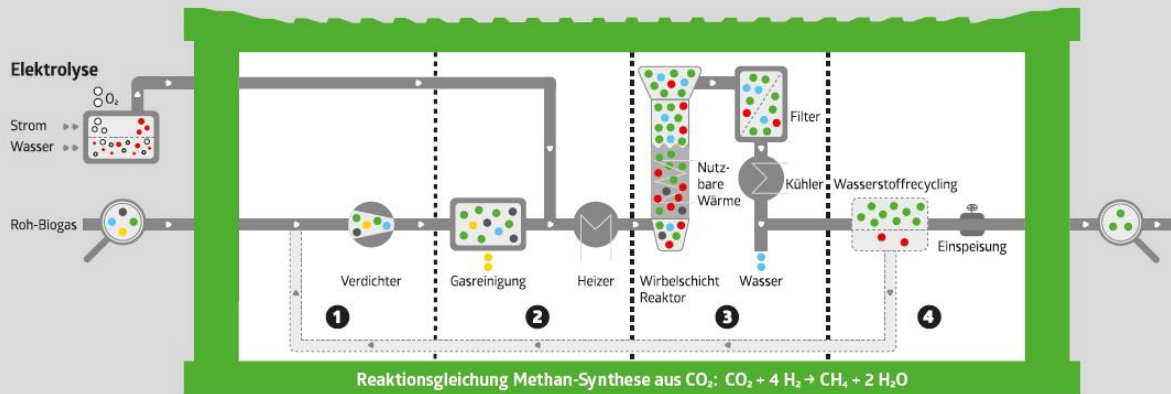


Final report

# Direct Methanation of Biogas

## Demonstrationsanlage «COSYMA»

Container-basiertes System einer Methanisierungsanlage



### Innenansicht Demonstrationsanlage



### Aussenansicht Demonstrationsanlage





**Date:** 10.8.2017

**Town:** Villigen, AG

**Publisher:**

Swiss Federal Office of Energy SFOE  
Biomass and wood energy Research Programme  
CH-3003 Bern  
[www.bfe.admin.ch](http://www.bfe.admin.ch)

**Co-financed by:**

Energie 360°, CH- 8010 Zürich  
Forschungs-, Entwicklungs- und Förderungsfonds der schweizerischen Gasindustrie (FOGA),  
CH-8027 Zürich

**Agent:**

Paul Scherrer Institut  
CH-5232 Villigen PSI  
[www.psi.ch](http://www.psi.ch)

**Author:**

Dr. Serge Biollaz, PSI, [serge.biollaz@psi.ch](mailto:serge.biollaz@psi.ch)  
Dr. Adelaide Calbry-Muzyka, PSI, [adelaide.muzyka@psi.ch](mailto:adelaide.muzyka@psi.ch)  
Dr. Tilman Schildhauer, PSI, [tilman.schildhauer@psi.ch](mailto:tilman.schildhauer@psi.ch)  
Julia Witte, PSI, [julia.witte@psi.ch](mailto:julia.witte@psi.ch)  
Andreas Kunz, energie360°, [andreas.kunz@energie360.ch](mailto:andreas.kunz@energie360.ch)

**Steering Committee:**

Peter Dietiker (E360)  
Martin Seifert/Peter Graf (FOGA)  
Sandra Hermle (SFOE)  
Helmut Vetter (Biogas Zürich)  
Urs Elber (EMPA)  
Peter Jansohn (PSI)

**SFOE head of domain:** Dr. Sandra Hermle, [sandra.hermle@bfe.admin.ch](mailto:sandra.hermle@bfe.admin.ch)  
**SFOE programme manager:** Dr. Sandra Hermle, [sandra.hermle@bfe.admin.ch](mailto:sandra.hermle@bfe.admin.ch)  
**SFOE contract number:** SI/501284-04

**The author of this report bears the entire responsibility for the content and for the conclusions drawn therefrom.**



**Swiss Federal Office of Energy SFOE**

Mühlestrasse 4, CH-3063 Ittigen; postal address: CH-3003 Bern

Phone +41 58 462 56 11 · Fax +41 58 463 25 00 · [contact@bfe.admin.ch](mailto:contact@bfe.admin.ch) · [www.bfe.admin.ch](http://www.bfe.admin.ch)



## Contents

<b>Abbreviation.....</b>	<b>6</b>
<b>Zusammenfassung.....</b>	<b>8</b>
<b>Summary .....</b>	<b>10</b>
<b>Overall Project Objectives.....</b>	<b>11</b>
<b>Analysis of biogas potential for PtG .....</b>	<b>13</b>
<b>Technical system analysis .....</b>	<b>16</b>
<b>Economics analysis of biogas PtG .....</b>	<b>29</b>
<b>Realisation of pilot plant COSYMA.....</b>	<b>34</b>
<b>Operation of COSYMA – Results on Methanation .....</b>	<b>37</b>
<b>Sorbent-based gas cleaning .....</b>	<b>50</b>
<b>Technical learnings for scale-up to 200 m<sup>3</sup>/h biogas plant.....</b>	<b>64</b>
<b>National collaborations.....</b>	<b>66</b>
<b>Annex.....</b>	<b>68</b>





<b>Abbreviation</b>	<b>Meaning</b>
BAFU	Bundesamt für Umwelt
bara	Absolute pressure
barg	Gauge pressure
BFB	Bubbling Fluidised Bed
BIOSWEET	Swiss Competence Center for Bioenergy Research
CAPEX	Capital expenditure
CCEM	Competence Center Energy and Mobility
CEDA	Coherent Energy Demonstrator Assessment
CH <sub>4</sub>	Methane
CO <sub>2</sub>	Carbon dioxide
COS	Carbonyl sulfide
COSYMA	Container Based System for Methanation
D4	Octamethylcyclotetrasiloxane
D5	Decamethylcyclopentasiloxane
DMS	Dimethylsulphide
DMDS	Dimethyldisulphide
DMTS	Dimethyltrisulphide
EMPA	Swiss Federal Laboratories for Materials Science and Technology
Energie360	Swiss utility supplying NG, biomethane and woodpellet
ESI	Energy System Integration platform
FB	Fixed Bed
FOGA	Forschungs-, Entwicklungs- und Förderungsfonds der schweizerischen Gasindustrie
GC	Gas Chromatograph
GC-FID	Gas chromatography–Flame Ionization Detector
GC-MS	Gas chromatography–Mass Spectrometry
GC-SCD	Gas chromatography–Sulfur Chemiluminescence Detector
GWh	Gigawatt hour



H <sub>2</sub>	Hydrogen
H <sub>2</sub> S	Hydrogen sulphide
LOD	Limit of detection
LOQ	Limit of quantification
LQ	Liquid quench system
mGC, $\mu$ GC	mini Gas Chromatograph
NDIR	Nondispersive infrared
NG	Natural gas
OPEX	operational expenditures
ppmv	parts per million by volume
PSI	Paul Scherrer Institut
PtG	Power-to-Gas (H <sub>2</sub> or CH <sub>4</sub> )
PtX	Power-to-X, where X are all products, which can be produced from power
R2	Mixed transition metal oxide dispersed on high surface area supports sorbent
R7	Mixed transition metal oxide sorbent
R8	Activated carbon with functionalized mixed transition metal oxides
S- $\mu$ GC	Sulphur-mini Gas Chromatograph
SCCER	Swiss Competence Center for Energy Research
SFOE	Swiss Federal Office of Energy
SNG	Synthetic Natural Gas
TRL	Technology Readiness Level
WWTP	Wastewater treatment plant



## Zusammenfassung

In Zusammenarbeit haben das PSI und Energie360° eine neue Power-to-Gas-Technologie validiert. Durch die "direkte Methanisierung von Biogas", wird die Methan-Ausbeute an Biogas deutlich erhöht. Zu diesem Zweck ist in einer Versuchsanlage Wasserstoff ( $H_2$ ) dem Roh-Biogas hinzugefügt worden, welches aus der Kläranlage bzw. dem Vergärwerk für biogene Abfälle am Standort Zürich- Werdhölzli stammt. Fünf Teilprojekte unterstützten die experimentellen Abklärungen und dienten der Fokussierung der Experimente.

Eines der Teilprojekte befasste sich mit der Frage nach dem Potential von geeigneten Biogasanlagen in der Schweiz die sich für die Integration der Power to Gas Technologie eignen. Der Fokus ist einerseits auf bestehenden Kläranlagen und andererseits auf industriellen Biogasanlagen, welche z.B. biogene Abfälle vergären. Landwirtschaftliche Biogasanlagen waren nicht Gegenstand dieser Betrachtung. Das wichtigste Ergebnis aus dieser Untersuchung ist, dass das grösste Potential in Bezug auf Anzahl Anlagen und Gas Produktionsmenge bei der mittleren Anlagengrösse mit  $200\text{ m}^3$  Biogas pro Stunde (11 GWh/a) liegt. Es gibt in der Schweiz ein Potential von 39 Anlagen in dieser Grösse.

In einem weiteren Teilprojekt wurde für die Anlagengrösse von  $200\text{ m}^3$  Biogas pro Stunde verschiedene Konzepte für die "direkte Methanisierung von Biogas" anhand einer technisch-ökonomische Modellierung beurteilt. Verglichen wurden sowohl verschiedene katalytische Methanisierungsvarianten als auch deren nachgeschaltete Abscheidung für Restwasserstoff (Membran versus zweistufige Methanisierung). Aufgrund dieser Untersuchung wird das Konzept der Wirbelschichtmethanisierung mit einer nachgeschalteten Wasserstoffmembran vertieft betrachtet, da bei diesem Konzept im Betrieb eine höhere Flexibilität möglich ist.

Die Pilotanlage COSYMA wurde am PSI erbaut und im November 2016 fertiggestellt. Die Anlage wurde anschliessend auf der ESI-Plattform am PSI in Betrieb genommen. Im Januar 2017 wurde die COSYMA an den Standort Werdhölzli transportiert und parallel zu der bestehenden Gasaufbereitungsanlage installiert und an das Gasnetz angeschlossen.

Für den Betrieb der COSYMA wurde in einem weiteren Teilprojekt die vorgeschaltete Gasreinigung festgelegt, welche mit einer Kombination von Sorptionsmitteln arbeitet. Vielversprechende Sorptionsmittel wurden ausgewählt und im Labor getestet. Für die kontinuierliche Dokumentation des Langzeitversuchs mit der Pilotanlage wurden verbesserte Gasanalysesysteme erfolgreich eingesetzt (mGC, Flüssigquench-System). Damit konnte frühzeitig erkannt werden, falls Störstoffe wie  $H_2S$ , Dimethylsulfid (DMS) oder Siloxane nicht mehr ausreichend von der Gasreinigung zurückgehalten werden.

In der erste Hälfte 2017 wurde erfolgreich mit einer einzigen Katalysatorcharge das 1'000 Stunden Langzeitexperimente in Werdhölzli gefahren. Im Dauerversuch wurden die vorhergesagten Gasqualitäten erreicht. Die experimentellen Resultate der Wirbelschichtmethanisierung und der Gasreinigung können vom Massstab der COSYMA auf den einer industriellen Anlage von  $200\text{ m}^3$  Biogas pro Stunde hochskaliert werden.

Über das Projekt wurde laufend in Fachzeitschriften und an Fachveranstaltungen berichtet. Im Rahmen dieses Langzeitversuches wurde das Projekt ebenfalls einer interessierten Öffentlichkeit vor Ort vorgestellt.





## Summary

A new Power-to-Gas technology was validated in collaboration between PSI and Energie360°. By way of "direct methanation of biogas", the CH<sub>4</sub> yield of biogas is considerably increased. For this purpose, H<sub>2</sub> was added in a test facility to the biogas from the sewage treatment plant as well as a bio-waste digestion plant on the Zurich-Werdhölzli site. Several subprojects supported the experimental investigations and helped to focus the experiments.

One of the subprojects dealt with the question of the potential of suitable biogas plants in Switzerland which are suitable for direct methanation of biogas (Power-to-Gas). The focus was, on one hand, on existing waste water treatment plants (WWTP) and on the other hand on industrial biogas plants, which are digesting green waste. Agricultural biogas plants were not the subject of this analysis. The most important results from this subproject are that the largest potential of units are plant with an average size of 200 m<sup>3</sup> of biogas per hour (11 GWh/a). There is a potential of 39 plants of this size in Switzerland.

A further subproject was the techno-economic assessment of several concepts for "direct methanation of biogas" for the plant size of 200 m<sup>3</sup> of biogas per hour. Various catalytic methanation processes were analysed with two different ways of hydrogen removal (membrane versus two-stage methanation). On the basis of this study, the concept of fluidised-bed methanation with a downstream hydrogen membrane was further investigated, as this concept is more flexible in the operation of a commercial plant.

The pilot plant COSYMA was built at PSI in 2016 for the long duration experiments. On the ESI platform the plant was commissioned and a first series of scientific methanation test were performed. In January 2017 the plant was installed on the Zurich-Werdhölzli site close to an existing biogas upgrading plant and connected to the gas grid.

In a further subproject, sorbent based gas cleaning was reviewed. Promising sorbent materials were selected and tested in the laboratory and integrated into the pilot plant COSYMA. For the continuous documentation and monitoring of the long-duration test with the pilot plant, improved gas diagnostic systems were successfully implemented (mGC, liquid quench system). This way, it could be detected at an early stage if impurities such as H<sub>2</sub>S, dimethylsulphide (DMS) or siloxanes were no longer sufficiently removed by the gas purification.

In the first half of 2017, the 1'000 hour long-time experiment was successfully carried out in Werdhölzli with a single catalyst charge. The predicted gas quality of the methanation was reached. The experimental results of fluidised bed methanation and gas cleaning can be scaled up from the COSYMA scale to that of an industrial plant of 200 m<sup>3</sup> biogas per hour.

Outcomes of the project have been regularly reported in journals and on events. Within the scope of this long-duration experiment, the project was also presented to an interested public.

## Overall Project Objectives

A new Power-to-Gas technology is validated in collaboration between PSI and Energie360°. By way of direct methanation of biogas, the CH<sub>4</sub> yield from biogas can be considerably increased. For this purpose, H<sub>2</sub> is added in a test facility to the biogas from the sewage treatment plant as well as from a bio-waste digestion plant on the Zurich-Werdhölzli site. The CO<sub>2</sub> in the biogas is converted by way of fluidized bed methanation to biomethane (see Figures 1 and 2). With this technology, conventional biogas upgrading plants separating CO<sub>2</sub> can be substituted.

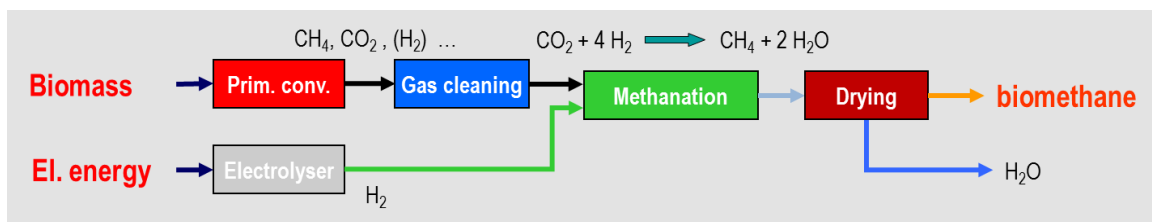


**Figure 1:** Block flow diagram of Power-to-Gas by way of "direct methanation of biogas".

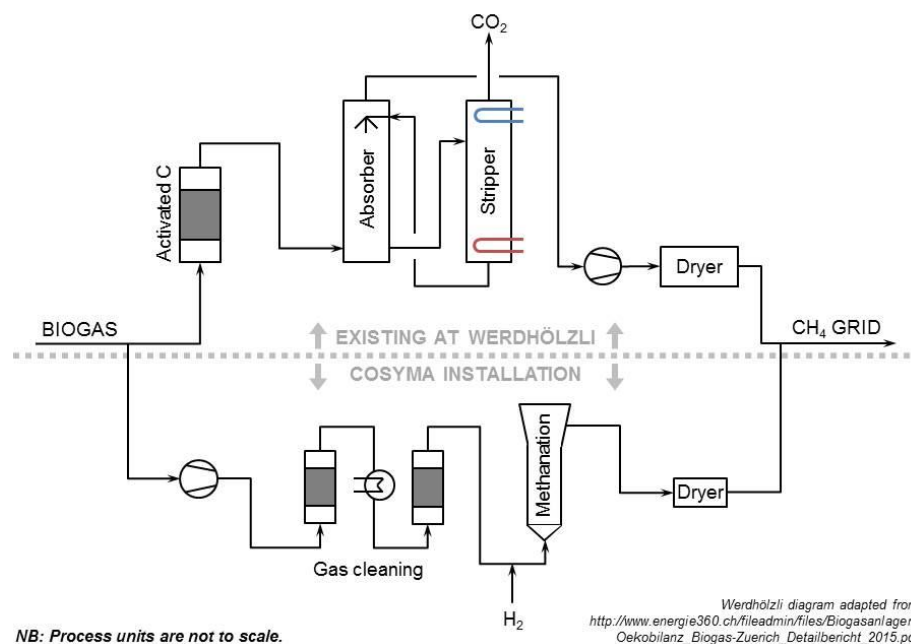


**Figure 2:** Simplified system schematic for integrating the test facility "COSYMA" into existing system.

The goal of this R&D project is providing technical and economic evidence for this technology at a Technology Readiness Level (TRL) of 5. The following main results are expected with this project:

- Key information about the economics and operation of an industrial installation for direct methanation of biogas
- Development and testing of essential process steps such as gas cleaning and methanation, of their technical integration into a complete system and the operation of these two units as a basis for the design of a system at TRL 7-8
- Experimental demonstration of gas cleaning and methanation at TRL 5, under real conditions in a long-duration field experiment from a slipstream of the biogas produced at Werdhölzli.



For the long-duration tests of direct methanation of biogas, experimental infrastructure must be built and put into operation. The required infrastructure consists mainly of three units:

- Gas sampling and analysis techniques for the main components and contaminants (Sulphur, siloxanes, terpenes), which is suitable for unmanned operation in the field
- Small sorbent test bed for accelerated breakthrough tests under synthetic (in house, TRL 2-3) and real biogas conditions (in field, TRL 4)
- Methanation installation integrated with gas cleaning, "COSYMA", (TRL 4-5) for long-duration field testing.



## Analysis of biogas potential for PtG

The assessment of the technical potential should answer the following questions:

- What potential exists in Switzerland to increase the production volume of bio-methane in a conventional biogas plant by using PtG?
- Which plant size is suitable for the integration of PtG into wastewater treatment plants or industrial biowaste digestion plants in Switzerland?

The potential number of additional plant sites in Switzerland is calculated, along with the corresponding potential for additional yearly production of renewable gas. The Analysis is based on the Swiss statistic of total energy [1] and renewable energy [2] and was adapted and verified with own experience and data of various studies [3, 4, 5, 6]. The aim is to define a plant size which is representative for an application at wastewater treatment plants (WWTP) and biowaste digesters in Switzerland.

In Switzerland, the proportion of biomethane in the natural gas grid has steadily increased over the last few years thanks to injections of gas produced by anaerobic digestion. In 2015, 262 GWh (HHV basis) of biomethane were injected into the Swiss gas grid [7]. This corresponds to 0.8% of the current gas consumption in Switzerland. In order to cover the steadily growing demand for biomethane from Swiss consumers, additional biomethane must already be imported from abroad today. The Swiss gas association aims to achieve 30% of renewable Gas of the total gas consumption for heating purposes by 2030.

If the CO<sub>2</sub> contained in the raw biogas at these existing biomethane injection sites was not separated as usual, but was instead methanized with renewable H<sub>2</sub>, 180 GWh (HHV basis) of additional biomethane could be produced each year. However, the existing biogas processing systems would have to be modified. Such a modification of the existing Swiss biomethane production plants would be realistic over the next 15 years as the plants get renewed. For the operation of these plants (mainly the production of the required hydrogen for the methanation process) an **amount of 300 GWh/a electrical energy would be required.**

In addition to the plants with existing biomethane injection systems, there are many more plants in Switzerland that today produce electricity and heat using a gas engine in combined heat and power (CHP) plants. As a result of existing feed-in tariffs for electricity (KEV/RPC), a large proportion of the raw biogas generated today in Switzerland is directly converted in CHP plants. However, the produced renewable electricity is then injected into the electric grid and cannot be stored. In addition, a considerable portion of the heat produced in this application is lost through cooling systems, particularly in the summer months when heat is not needed. Part of this lost potential could be recovered by production and injection of biomethane if a gas network was available in the vicinity. In Switzerland, an additional 570 GWh per year (HHV basis) of raw biogas could be recovered from all wastewater treatment plants or green waste digesters currently producing at least 3 GWh of biogas. If this raw biogas was not combusted in a gas engine, but converted into grid-injectable methane by a Power-to-Gas technology using renewable hydrogen, an additional 385 GWh of biomethane could be produced from conversion of the CO<sub>2</sub>. Therefore, in total an additional 955 GWh per year of biomethane could be produced from existing CHP plants. An investment in the replacement process for this transformation is also realistic in the next 15 years, for a large part of installations that currently generate electricity. For the operation of these modified plants (mainly the production of the required hydrogen for the methanation process) an **amount of 640 GWh/a electrical energy would be required.**

Through these measures, the rate of grid injection of biomethane in Switzerland could increase by more than fivefold – from 262 GWh to 1.4 TWh/year. This corresponds to an increase in the share of



renewable gas in the gas network to 4% of the current gas consumption in Switzerland. This increase solely would be realised by the conversion of existing plants to PtG using the same amount of available biomass. It would be a major step in direction of the target given by the Swiss gas association.

**Table 1:** Biomethane potential of all plants in Switzerland with >3 GWh per year of biogas production. (data 2015)

Potential analysis in GWh/year (HHV)	Existing bio-CH <sub>4</sub> grid injection	Potential, adding PtG at existing bioCH <sub>4</sub> plants	Potential, new bioCH <sub>4</sub> injection (conventional)	Potential, new bioCH <sub>4</sub> injection (PtG increase)	Total potential through PtG
WWTP	150	100	460	310	410
Biowaste-Digestion plants	112	80	110	75	155
<b>Total</b>	<b>262</b>	<b>180</b>	<b>570</b>	<b>385</b>	<b>565</b>

The biomethane potential in Switzerland is described in **Table 1**. This increase solely would be realised by the conversion of existing plants to PtG using the same amount of available biomass. **Table 2** includes nearly 100 plants. The largest proportion (64 plants) are located at wastewater treatment plants which do not have yet a gas grid injection systems today, but instead produce electricity from the produced biogas (CHP plants).

**Table 2:** Biomethane potential, in number of installations with >3 GWh per year of biogas production. (Data 2015)

Potential analysis in number of plants	Existing bioCH <sub>4</sub> grid injection	Potential, new bioCH <sub>4</sub> injection	Total potential through PtG
WWTP	15	64	79
Biowaste-Digestion plants	8	9	17
<b>Total</b>	<b>23</b>	<b>73</b>	<b>96</b>

The potential plants (WWTP and anaerobic digestion plants) were divided into three typical plant sizes: plants with a raw biogas production per year of (1) less than 5 GWh; (2) between 5 and 15 GWh, and (3) greater than 15 GWh. The resulting number of installations for each size is shown in Table 3.



The greatest potential with regard to the number of plants is for plants with less than 5 GWh per year of biogas production (HHV basis). The greatest potential with regard to the raw biogas production is for plants in the range of 5 – 15 GWh per year. Since the focus is on a balance of the biomethane total production volume and the number of realizable plants, the middle range (5 – 15 GWh) was considered in the economic analysis.

**Table 3:** Biomethane potential (number of plants and raw biogas) for three representative plant sizes.

Plant size (HHV)	< 5 GWh/year		5 – 15 GWh/year		> 15 GWh/year	
	Number of plants	GWh/year Total with PtG	Number of plants	GWh/year Total with PtG	Number of plants	GWh/year Total with PtG
WWTP	42	262	30	428	7	330
Biowaste Dige- stion plants	5	31	9	158	3	188
<b>Total</b>	<b>47</b>	<b>293</b>	<b>39</b>	<b>586</b>	<b>10</b>	<b>518</b>

### Summary of chapter

Converting all potential biogas plants (existing biomethane injection plants and plants currently producing electrical power) with the PtG technology and gas grid injection could increase the renewable gas production by more than fivefold – from 262 GWh to 1.4 TWh/year. To realise this, the amount of 940 GWh/a electrical power (mainly the production of the required hydrogen for the methanation process) would be required.

### References for chapter “Analysis of biogas potential for PtG from WWTP & green waste AD”

- [1] BFE (2015), Schweizerische Gesamtenergiestatistik 2014
- [2] BFE (2015), Schweizerische Statistik der Erneuerbaren Energien-Ausgabe 2014
- [3] BFE (2010), Strategie zur energetischen Nutzung der Biomasse in der Schweiz
- [4] BFE (2015), Thermische Stromproduktion inkl. Wärmekraftkopplung (WKK) - Ausgabe 2014
- [5] Energie360, Potenzialanalyse (not public).
- [6] Triple E&M, ZHAW (2016), Meta Studie Inländisches Biogaspotential der Schweiz, 2016 (not public).
- [7] VSG (März 2015), Biogas-Anlagen mit Einspeisung ins Erdgas-Netz



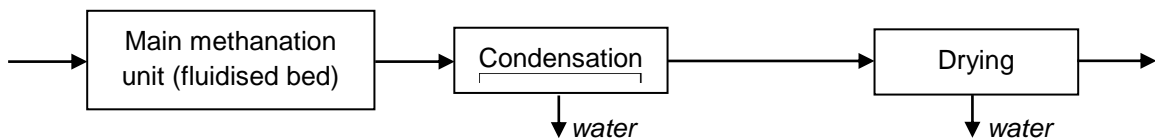
## Technical system analysis

In order to explore the technical feasibility of the concept "direct methanation of biogas" in detail, possible PtG process designs, integrated in a biogas plant serving as upgrading unit, are simulated and evaluated in terms of product quality and cost effectiveness. For this, two different methanation technologies, Bubbling Fluidized Bed (BFB) and Fixed Bed (FB), are considered and combined with further upgrading methods, i.e. second methanation step or membrane with hydrogen recycle.

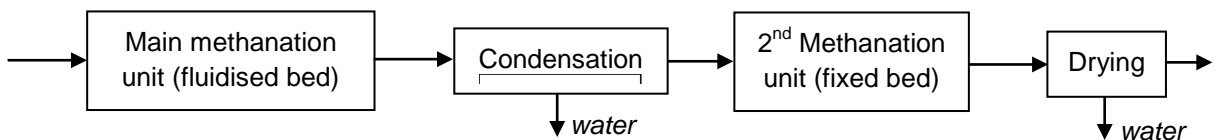
In order to determine optimal operation conditions, which lead to target concentrations in the bio-methane, the behaviour of single units as well as the interplay of the units in the flowsheets was investigated. A commercial scale (TRL 7/8) plant is considered with a biogas input of 200 Nm<sup>3</sup>/h. For this size, the methanation reactor and the up-grading unit are modelled in detail, while for the remaining units, thermodynamic short-cut- models have been applied. This resulted in a good estimate of the design of different units (reactor size, compressors etc.) and the mass and energy flows, which forms a basis for appropriate cost calculation.

The process concepts investigated in detail are shown below:

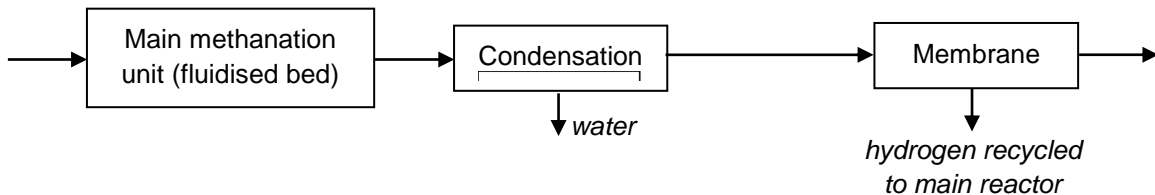
*Process I (BFB only: Bubbling fluidized bed with Drying as upgrading)*



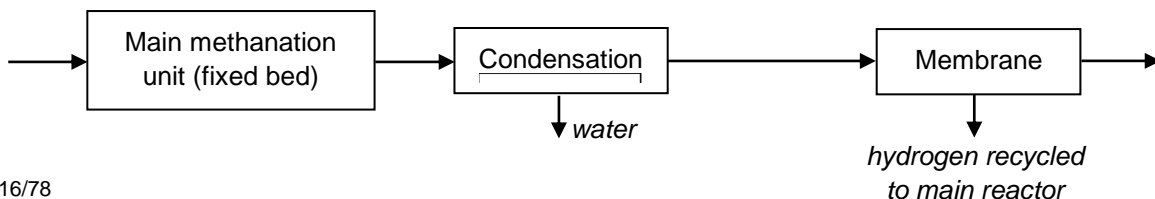
*Process II (BFB-FB: Bubbling fluidized bed with Fixed bed as upgrading)*



*Process III (BFB-Memb: Bubbling fluidized bed with membrane as upgrading)*



*Process IV (FB-Memb: Fixed bed with membrane as upgrading)*



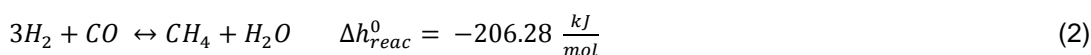
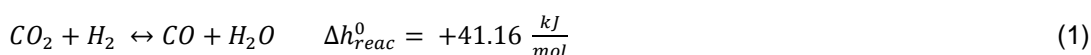


## Process Design and Modelling Procedure

Rigorous process models were developed for the gas upgrade of biogas from anaerobic digestion to bio-methane within the PtG concept on the base of the scheme described above. The software products Athena Visual Studio<sup>®</sup> and Matlab<sup>®</sup> are used for the implementation.

For the Fixed bed (FB) and the Bubbling fluidised bed (BFB) model, rate-based models are implemented with kinetic data and correlations for heat and mass transfer from literature and own research. The fixed bed reactor is described by a pseudo homogeneous one-dimensional model of a multi-tubular reactor. The bubbling fluidised bed is represented by the two-zone one-dimensional model developed at PSI in previous work (Kopyscinski, Schildhauer, Biollaz, 2011). Both reactors are cooled. The overall reaction is highly exothermic (- 165.12 kJ/mol), which results in high demands on the heat exchange performance of the reactor. The membrane performance is determined by a rate-based two stage model. All other unit operations are calculated by short-cuts or thermodynamic models.

Two independent chemical equations are considered; the fully reversible water gas shift (Equation 1) and the methanation reaction (Equation 2):



Both reactions are influenced by thermodynamic equilibrium.

Four different processes were developed where different methanation technologies and further upgrade units are included. In all models, the state-of-the-art gas cleaning for removal of sulphur species etc. unit is not included (as it does not change the main gas composition), but it is considered in the economic analysis. The processes operate in steady-state mode. The purpose of the biogas upgrade processes is the production of bio-methane injectable into the existing gas grid in Switzerland. Hence the produced bio-methane must fulfil the gas grid requirements, listed in Table 4. The process concepts with membrane or 2<sup>nd</sup> methanation unit reach this defined product gas quality, whereas the process concept comprising only the once-through fluidised bed methanation with water removal by condensation and drying, is considered to show which savings would be possible if lower methane and higher hydrogen content were accepted for injection.

**Table 4:** Gas grid requirements of Switzerland and Germany for main components issued for the simulation (Schweizerischer Verein des Gas- und Wasserfaches (SVGW), 2016), (Deutscher Verein des Gas und Wasserfaches, 2011, 2013).

Components	Requirements
Methane	CH <sub>4</sub> ≥ 96 vol%
Hydrogen	H <sub>2</sub> ≤ 2 vol%
Carbon Dioxide	CO <sub>2</sub> ≤ 4 vol%
Water	Dew point at – 8 °C at pressure level of injection point of the gas grid



The inlet volume stream is fixed at 200 Nm<sup>3</sup>/h, which represents a medium size biogas plant. The inlet composition of biogas is set to 40% carbon dioxide and 60% methane, which represents the maximum amount of carbon dioxide in the biogas plant.

*Upgrade process via two-stage methanation (Process concept BFB-FB)*

Cleaned biogas is compressed to operational pressure (up to 7 bara). Then steam, provided by an evaporator and hydrogen is mixed to the raw biogas at operational pressure. Hydrogen and oxygen are produced via electrolysis out of water at 30 bar, whereas oxygen may be stored in bottles for selling purposes. Hydrogen is hold by a tank for further processing. The added steam prevents the catalyst in the next step from deactivation. After a preheating step, the gas mixture is entering a bubbling fluidized bed methanation (concept BFB-FB) where carbon dioxide together with hydrogen is converted to methane and water over a nickel catalyst.

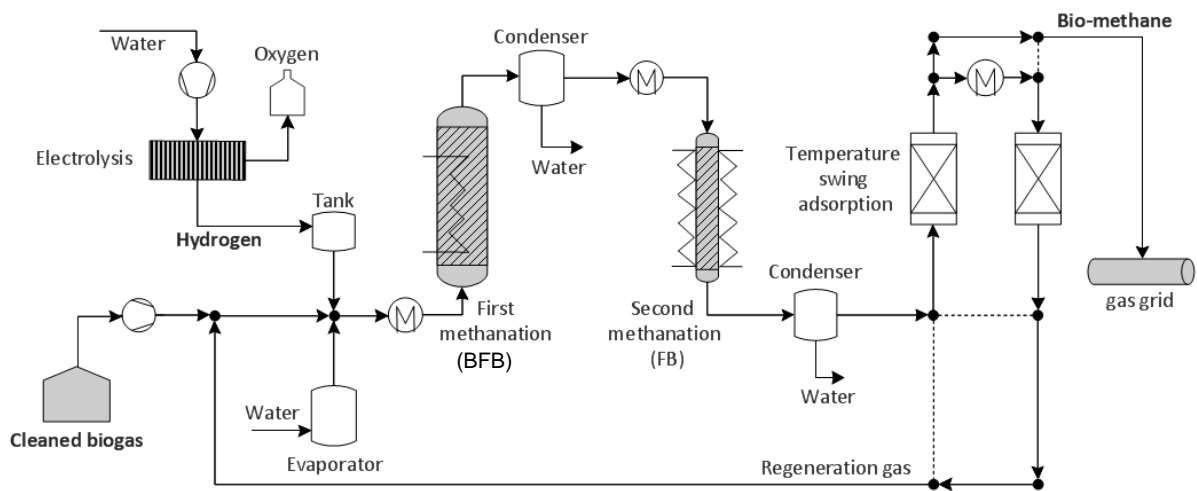


**Figure 3:** Flowsheet for the upgrade process of biogas via two-stage methanation (process concept II BFB-FB); the process concept I (BFB only) is similar, but omits the 2<sup>nd</sup> methanation and the second condenser

After leaving the BFB reactor, the gas stream is cooled down to 20°C in a condenser unit, where the added steam and water formed during the reaction is separated from the gas down to saturation concentration. Because the gas stream is not fulfilling the gas grid requirements after the first stage of methanation, further upgrading is needed. Due to the water separation, the thermodynamic equilibrium is influenced towards the product side.

Therefore, a second stage methanation was implemented, where the remaining carbon dioxide together with the remaining hydrogen is converted to methane (Equation 1 and Equation 2) in a fixed bed reactor until product quality is reached. Again, during the reaction water is produced. It is separated in a subsequent condenser unit down to saturation concentration at 20°C and operational pressure. For the injection into the gas grid the gas stream must be technically free of water, which means a dew point of -8°C at injection pressure must be reached. For that reason, a dryer unit is necessary, which is realized via temperature swing adsorption (TSA) technology. As drying agent silica gel is used. A part of the product gas is used as regeneration gas to ensure product purity, which is about 10% of the whole stream (Tentarelli & Gibbon, 2011). It is not possible using air as regeneration gas because of the contamination of the product gas with oxygen and nitrogen, while switching desorption

and adsorption vessels. In order not to lose 10% of the product gas and to avoid emissions of methane, the saturated regeneration gas is redirected to the biogas stream as recycle loop. The dried product gas stream is compressed or expanded to the pressure level of the injection point of the gas grid, which is dependent on the site and varies between 5 bar (low pressure transportation grid) and 0.02 – 0.1 bar (distribution grid) (Verband der Schweizerischen Gasindustrie (VSG), 2015).

*Process concept I Bubbling fluidised bed methanation and drying (BFB only)*

This simpler process scheme comprises only a single step methanation and water removal as upgrading. It therefore resembles the one with 2<sup>nd</sup> methanation unit; just the 2<sup>nd</sup> methanation unit and the 2<sup>nd</sup> condenser are omitted.

*Upgrade process III/IV via methanation and H<sub>2</sub>-membrane (BFB-Memb, FB-Memb)*

The first part of the process until the first condenser is similar to the flowsheet in figure 3. The model BFB-Memb differs from model of the previous section by the processing of the remaining hydrogen after the main methanation unit and the subsequent condenser (see figure 4). Here the remaining hydrogen is separated from the product gas stream by a hydrogen membrane and is recycled to the methanation unit. Remaining water in the gas stream is condensed at 20 °C and membrane pressure. The gas stream passes the hydrogen membrane, where hydrogen and water, but also part of methane and carbon dioxide are separated from the product stream bio-methane. The bio-methane stream is technically free of water and does not need further drying. The recycled hydrogen stream is mixed with the biogas stream and compressed again to the operational pressure in order to be fed into the methanation reactor. The pressure of the product gas stream is adjusted by mean of a pressure control valve to the gas grid pressure level.

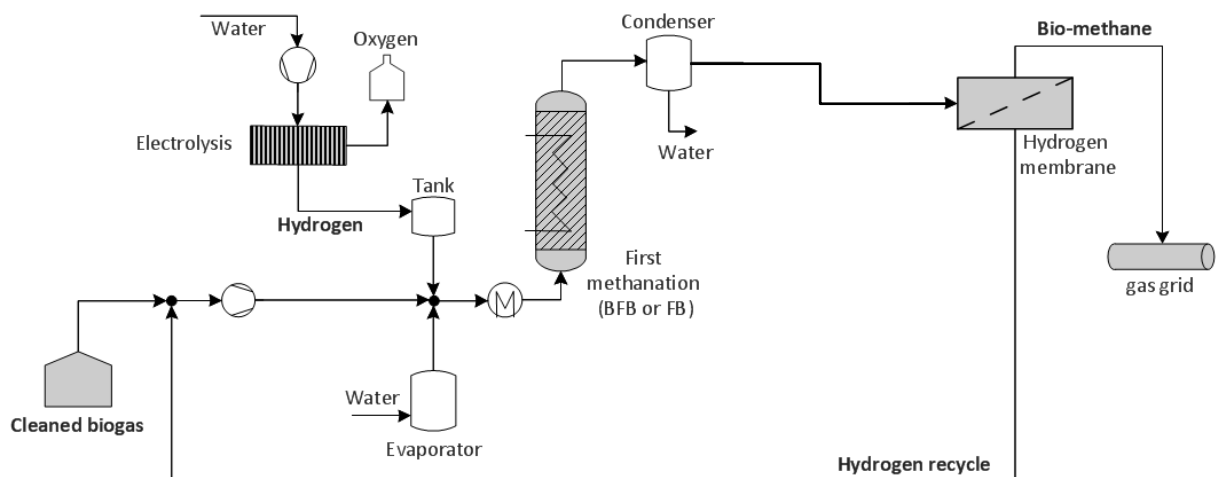


**Figure 4:** Flowsheet for the biogas upgrade via methanation and hydrogen membrane (process concepts III (BFB-Memb) and IV (FB-Memb))



## Modelling and Simulation Results

### *Isothermal fluidised bed as main reactor*

The performance and geometry of the fluidised bed methanation reactor (BFB) depends on pressure and temperature as well as on fluidisation conditions and heat dissipation performance for isothermal conditions. In figure 5 and 6, the influence of the operational conditions to the reactor geometry is illustrated. The ratio of gas velocity and minimal fluidisation velocity  $u/u_{mf}$  is set sufficiently high for a sufficient particle movement. The particle movement ensures isothermal conditions over the height of the reactor, as well as a regeneration of catalyst particles, transported from areas with high catalyst stress and heat generation to areas with low catalyst stress and heat generation, respectively. The inlet volume stream is constant.

In order to meet the fluidisation number  $u/u_{mf}$ , the reactor diameter is adjusted, also depending on the pressure and temperature in the reactor. With higher pressure, the volume flow of the gas decreases, hence the diameter must decrease to ensure the same velocity of gas inside the reactor. Higher temperatures require a bigger diameter, due to the volume increase. Therefore, the diameter of the reactor is influenced by the fluidisation number  $u/u_{mf}$  as well as by temperature and pressure. The heat

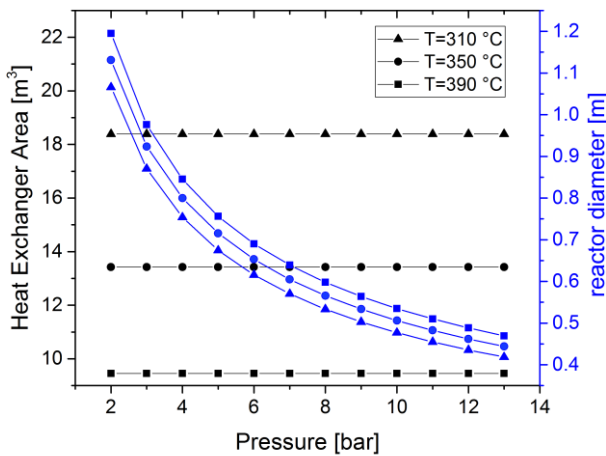


**Figure 5:** Influence of temperature and pressure to the reactor geometry of the fluidized bed reactor

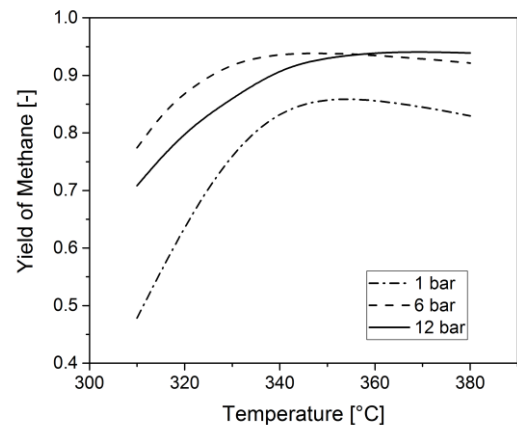


**Figure 6:** Performance of the fluidized bed reactor over temperature and pressure

exchange area inside of the reactor and with that the height of the reactor is determined by the maximum of released reaction heat assuming 100% conversion. The heat has to be dissipated to operate isothermally, which requires a corresponding heat transfer area. Over the pressure, the heat transfer area is set constant, because of the constant inlet flow and therefore the constant maximum heat generation. But the area decreases with higher temperatures, due to the increasing temperature difference between the reactor and the cooling agent, which results in improved heat transfer. In figure 7 the yield of methane over temperature and pressure in the fluidised bed reactor is illustrated. For every temperature and pressure, the corresponding adaptations in the geometry of the reactor are made. The diagram shows that the graphs of the corresponding pressures form maxima. Hence, for every pressure an optimal temperature exists, where the yield of methane is at maximum. This can be explained by the activity of the catalyst and the thermodynamic equilibrium. The activity is increasing and



the thermodynamic equilibrium of the reaction is decreasing with higher temperatures. At lower temperatures, the reaction cannot reach thermodynamic equilibrium because of the low activity of the catalyst. With increasing temperatures, the catalyst become more active until thermodynamic equilibrium can be reached at the corresponding temperature. This point forms the maximum. At higher temperatures, the yield is decreasing together with the thermodynamic limit of the reaction. The maximum yield first is moving with higher pressures until 6 bara towards lower temperatures. With further increase of pressure, the maximum yield is shifted towards higher temperatures. Here changing pressure and hydrodynamic behaviour, caused by the geometry adaptations, are influencing the reaction. With lower pressure until 6 bara, the pressure is the dominant effect; above 6 bara hydrodynamic effects are prevalent. With increasing pressure, the reaction is faster and reaches therefore at lower temperature the thermodynamic limit. Above 6 bara, hydrodynamic effects become more important, caused by the adaptations to diameter and height of the reactor. Now, more gas stays in the bubble phase, hence the reaction is limited more strongly by mass transfer from the bubble into the dense phase. The reaction is slowed down and reaches the thermodynamic limit only at higher temperatures. Between 1 and 6 bara, an increase of the maximum yield for methane is apparent. Then, with further increasing of the pressure, no significant improvement of the yield is obtained. The maximum yield is about constant between 6 bara and 12 bara at 94% for the assumed feedgas composition (i.e., the chosen ratios of  $H_2/CO_2$ ,  $H_2O/CO_2$ ,  $CO_2/CH_4$ , etc.).

#### *Cooled fixed bed as main reactor*

In Figure 7, concentration profiles of the main components  $H_2$ ,  $CH_4$ , and  $CO_2$  over the length of the main fixed bed reactor for different pressures are illustrated. Increased pressure in the reactor results in a steeper increase of methane concentration due to a faster conversion of carbon dioxide to methane over the reactor length. Also the outlet concentration of methane is slightly higher for increased pressure, which is expected from thermodynamics and Le Chatelier's principle, because the reaction in mole reducing. The increased reaction extent due to increased pressure is also reflected in the corresponding temperature profiles. Here temperature peaks are formed in the area with the highest reaction extent. Then, over the length of the reactor, the temperature is falling again due to cooling. The maximum peak temperature is increasing with the pressure. The pressure also influences the heat transfer properties of the reactor, reflected in the overall heat transfer coefficient.

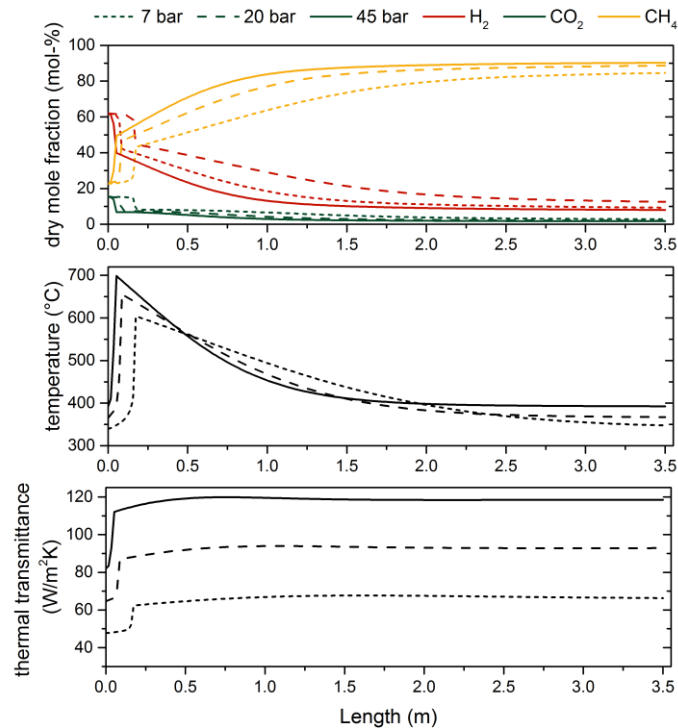


**Figure 7:** Concentration profiles of main components and corresponding temperature profiles for different pressures ( $T_{\text{cool}} = T_{\text{in,FB}} - 30\text{K}$ ,  $V_{\text{biogas}} = 200 \text{ Nm}^3/\text{h}$ ,  $\text{H}_2/\text{CO}_2 = 4.03$ ,  $\text{H}_2\text{O}/\text{CO}_2 = 0.5$ )

Despite cooling, in the main fixed bed reactor hot spots at beginning of the reactor up to 700°C are formed. Then the temperature decreases faster for increased pressure over the reactor length, due to increased overall heat transfer for higher pressures. Before the temperature peak in the reactor, the reaction is determined by kinetic effects. Downstream of the peak, thermodynamic equilibrium sets a limit for the conversion of carbon dioxide to methane. The concentrations of the components follow the equilibrium composition at the corresponding temperature. (With decreasing temperatures over the reactor length, more CO<sub>2</sub> conversion becomes possible, due to more beneficial thermodynamic conditions.) This means the length of reactor is also determined by the cooling performance in order to reach thermodynamically beneficial temperatures inside the reactor. As a result, fluidized bed reactors are usually smaller due to the significantly better heat transfer caused by the movement of the catalyst particles.

#### *Process performance of two-stage methanation (process concept II, BFB-FB)*

In process concept II, the yield in the bubbling fluidised bed (BFB) shall be maximised to ensure low heat production in the subsequent fixed bed (FB) reactor. Figure 8 showed that this target does not determine the operational conditions in the BFB, because the same maximum yield for different pressures was reached. Economic considerations lead to an optimal pressure for this process layout. The ratio of added hydrogen from electrolysis and carbon dioxide from raw biogas can be set only slightly over-stoichiometrically with 4.03 at maximum, because otherwise the upper limit of hydrogen in the product gas cannot be reached. This procedure makes it necessary to adjust the hydrogen flow permanently to the carbon dioxide fraction in the raw biogas, which may fluctuate over time, especially in anaerobic digestion of green wastes. In order to prevent catalyst deactivation, evaporated water is



added to the reactor with a water-to-carbon dioxide ratio of 0.5. The system pressure was varied between 6 and 20 bar. With a certain pressure, the temperature and the geometry of the BFB are defined to reach the maximum yield of methane. Also the fixed bed is pre-defined by the pressure, which sets the necessary length of the reactor with constant diameter to reach gas grid requirements. In figure 8, the concentration profiles of methane, hydrogen and carbon dioxide over the length of the fixed bed reactor are illustrated. Methane must exceed the limit of 96% and hydrogen must fall below the limit of 2%. For high pressures the reaction is faster, which results in a steeper increase of methane and a steeper decrease of hydrogen concentration, so that a shorter length is sufficient to reach the desired concentrations. The higher activity of the reaction is also visualized by the temperature profiles, which corresponds with the development of reaction heat. The increase of the temperature for high pressures is much steeper than for low pressures. Low pressures result in a longer reactor, hence a bigger amount of catalyst mass is needed. It can be seen as well, that the requirement for methane can be reached with less catalyst than the requirement for hydrogen; hence the bigger issue is to fall below the 2% limit of hydrogen than to reach 96% methane concentration.

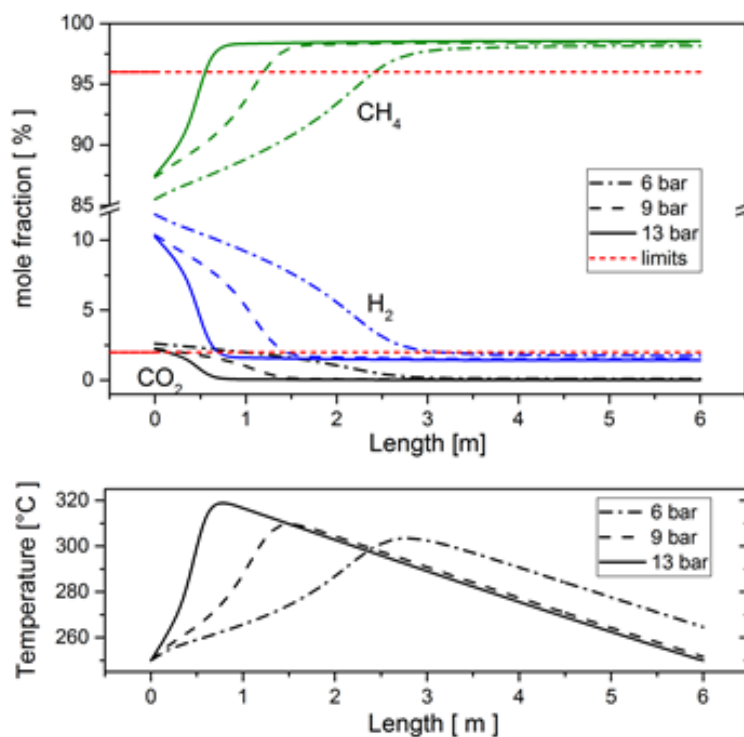


**Figure 8:** Concentration profiles of carbon dioxide, hydrogen and methane over the length of the second-stage fixed bed reactor for different pressures and corresponding temperature profiles; further conditions:  $H_{2,in}/CO_{2,in} = 4.03$ ,  $H_2O/CO_2 = 0.5$ , diameter fixed bed = 0.44 m,  $T_{cool,FB}=20^\circ C$

With the hydrogen-carbon dioxide ratio of 4.03, hydrogen conversion of more than 99% must be reached to fall below the upper limit of hydrogen. This high conversion is only achievable with a cooling of the fixed bed reactor, so that the temperature stays in a range favourable for thermodynamic equilibrium. The reactor is cooled at the shell of the reactor tube, which is sufficient because only



small amounts of reactive gas are left after the fluidized bed methanation, so that the heat generation is moderate.

The next figure (Figure 9) shows a flow diagram for energy flows and mass flows. It shows the electricity consumption which is dominated by the electrolysis which needs 70-75 times more electricity than the compressor. Further, the water consumption and production are shown as well as the heat production from electrolysis, reactor cooling and condensation of steam produced during methanation. The recycled methane stream stems from the regeneration of the temperature swing adsorption.

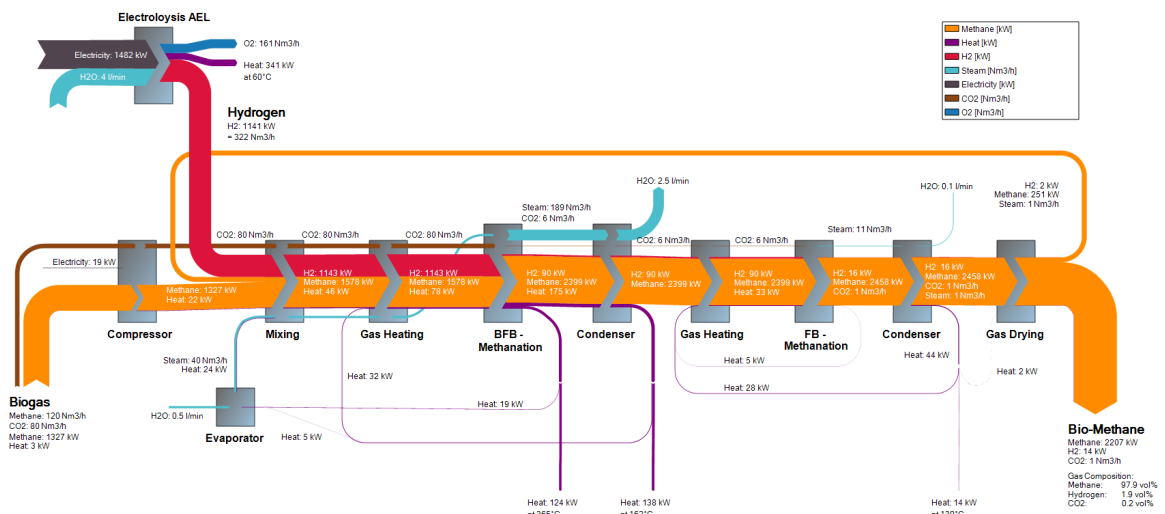


**Figure 9:** Flow diagram for energy flows and mass flows for process concept II (BFB-FB) with two stage methanation at 7 bara, applying isothermal fluidised bed methanation for the main reactor and cooled fixed bed methanation for the upgrading reactor.

*Process performance of single-stage methanation (process concept I, BFB only)*

The simplified process which consists of only one bubbling fluidised bed reactor and water removal shows a relative similar Energy and Mass flow diagram (Figure 10) as the two stage methanation. In most aspects, similar numbers are reached (amount and temperature level heat removal, electricity consumption etc.). Only the final gas composition differs strongly, as now around 2% CO<sub>2</sub> and up to 10% hydrogen are obtained in the biomethane which allows only restricted injection into the gas grid according actual net injection specifications. Again, part of the methane is recycled during the regeneration of the TSA drying section.

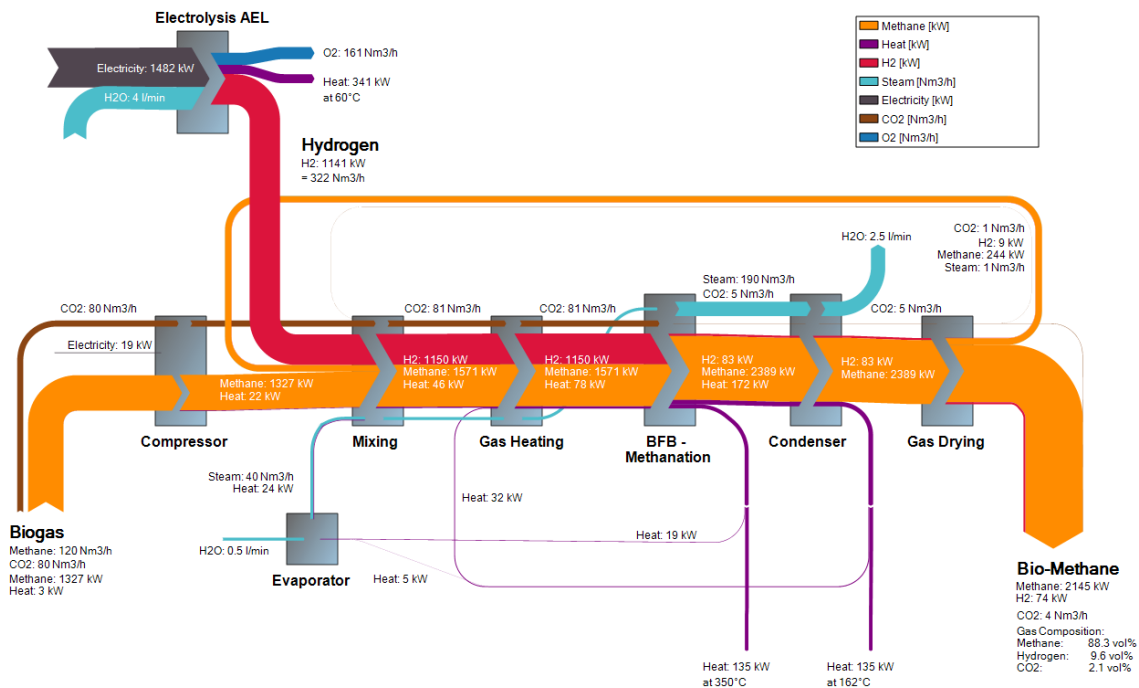


**Figure 10:** Flow diagram for energy flows and mass flows for single stage methanation at 7 bara (Process concept I, BFB only), applying isothermal fluidised bed methanation and only drying for gas upgrading

### *Performance of methanation and upgrading by H<sub>2</sub>-membrane (process concepts III and IV, BFB-Memb and FB-Memb)*

In these two process concepts, two parameters determine the other process conditions. The first parameter is the pressure existing in evaporator, fluidised bed and subsequent condenser. The second parameter is the H<sub>2</sub> - CO<sub>2</sub> ratio in the feed  $(H_2/CO_2)_{Feed}$ , which is different to the ratio  $(H_2/CO_2)_{BFB}$  in the methanation reactor due to the recycle stream of hydrogen. All variations were made such that the process produces biogas with the desired quality. For the membrane, a one-dimensional rate-based-model is implemented. In Figure 11, the hydrogen mole fraction falls below the 2% limit with corresponding pressure and membrane area such that the gas grid requirements regarding hydrogen are fulfilled. In this case, methane and carbon dioxide diffuse in bigger amounts through the membrane and reach a fraction of more than half of the hydrogen recycle stream. Further, all steam is fed through the membrane and recycled to the reactor, which allows to omit the temperature swing adsorption drying and the according costs. Further, the hydrogen recycle decouples the H<sub>2</sub>/CO<sub>2</sub> ratio in the reactor from that at the reactor inlet, i.e. higher hydrogen content can be supplied in the reactor (where it is needed) while overall less hydrogen is necessary. Therefore, the membrane based processes can operate with a just or even slightly understoichiometric hydrogen content which saves some hydrogen compared to the process concepts without H<sub>2</sub> recycle.

The correct calculation of the membrane and hydrogen recycle is a challenge, as the prediction quality depends completely on the properties given in literature. Using different parameters from various articles, relatively large recycle streams are found, which do not fit well to preliminary information given by membrane suppliers. Therefore, for correct membrane representation in the models, own measure-



ments with the targeted membrane are necessary that should be conducted in follow-up activities. Especially, it is necessary to determine the permeability and selectivity of the membranes for hydrogen, CO<sub>2</sub>, steam and hydrogen as function of the concentrations for the desired pressure range. With these parameters, the real value of the recycle flow and its composition can be calculated. Further, the real cost optimum is found between elevated pressure within the membrane (which decreases capital cost for membrane area) and the connected costs of the compressor, be it higher operation costs due to the higher pressure level change, be it the costs for a second compressor for the membrane unit.

Based on the information from a membrane supplier (private communication), an estimated flow diagram is presented in Figure 11 that gives an indication of the realistic recycle ratio. Again, it can be seen that injectable gas quality can be reached. For the energy flow diagram, hardly any differences between fluidised bed or fixed bed methanation in the main reactor can be found because both reactor types are limited by thermodynamic equilibrium while the membrane properties dominate the rest.

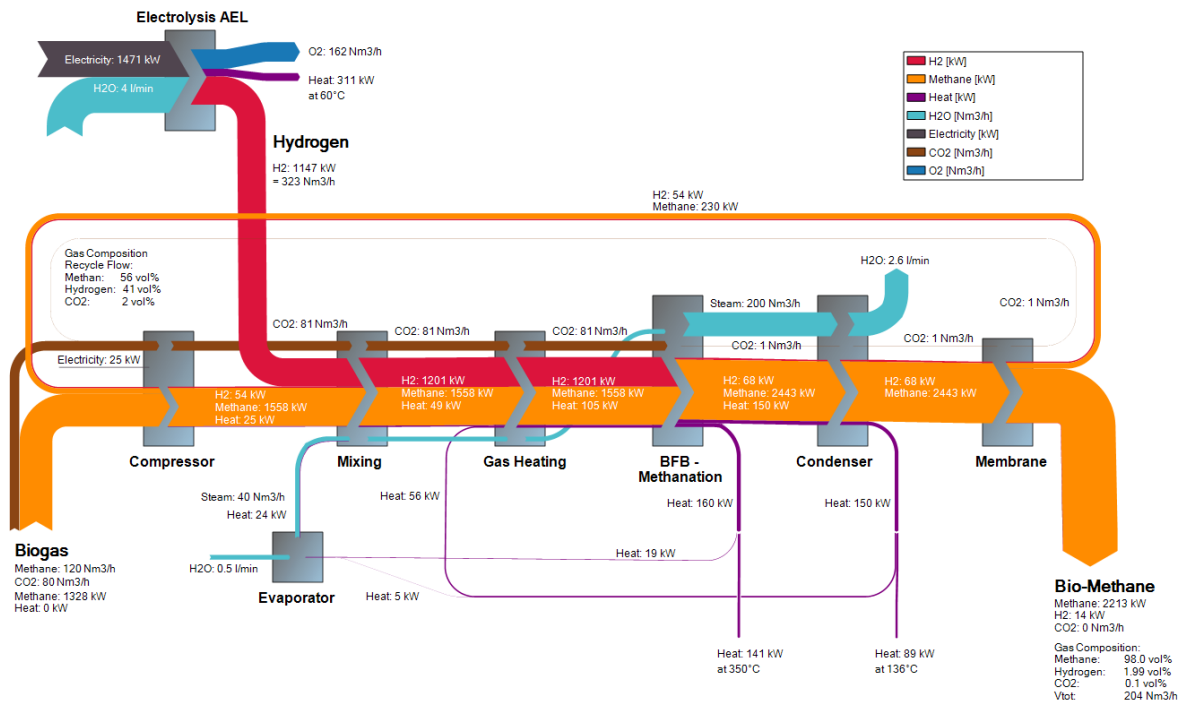


**Figure 11:** Flow diagram for energy flows and estimated mass flows for single stage methanation and membrane upgrading at 7 bara (process concepts III and IV, BFB-Memb and FB-Memb); As both methanation reactors (BFB and FB) are limited by thermodynamics, no significant differences are visible in the energy and mass flow diagram.

### Comparison

In process concepts III and IV (BFB-Memb and FB-Memb), it is possible to adjust the product gas quality in terms of the ratios of hydrogen, methane and carbon dioxide. The feed of hydrogen to the overall system can be decreased to stoichiometric conditions, while in the two stage methanation and single BFB reactor without H<sub>2</sub> recycle, the H<sub>2</sub>/CO<sub>2</sub> ratio is minimum 4.03. From the technical analysis, it was found that all processes with upgrading fulfil the gas grid requirements. Only the process concept without further upgrading leads to high hydrogen contents in the biomethane. Table 5 shows important parameters of the four processes indicating only moderate differences. As operation and capital costs of the electrolysis have the biggest impact on the costs, process concepts III and IV (with H<sub>2</sub>-recycle,



BFB-Memb and FB-memb) has the potential to be more profitable because of H<sub>2</sub> saving potential. Further, the two other processes are less robust, because they require permanent adaption of hydrogen to maintain the optimal ratio with respect to carbon dioxide in the feed to avoid too low hydrogen to CO<sub>2</sub> ratios. This is especially important when the CO<sub>2</sub>-content in the biogas is not constant. This is the case e.g. for plants digesting bio-wastes where the CO<sub>2</sub> content may change between 40% and 50% within hours. Therefore, methanation in combination with H<sub>2</sub>-membranes is considered the most promising concept with a reactor pressure of around 6 bar and a temperature of around 350-360°C.

**Table 5:** Important parameters of the four processes investigated

Parameter	Einheit	BFB only	BFB-FB	BFB-Memb	FB-Memb
H <sub>2</sub> /CO <sub>2</sub> ratio	-	4.03	4.03	4.00	4.00
Druck in Methanisierung	bar	7.00	7.00	7.00	7.00
Umsatz CO <sub>2</sub> im Gesamtprozess	%	95.00	99.50	98.90	98.80
Methanausbeute im Gesamtprozess	%	92.40	99.40	98.70	98.70
Umsatz H <sub>2</sub> im Gesamtprozess	%	93.50	98.80	98.70	98.70
spezif. Leistung Kompressor Biogas	kWh/Nm <sup>3</sup> Biogas	0.09	0.09	0.22	0.22
spezif. Nutzbare Reaktionswärme	kWh/Nm <sup>3</sup> Biogas	0.64	0.62	0.61	0.61
spezif. Nutzbare Kondensationswärme	kWh/Nm <sup>3</sup> Biogas	0.68	0.69	0.82	0.81
<b>Modell Einstellungen</b>	<b>Einheit</b>	<b>nur BFB</b>	<b>BFB +FB nach</b>	<b>BFB + H<sub>2</sub> Mem, 1 Kompr</b>	<b>FB+Mem</b>
pMeth	bar	7	7	7	7
Tmeth	°C	350	365	365	360
pMem	bar			7	7
H <sub>2</sub> /CO <sub>2</sub>	-	4.03	4.03	4	4
Länge 2. FB	m		2.5		
Temperatur 2.FB	°C		280		
Länge 1.FB	m				5
Anzahl Rohre a 15mm, 1. FB	-				220

### Summary of chapter

Four different process concepts were modelled in detail to obtain mass and energy balances for an industrial size plant of 200 m<sup>3</sup> biogas per hour. From the technical analysis, it was found that all processes with upgrading fulfil the gas grid injection requirements. As operation and capital costs of the electrolysis have the biggest impact on the costs, process concepts with membrane and H<sub>2</sub> recycle have the potential to be more profitable because of H<sub>2</sub> saving potential. Nevertheless too low hydrogen to CO<sub>2</sub> ratios lead to deactivation of the methanation catalyst. Therefore the fluidised bed reactor with membrane is more robust and flexible during commercial operation, as there is no need for permanent and precise adaption of hydrogen addition in order to maintain the optimal ratio with respect to carbon dioxide in the feed gas.

### References for chapter "Technical system analysis"

- [1] M. Piot, "Energierstrategie 2050 der Schweiz," in *13. Symposium Energieinnovation*, 2014, no. Kapitel 5, pp. 21–23.
- [2] A. Zervos, C. Lins, and L. Tesnière, "Mapping Renewable Energy Pathways towards 2020," *Eur. Renew. Energy Counc.*, p. 28, 2011.
- [3] P. Graichen, M. M. Kleiner, P. Litz, and C. Podewils, "Die Energiewende im Stromsektor: Stand der Dinge 2015," 2015.
- [4] Bundesamt für Energie, "Schweizerische Gesamtenergiestatistik 2014 Statistique globale suisse de l' énergie 2014," 2015.



- [5] Schweizerischer Verein des Gas- und Wasserfaches (SVGW), "Richtlinie für die Einspeisung von erneuerbaren Gasen - G13/G18," 2016.
- [6] Deutscher Verein des Gas und Wasserfaches, "Technische Regel Arbeitsblatt G260," 2013.
- [7] Deutscher Verein des Gas und Wasserfaches, "Technische Regel Arbeitsblatt G262," 2011.
- [8] S. C. Tentarelli and S. J. Gibbon, "Adsorbent bed support," WO2011138612 A1, 2011.
- [9] Verband der Schweizerischen Gasindustrie (VSG), "Gas in Zahlen 2015 Erdgas / Biogas," 2015.



## Economic analysis of biogas PtG

The economic analysis should answer the following questions:

- What are the main cost drivers (investment and operating costs)?
- Are specific investment and operating costs comparable to a conventional plant?
- Can a Power-to-Gas plant be operated economically?
- What are optimal operating conditions for the plant when the raw biogas is continuously produced in the WWTP or the biowaste digestion plant?
- Which gas (raw biogas or H<sub>2</sub>) can be stored more economically?
- Which maximum electricity costs (including grid fees and charges) are acceptable for an economic operation?

Compared to natural gas today, biogas has an ecological added value as well as higher production costs. The resulting higher price for biogas is fully accepted by the customers who demand an energy source with a low CO<sub>2</sub> footprint. However, biogas is exempt from the mineral oil tax and the CO<sub>2</sub> tax. Under these conditions, today's conventional biogas processing plants can be operated without state subsidies. In the economic analysis, the conventional process is therefore used as the benchmark to compare a Power-to-Gas plant. An analysis is done to determine whether it is possible to operate the PtG plant with comparable or even lower investment and operating costs per kWh product gas. Only if this condition is met, the substitution of a conventional biomethane production plant with a PtG plant would then be economically justified. The cost data is based on published data for electrolyzers [6, 7] and various studies and literature [1-4] and adapted with own experience and builds the basis of the cost database [5] for the model.

Since 2016, the exemption from mineral oil tax and CO<sub>2</sub> tax has also been applied to renewable methane (analogously to biogas). This is valid as long as the hydrogen is produced from renewable energy sources, and the CO<sub>2</sub> does not have an origin from processes that explicitly produce CO<sub>2</sub> only for methanation. Based on these conditions, synthetic methane is equated with today's biogas. It is therefore assumed that the market price to be reached by biomethane with conversion of CO<sub>2</sub> will then be identical to the prices for conventional biomethane from biogas.

Accordingly, an estimation of 10 to 12 Rp/kWh was chosen for grid-injectable biomethane at the outlet of the production plant and before distribution, trading and sale. In addition to the energy price of the gas without the mineral oil tax and CO<sub>2</sub> tax, this price also includes the ecological added value. This is a rather optimistic assumption as the biogas market also becomes more competitive. It is to be expected that this value will decrease in the future.

A plant size of 200 Nm<sup>3</sup> of raw biogas per hour was defined for comparing the Power-to-Gas plant to a conventional biogas upgrading plant. This is a typical plant size for Switzerland and corresponds to approximately 11 GWh per year in the case of continuous conventional production. Depreciation over 15 years and an interest rate of 5% were used for both cases.

### Capital costs

By using the CO<sub>2</sub> from raw biogas in the PtG process, the biogas production can be increased to 160%. The investment costs of the PtG plant increase to 190% compared to the conventional plant. Consequently, the specific investment costs per kWh are slightly higher, but not so much higher that a business case would be unthinkable. In figure 12 the breakdown of investment cost and in figure 13 the itemised portion of the total plant cost is shown in a comparison for conventional biogas processing plant and a power-to-gas plant. For biogas processing plants actual cost level and for PtG



plants estimated cost of a near future commercial plant were considered (Costlevel 2020). In the long-term future, the investment costs of the power to gas technology is expected to drop markedly, especially with increasing scaling.

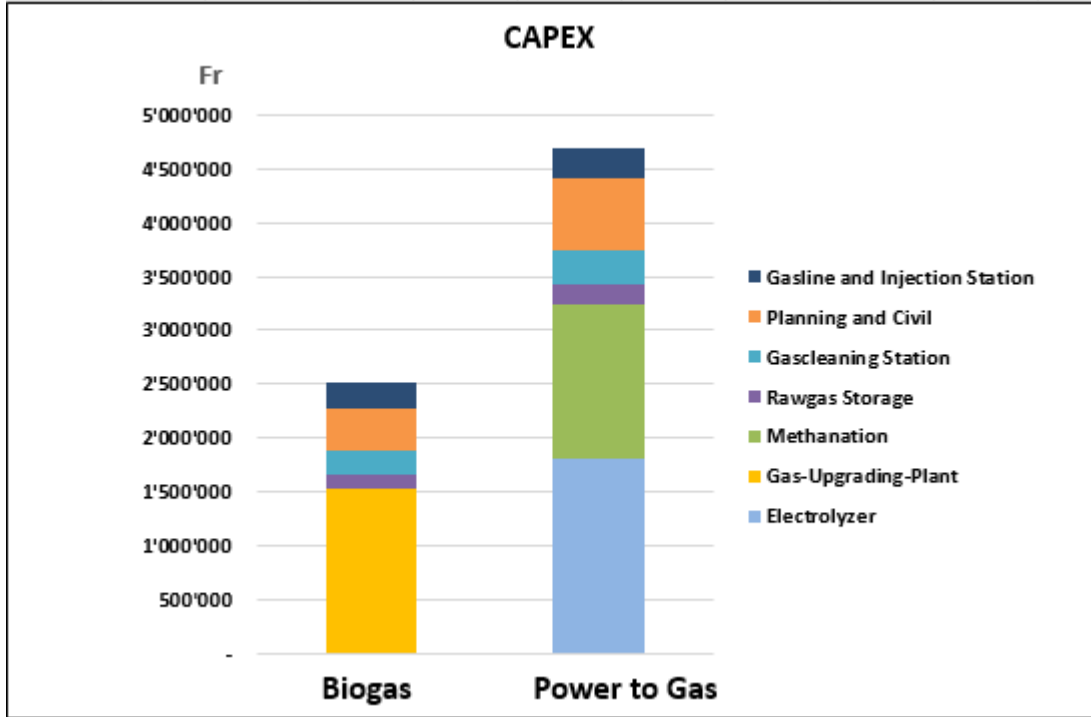


**Figure 12:** Investment cost comparison (conventional biogas processing plant vs. a power-to-gas plant)

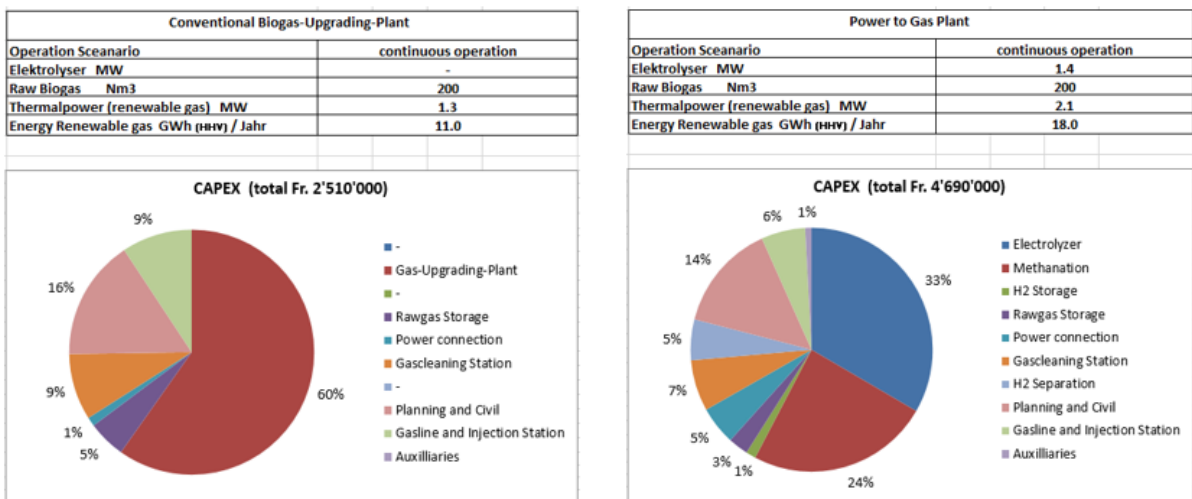


**Figure 13:** Itemized portion of total Investment cost comparison (conventional biogas processing plant vs. a power-to-gas plant)



The specific investment costs per kWh based on continuous plant operation over 15 years:

- 2.2 Rp / kWh Conventional gas processing plant
- 2.5 Rp / kWh PtG system

The main contributors to capital costs are electrolysis, methanation, construction / planning and gas purification.

When comparing the two electrolysis technologies Alkaline (AEL) and Proton Exchange Membrane (PEM), it becomes apparent that from today's point of view, an AEL electrolyser is more economical than a PEM electrolyser. The AEL electrolyser currently has lower investment costs and equivalent efficiency as a PEM electrolyser. It is assumed that the costs of the PEM electrolysers will decrease in the future and then, a PEM electrolyser would be preferred.

### Operating costs

Converting the CO<sub>2</sub> from raw biogas using the power-to-gas technology increases the amount of produced biogas to 160%. The costs for operation and maintenance decrease specifically with increasing production quantities and thus compensate for the higher capital costs of PtG compared to a conventional biomethane production plant. In the model, the costs for raw biogas as well as the price for injectable biogas are identical in both variants. For an economic operation, without cross-subsidisation between methane from raw biogas to the additional generated methane, electricity costs are determined.

In figure 14 specific costs per kWh are compared for conventional biogas processing plant and a power-to-gas plant. In figure 15 annual operating costs for conventional biogas processing plant and a power-to-gas plant are compared.

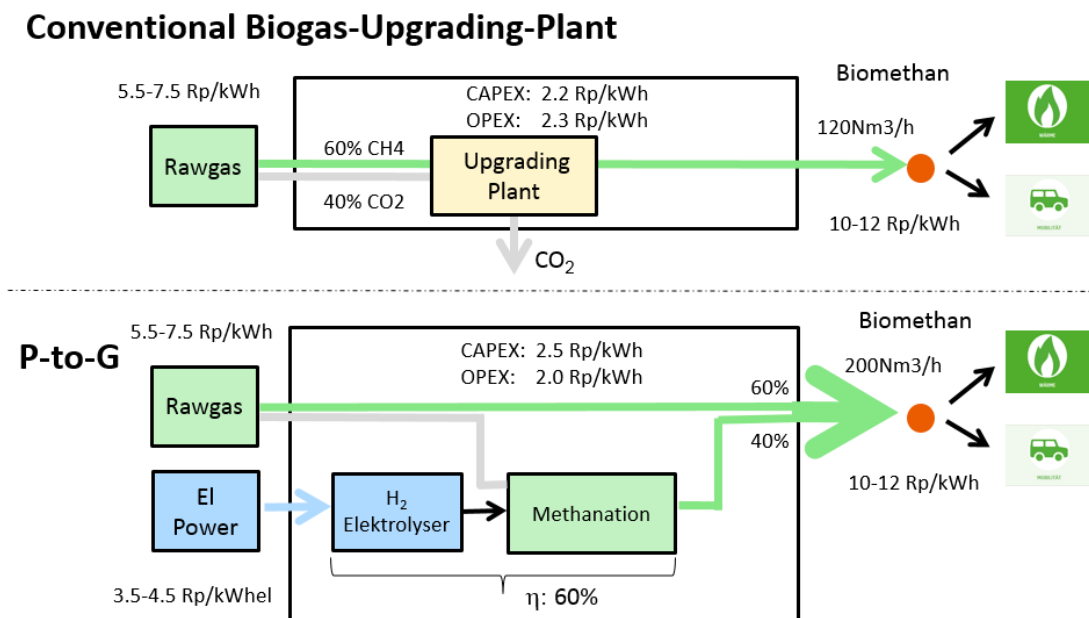


**Figure 14:** Comparison of specific costs per kWh (conventional biogas processing plant vs. a power-to-gas plant)



Based on the model calculations, the resulting maximum electricity costs are 3.5 to 4.5 Rp/kWh, including grid charges and taxes. The lower the power costs, the more economical the PtG technology operates. If higher electricity costs are to be expected, PtG is not worthwhile compared to a conventional system.

The heat generated in a PtG plant as well as the oxygen from the electrolysis can be utilized to improve the economy. In the present study, however, this has not yet been taken into account since these parameters are strongly dependent on the project and location. The economic efficiency of the PtG plant should primarily be provided by the sale of gas, and other sources of revenue should only be used for optimization. In the given plant size, an additional approximately 0.7 Rp/kWh of injected gas can be assumed by the marketing of joint products.

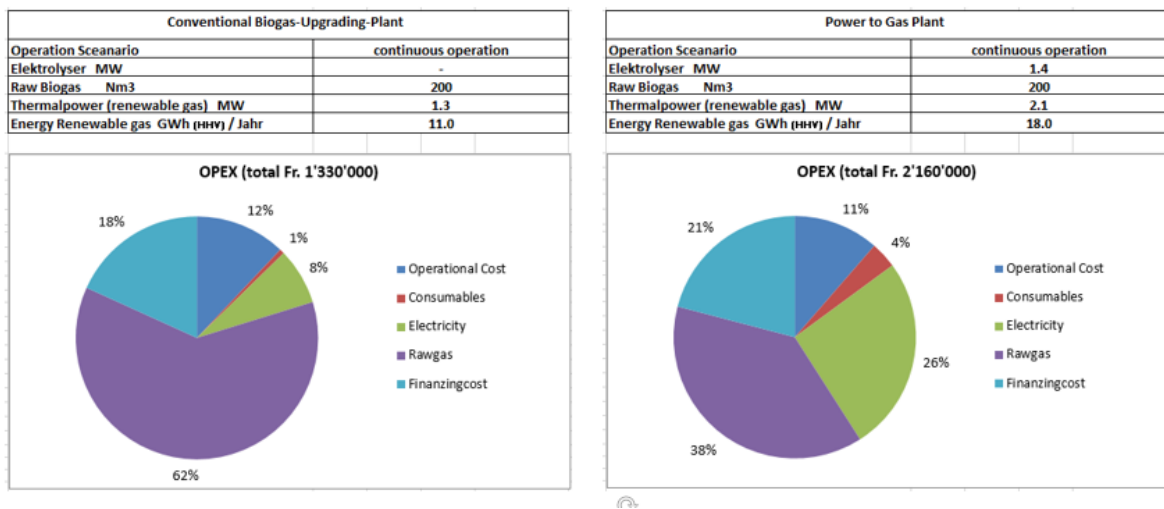


**Figure 15:** Comparison of annual operating costs (conventional biogas processing plant vs. a power-to-gas plant)

### Operating regime

The above presented case is based on continuous plant operation. In order to optimize the electricity consumption for the operation of the electrolysis, various scenarios were investigated which allow a periodically changing current demand. In this case, raw biogas or hydrogen must be buffered. Storage of hydrogen (including compression, if necessary) is more economical than storage of raw biogas. When storing raw biogas, not only the electrolyser, but also the methanation plant has to be built larger, which leads to higher costs.

In general, the analysis shows that a periodic operation of a PtG system only in times of power oversupply is not economical when connected to an anaerobic digester or waste water treatment plant. This is caused by the low number of operating hours, which requires in turn large storage tanks to process the continuous raw gas flow.

### Part time operation 12 h / day:

If the electrolysis is operated daily only for twelve hours, for example to use day / nighttime tariffs, the electrolyser must have a doubled capacity. Only in this way can sufficient hydrogen be produced to methanate the same continuously produced flow of raw biogas. The hydrogen must be able to be stored in order to guarantee a continued operation of the methanation during the non-operating period



of the electrolyser. Higher capital and operating costs of CHF 340'000 are incurred annually. Accordingly, an additional revenue or savings of more than 340'000 CHF must be achieved through the optimization.

*Part load operation, standstill 4h / day:*

Analogously to the partial operation during 12 hours per day, the electrolyser must be dimensioned larger than in full load operation. In addition, a small hydrogen storage tank must be installed. Higher capital and operating costs of CHF 110'000 are incurred annually. Accordingly, an additional revenue or savings of more than 110'000 CHF must be achieved through optimization.

*Operation on partial capacity electrolysis:*

The electrolyser has a capacity reserve of additional 0.5 MW, in order to provide this as a positive as well as negative control energy to the power grid. Accordingly, a hydrogen storage device must be present in order to be able to methanate the continuously produced raw biogas at reduced electrolysis capacity. In case of overcapacity, the gas storage tank must be able to absorb the additional amount of hydrogen. Higher capital and operating costs of CHF 130'000 are incurred annually. Accordingly, an additional revenue or savings of more than CHF 130'000 must be achieved through optimization and participation in the regulatory energy market.

### **Summary of chapter**

The specific investment and operation cost (without the cost for electrical power for the production of the hydrogen) is for a PtG plant at the level of a traditional biogas upgrading plant. Based on an assumed 10 to 12 Rp/kWh for grid-injectable biomethane the resulting maximum electricity costs are 3.5 to 4.5 Rp/kWh, including grid charges and taxes.

### References for chapter "Economics analysis of biogas PtG "

- [1] Fachagentur Nachwachsende Rohstoffe e V (2014), Leitfaden Biogasaufbereitung und –Einspeisung
- [2] Science Direct (2015), Renewable Power-to-Gas: A technological and economic review, M Götz
- [3] Science Direct (2014), State of the Art of commercial electrolyzers, M Felgenhauer
- [4] Dena (Okt2015), System Lösung Power to Gas
- [5] PSI (2016), Datenbank ESI, Power to Gas Technology (nicht veröffentlicht).
- [6] DVGW (2014), Techno-ökonomische Studie von Power to Gas Konzepten
- [7] Fuel cells and hydrogen (2014), Development of Water Electrolysis in the European Union Final Report ]



## Realisation of pilot plant COSYMA

COSYMA stands for Container Based System for Methanation. The entire methanation process, including compressor and gas cleaning, is integrated into a standard 20 feet container with customised openings (doors, windows, etc.). This also means that the space inside the container is limited since one side of the container is fitted with desks as workplace for the researcher. At the same time, the installation is appropriate to explain the concept of direct methanation of biogas to interested visitors where the process is visible behind transparent doors.

COSYMA is based on a similar installation built in 2004 at PSI. The first installation was successfully operated with syngas from biomass gasification. In total, 3'000 hours of experimental hours were accumulated. For the long duration test in Werdhölzli, this plant had to be rebuilt in order to fulfil the actual requirements. Except of the core process vessels, all other equipment had been replaced with new installations.

In Figure 16, the technical concept is shown as well as the technical realisation. The installation consists of five sections. Section 1 is the gas compressor/gas supply, section 2 contains the gas cleaning, section 3 is the fluidised bed methanation and section 4 comprises the gas conditioning, i.e. the gas drying. In section 5, the gas diagnostics and the necessary installations for the injection into the natural gas grid are placed.

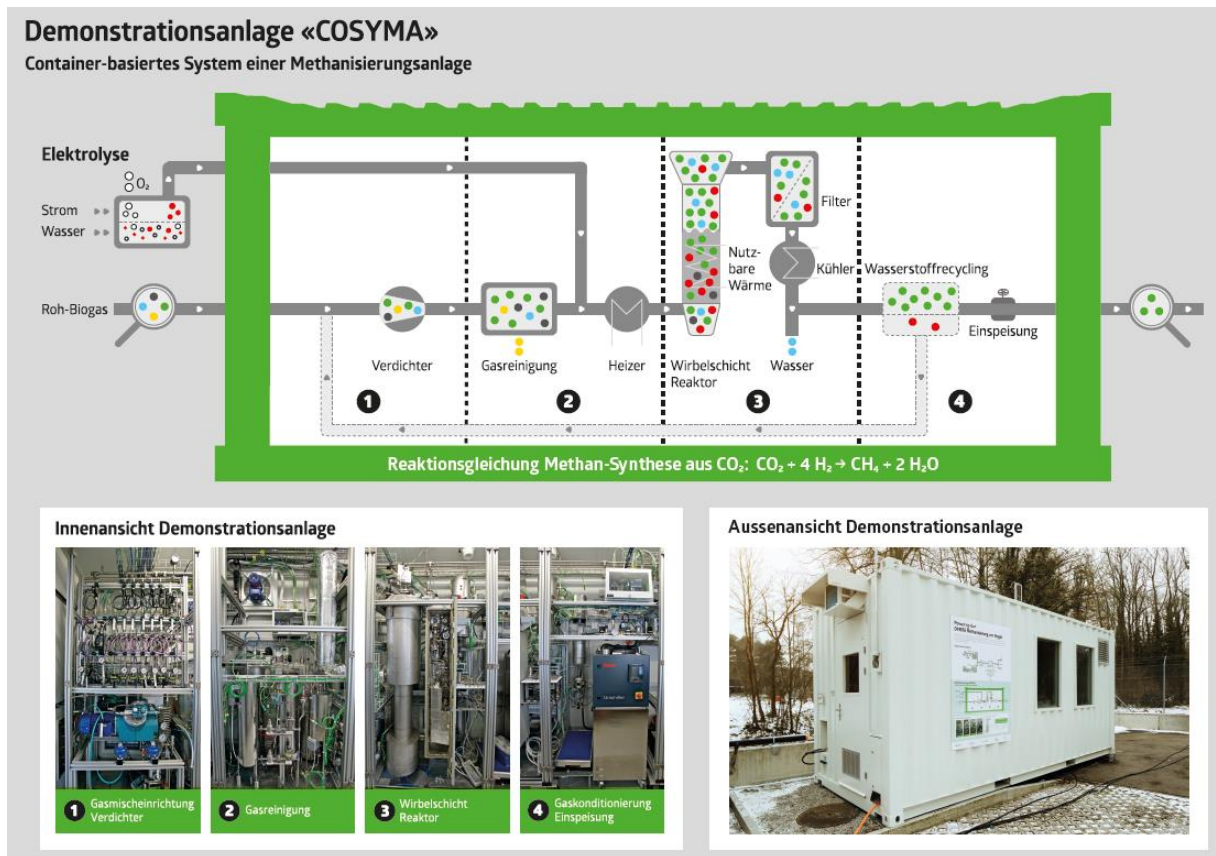


**Figure 16:** Pilot plant COSYMA, consisting of a compressor/gas supply (1), gas cleaning (2), fluidised bed methanation (3) and a gas conditioning (4).



In table 6 the list of equipment for the gas diagnostics is shown, which is applied for the long duration test in Werdhölzli with the COSYMA.

**Table 6:** Diagnostic toolbox applied for the COSYMA long duration test in Werdhölzli. Multiple on-line and off-line sampling systems and analytical instruments are applied.

	Tool	Compounds measured
To be used on site at Werdhölzli for COSYMA	NDIR ( <b>on-line, continuous</b> )	• Bulk: CO <sub>2</sub> , CH <sub>4</sub> , CO
	O <sub>2</sub> sensor ( <b>on-line, continuous</b> )	• O <sub>2</sub>
	Sulfur- $\mu$ GC ( <b>on-line</b> )	• Bulk: CO <sub>2</sub> , CH <sub>4</sub> , H <sub>2</sub> • <b>H<sub>2</sub>S, COS</b>
	FTIR ( <b>on-line</b> )	• Bulk: CO <sub>2</sub> , CH <sub>4</sub> , ... • Moisture • <b>Siloxanes, COS, HC</b>
	TDA SulfaTrac ( <b>off-line</b> )	• <b>Total sulphur</b>
	Sampling system for off-line analysis at PSI: <b>Liquid quench</b>	• Tars, other trace contaminants • Compounds with BP > 80 °C
Available at PSI	Sampling system for off-line analysis at PSI: <b>Gas Sample Cylinders</b>	• Sulphur compounds • Compounds with BP > - 60 °C
	MS, GC/FID, GC/SCD, GC/MS, ICP/MS for on-line and off-line applications	• <i>Various</i>

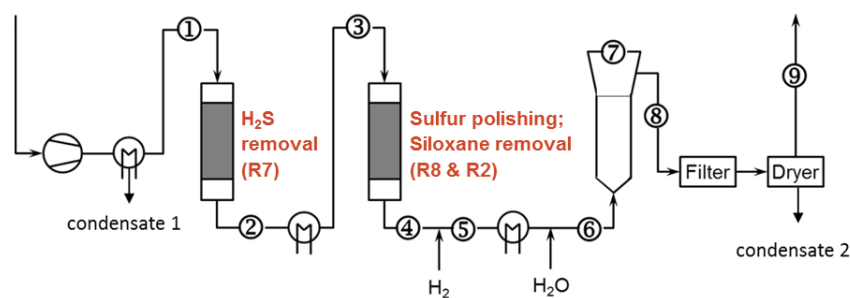
BP: Boiling point

The NDIR and the O<sub>2</sub> sensors are process diagnostics. If these diagnostics do not work properly or predefined limits are exceeded, COSYMA is switched automatically into standby mode. Therefore NDIR and the O<sub>2</sub> sensors are process gas diagnostics and critical for the operation of COSYMA.

In principle the long duration test could be performed only with the process gas diagnostics. Further gas diagnostic tools are needed in order to identify much earlier unwanted trends, i.e. breakthrough of contaminants in the gas cleaning section or deactivation of the methanation catalyst. The so-called research gas diagnostics is not critical for a safe operation of COSYMA.

One high-end research analytical instrument is the Sulphur- $\mu$ GC. This instrument is an on-line research diagnostic tool and operated unmanned. Data support the operation of the COSYMA, i.e. replacement of sorbent materials or adaptation of operation conditions in the bubbling fluidised bed methanation. The liquid quench system (LQ) is operated in batch mode. These sampling systems allow taking samples any time if needed. Samples are off-line analysed at PSI. The indicators "Dräger" are used for on-site off-line analysis of low concentration of H<sub>2</sub>S.

In figure 17 the multiple sampling points, sampling systems and online analytical instruments of the COSYMA installation are shown. Sulphur- $\mu$ GC is a one single measuring cell. Therefore this system is equipped with switch valve systems, which allow the analysis of gases from different sampling points. The LQ system has to be connected manually to the different sampling points.



Locations	①	②	③	④	⑤	⑥	⑦ (Lance)	⑧	⑨
AI-1	S-mGC (VA202)	S-mGC (VA206)	---	Indicators (VA303)	2x2 mGC (VA305)	---	S-mGC (VA501)	---	NDIR
AI-2	Liq. Quench (VA204)	Indicators (VA205)	---	Liq. Quench (VA303)	S-mGC (VA305)	---	---	---	2x2 mGC (VA702)
AI-3	---	Liq. Quench (VA205)	---	---	---	---	---	---	S-mGC (VA702)
AI-4	---	---	---	---	---	---	---	---	---
# of parallel sampling pts. available	4	2	1	2	1	0	1	2	1 (+NDIR)

**Figure 17:** Sampling points, sampling systems and online analytical instruments of the COSYMA installation for testing sorbent based gas cleaning (1 kg of sorbent) and fluidised bed methanation (1 kg of catalyst).

## Operation of COSYMA – Results on Methanation

A simplified version of the COSYMA set-up is illustrated in Figure 18. The set-up can be operated either by synthetic bottled gas or by real biogas coming from the anaerobic digester. Starting from real biogas, the stream first is compressed to the desired system pressure thereafter the flow is measured by means of an orifice measurement. After this, the biogas enters the gas cleaning unit, where harmful trace components like (organic) sulphur compounds are removed. These contaminants lead to deactivation of the catalyst even in small amounts, so it is essential to remove them. A detailed description of the gas cleaning unit can be found in chapter 'Gas Cleaning'. Subsequently, biogas is mixed with hydrogen and trace amount helium from the bottled gas section. The mass flows of bottled gases are measured and controlled by mass flow controllers (MFC). The addition of a known amount of helium allows determining the standard volume flows of all components via concentration measurements. Next, a small volume flow of the gas mixture is continuously directed to a Micro Gas Chromatograph (mGC) to measure bulk gas concentrations including helium. Then the stream is preheated to reactor inlet temperature and mixed with vapour. For this, water from a closed tank is heated to 360°C and evaporated. The decreasing mass of water in the tank is measured by scale I, which allows determining the inlet mass flow of water. Water addition is supposed to prevent coking of the catalyst.

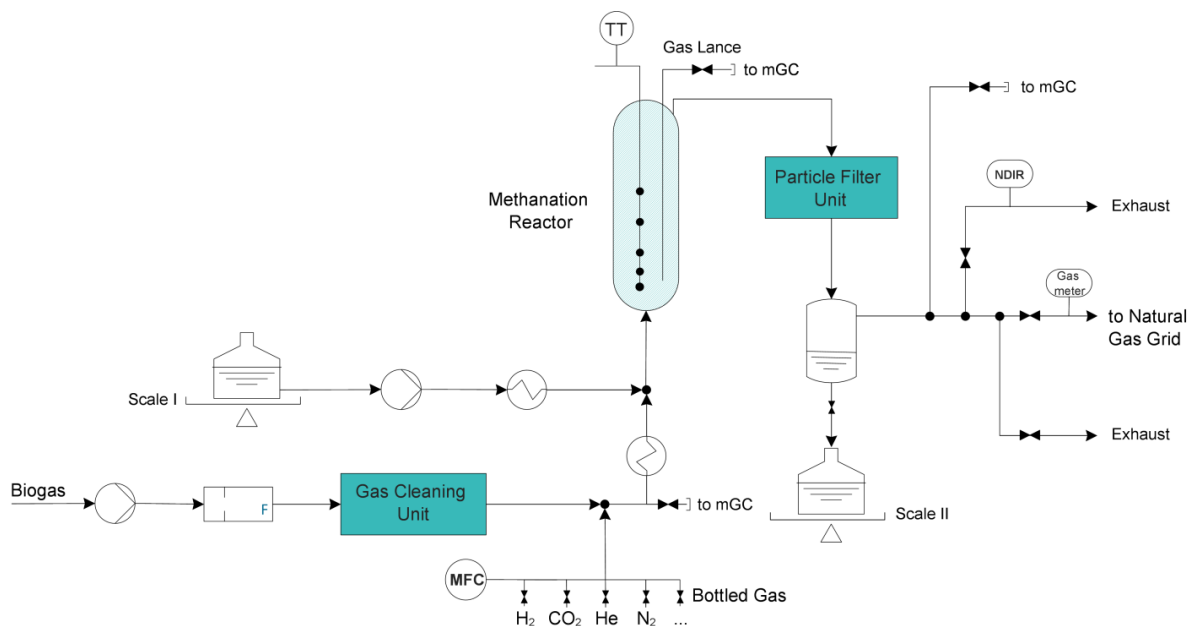


**Figure 18:** Simplified flowsheet of the COSYMA set-up

Now, the wet gas mixture is entering the bubbling fluidised bed reactor, where the methanation reaction takes place with a nickel catalyst of Geldart B type particle. The exothermic methanation reaction converts carbon oxides and hydrogen to methane and steam. The reactor diameter is 5.2 cm and the predominant catalyst mass was 800 g at the beginning of operation. The corresponding non-fluidised bed height is 58 cm. Inside the reactor, two lances are present. One lance measures temperatures at different heights. The other lance is taking gas probes at 7 cm bed height, which are directed to a mGC for measuring bulk gas concentration including helium.

The reacted wet gas mixture leaves the reactor and enters the particle filter unit. The filter safely removes fine dust that stems from attrition of the moving catalyst particles in the fluidised bed, whose amount however is not significant for operating such a system.



In a next step, the wet gas mixture is cooled to 4°C, so that the water present in the reacted gas condensates. The condensate is directed to a tank, which is weighed by scale II. With this procedure, it is possible to determine the entering water flow and the one leaving the reactor. The difference of these two streams equals the produced water during reaction. The dry gas leaving the condenser is analysed continuously via mGC and non-dispersive infrared sensor (NDIR sensor). If the NDIR sensor displays permissible concentrations of methane ( $\text{CH}_4 > 85\%$ ), the gas, which is now referred to as 'bio-methane', flows via gas meter into the natural gas grid (restricted injection). If the methane content is below the mentioned limit, the set-up turns into stand-by (keeping pressure and temperature while flushing with  $\text{N}_2$ ). During start-up (which is achieved in less than 15 min), the gas leaves the set-up as exhaust.

### Measurements and Data Evaluation

Operational conditions that can be measured directly are recorded and visualised by an Intermodulation Analysis System (IAS); e.g. temperatures, pressures, weights, concentrations by NDIR sensor etc. (155 measurement points in total). Concentration measurements via mGC have to be evaluated separately. The same holds for calculating operational parameters based on data from IAS or mGC. A redundant measurement system was established, such that relevant operational conditions could be measured or calculated in multiple ways independently from each other. This allows a direct verification of the redundantly obtained values for one operational condition. Also, an elementary mass balance was done for the whole set-up considering the elements carbon, hydrogen and oxygen. For this, a data processing tool (DP tool) programmed in Matlab<sup>®</sup> was established. First, the DP tool merges the data from the different sources. For this, the same time stamp must be applied to every source. This was necessary because different frequencies of recording were predominant from the different data sources. In order to obtain a value within two measured data points, linear interpolation between those two data points was applied. Operational parameters not accessible directly (e.g. inlet volume flow of biogas, hydrogen-to- $\text{CO}_2$  inlet ratio, conversion of  $\text{CO}_2$  etc.) were calculated by means of IAS and mGC data. In a last step, selected data is visualised in diagrams.

The explained procedure allowed an identification of reliable measurement values with which mass balances can be closed with an average error of +/- 5%. Redundantly obtained values are in agreement with each other. A prompt tracking and evaluation of the course of operation in a detailed way over 1000 h of operation become possible with the help of data processing tool.

**Regular Operation** Regular operation hours are defined as the time, where biogas from the plant in Werdhölzli was directed to the COSYMA reactor and bio-methane produced by COSYMA was injected into the gas grid. The 1'000 hours of operation time can be divided into two phases.

In the first phase (0h – 429h), operational conditions were varied in order to find optimal conditions for maximum methane content in the reactor outlet gas. This goal represents the need of a single methanation rather than the operation conditions for combining methanation with a hydrogen separation membrane. The latter would suggest significantly over-stoichiometric hydrogen addition. Within this experimental campaign however, the more challenging maximisation of the methane was targeted. During the optimisation phase, reactor temperature and hydrogen feed were varied. The amount of hydrogen added to the system is expressed by the hydrogen-to- $\text{CO}_2$  ratio, where the hydrogen feed is set into relation to the carbon dioxide mole flow of the raw biogas. Therefore, variations in the biogas feed when the hydrogen feed was constant lead to a change of this ratio.

The pressure was set to 5.7 barg for the whole regular operation time. Vapour was added to the reactor in order to prevent deactivation of the catalyst from coke forming. Here, a ratio of water-to- $\text{CO}_2$  of 0.5 was chosen.



In the second phase (430 h – 1'000 h), operational conditions were held constant within a range with the identified optimal conditions for temperature and hydrogen-to-CO<sub>2</sub> ratio. Pressure and water-to-CO<sub>2</sub> ratio remained the same as in the first phase. It turned out that the compressor for the biogas feed was not temperature-controlled and hence influenced by ambient temperature variations from day to night, which resulted in changing volume flows. In order to maintain a constant hydrogen-to-CO<sub>2</sub> ratio, hydrogen had to be readjusted. However, fluctuations of hydrogen-to-CO<sub>2</sub> ratios could not be fully avoided.

In the following figures, operational conditions and the performance of the reactor are illustrated. The different ratios, catalyst stress and yield of methane shown in the figures are defined as follows:

$$\frac{H_2}{CO_2} = \frac{\dot{n}_{H_2,in}}{\dot{n}_{CO_2,biogas}} \qquad \frac{H_2O}{CO_2} = \frac{\dot{n}_{H_2O,in}}{\dot{n}_{CO_2,biogas}}$$
$$cat\ stress = \frac{\dot{V}_{CO_2,biogas}^{std}}{m_{cat}} \qquad Y_{CH_4} = \frac{\dot{n}_{CH_4}^{out} - \dot{n}_{CH_4}^{in}}{\dot{n}_{CO_2}^{in}}$$

During the first phase, the reactor temperature was changed between 320°C and 360°C and for a short time until 380°C, which is illustrated in Figure 21. The system pressure was set constant. Especially during the first 200 hours, the temperature was varied strongly to identify an optimal temperature at given other conditions. The same holds for the hydrogen-to-CO<sub>2</sub> ratio (Figure 20). For low temperatures, the catalyst is less active, whereas high temperatures are thermodynamically unbeneficial. For low H<sub>2</sub>/CO<sub>2</sub> ratios (3.8 – 3.95), less hydrogen remains in the outlet stream, but CO<sub>2</sub> conversion is decreased due to sub-stoichiometry. Whereas for high H<sub>2</sub>/CO<sub>2</sub> ratios (4.0 – 4.2), CO<sub>2</sub>-conversion is increased, but more hydrogen remains in the outlet gas due to the bigger hydrogen feed. All aspects together form an optimal point for maximum methane content in the outlet gas.

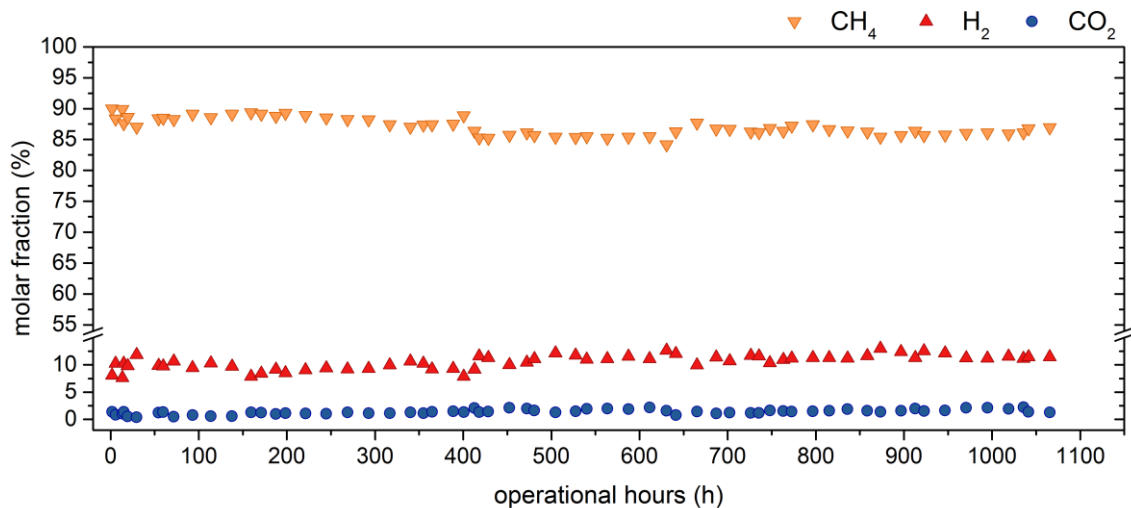


**Figure 19:** Molar fractions of bulk components after the methanation reactor over operational hours

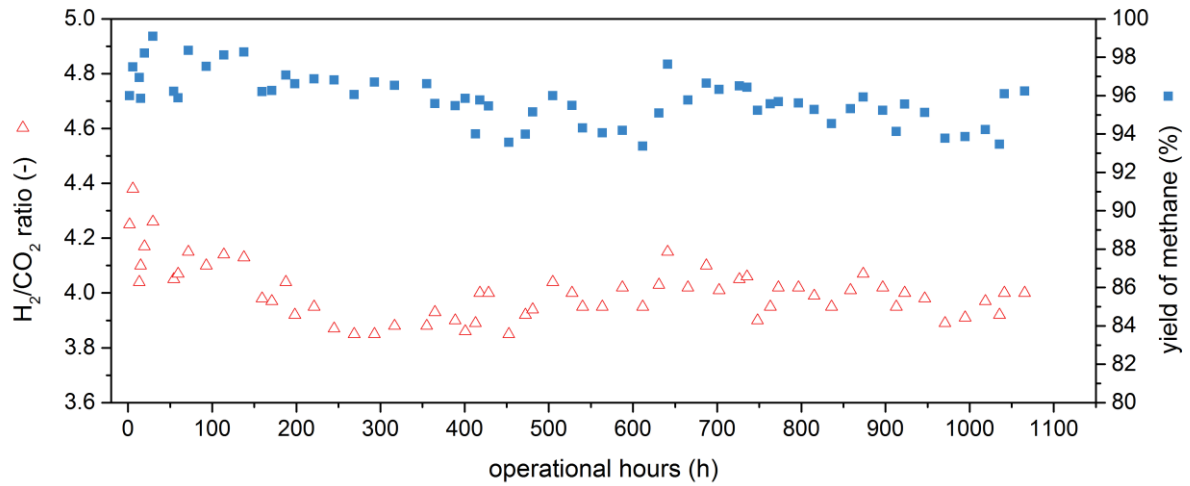


**Figure 20:** Inlet ratio of hydrogen-to-CO<sub>2</sub> and yield of methane over operational hours

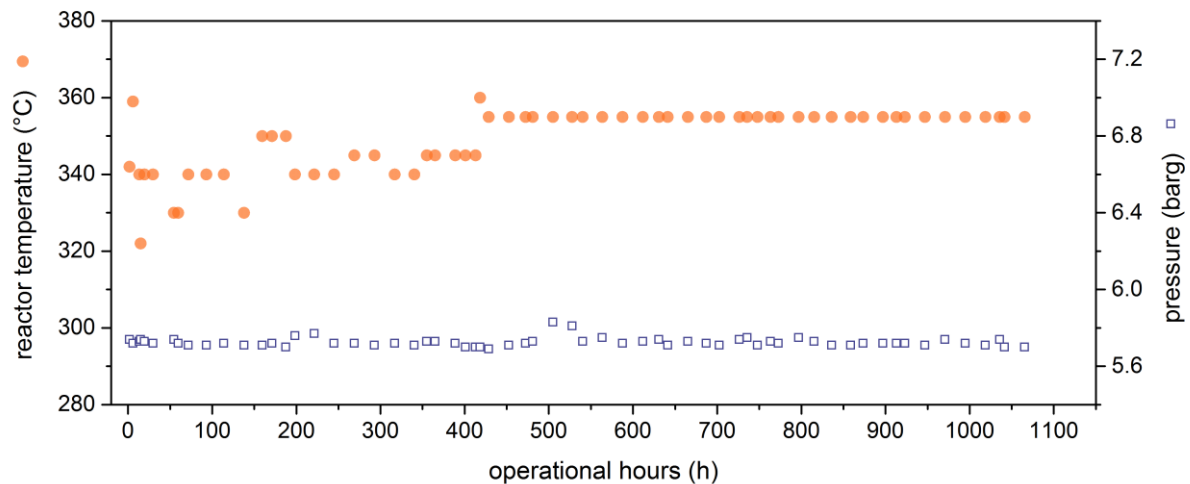


**Figure 21:** Reactor temperature and system pressure over operational hours

Due to the pronounced changes of those parameters, the dry concentration of the bulk components in the outlet gas (Figure 19) strongly vary at the first 200 operational hours. In the first phase, yields were reached between 94 vol-% and 99 vol-% with corresponding methane concentrations in the outlet stream between 85 vol-% and 90 vol-%. Almost the whole amount of reacted carbon dioxide is converted to methane. Hence, it can be assumed that the yield of methane equals the conversion of CO<sub>2</sub>.

During the second phase, operational parameters were mainly set constant within a range. Temperature and pressure were set to 355°C and 5.7 barg (Figure 21). The H<sub>2</sub>O/CO<sub>2</sub> ratio was about 0.55. Since it was not possible to hold the H<sub>2</sub>/CO<sub>2</sub> ratio constant due to the changes of the compressor flow, the ratio varies between 3.85 and 4.15 (Figure 20). In the second phase, methane yields reached 93 vol-% to 98 vol-% with methane outlet gas concentrations between 84% and 88%.



In general, changes in catalyst stress and vapour addition within the given ranges have only minor influences on the reactor performance, while variations of hydrogen addition impacts the dry outlet concentration of the reactor strongly. The yield of methane correlates directly with the predominant hydrogen-to-CO<sub>2</sub> ratio (Figure 20); however catalyst deactivation may also play an important role.

Effects of deactivation can be observed after 200 hours of operation. From 50 to 200 operational hours, the average methane content was 88.9 vol-% in the outlet gas. Then, the methane content decreases slightly such that during the operational hours from 430 to 600, the average methane concentration was 85.4%. After 640 hours of regular operation, 150 g of new catalyst were added to the reactor. As a result, methane content is increasing at that time and reaches an average methane concentration of 86.7 vol-% for the next 100 hours. But again a slightly decreasing trend can be observed, indicating that the source of deactivation may not be eliminated until that time (see chapter 'Gas cleaning'). After 735 hours, the critical adsorber bed of the gas cleaning unit was heated in order to remove adsorbed water blocking the sites of the adsorber material. According to the measure, the average methane concentration in the outlet gas is slightly increasing again for the next 61 hours.

At 815 hours, methane content starts decreasing again, where it reaches at the last recorded point a concentration of 85.4 vol-%. However, operational conditions were continuously changing over the time, thus a clear comparison of the results over the operational hours regarding deactivation is not possible. In order to gain reliable information about the effects of deactivation, separate experiments were conducted repeatedly in certain intervals at reference conditions. The procedure for these experiments is described in the next section.

#### Investigation of Deactivation via Reference Experiments with Bottled Gas

By means of repeated reference experiments, it was possible to create exactly the same conditions in the reactor such that the performance of the reactor can be compared over time regarding deactivation of the catalyst. Since the biogas concentrations from the biogas plant are subject to fluctuations, only bottled gas was used for the reference experiments in order to achieve stable. The reference experiments were repeated about every 100 operational hours (starting after 400 hours) or when there was a specific incident like catalyst addition etc. An average biogas composition of 40 vol-% CO<sub>2</sub> and 60 vol-% methane was simulated with bottled gas as feed, where methane was substituted by nitrogen for technical reasons. This procedure is valid, since the influence of the replacement of methane with nitrogen to the chemical equilibrium is minor. The predominant conditions of the reference experiments are listed in Table 7.

**Table 7:** Operational conditions during reference experiments with bottled gas

<b>H<sub>2</sub>, NI/min</b>	<b>CO<sub>2</sub>, NI/min</b>	<b>N<sub>2</sub>, NI/min</b>	<b>He, NI/min</b>	<b>H<sub>2</sub>/CO<sub>2</sub>, -</b>	<b>H<sub>2</sub>O/CO<sub>2</sub>, -</b>	<b>p, barg</b>	<b>T<sub>reac</sub>, °C</b>
53.4	12.8	18.6	0.4	4.17	0.86	6.1	320; 350

During the reference experiments, lance measurements were executed besides the regular measurements. Changes of concentration profiles over the reactor height give information regarding deactivation and the reaction mechanism.



In Figure 22, dry molar concentrations of the components methane, hydrogen and carbon dioxide after the reactor for reference experiments are illustrated. The concentrations of the mentioned components are normalised to 100% so that nitrogen and helium are not illustrated in the graph. Additionally, the yield of methane is shown for the corresponding experiment. At hour zero, a reference experiment was conducted, before real biogas was entering the COSYMA setup. This point can be seen as reference state for a fresh catalyst with a yield of 96.1 vol-% and a normalised methane concentration after the reactor of 82.5 vol-%. The normalised concentration of methane is not directly comparable with the results of the previous section, since only the produced methane is shown in Figure 22 and not the sum of methane from biogas and the produced methane like in Figure 19. Theoretically, the methane content for this experiment would have been 91 vol-%, if instead of nitrogen methane would have been added to the feed, which corresponds with the conditions of the regular operation.

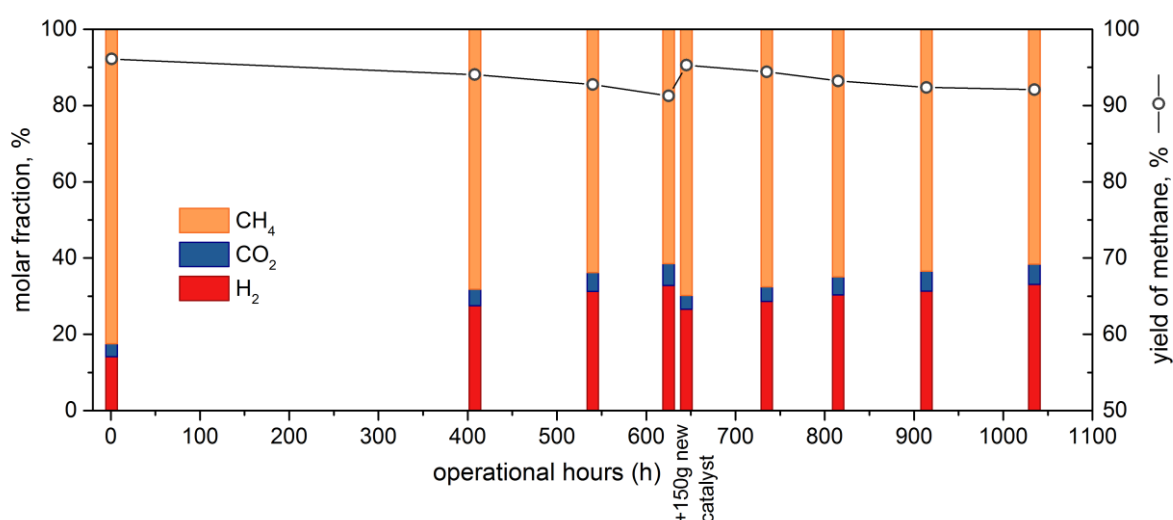


**Figure 22:** Normalised dry molar fraction of bulk components after the reactor and Yield of methane over operational hours with reference gas mixture at  $T=350^{\circ}\text{C}$  reactor temperature

At about 400 hours of operation, the first reference experiment was conducted since the reactor was operated with real biogas. A decreased yield can be observed together with a decreased normalised concentration of methane after the reactor. Corresponding to this, hydrogen and carbon dioxide content is increasing due to the lower conversion rates. Within the course of further operational hours, deactivation progresses until a yield of 91.3 vol-% and a normalised methane concentration of 61.5 vol-% at about 630 hours, which corresponds to methane content of 81 vol-%. The yield in total decreased with 5% over 630 hours of operation. The reason was the breakthrough of a sulphur compound in the biogas which was not expected during the design of the gas cleaning section. As discussed in section (Gas cleaning), it was possible to adapt the gas cleaning system to remove this sulphur species.

At about 640 hours, 150 g of new catalyst was added to the 800 g of catalyst inside the reactor. As a result, yield and methane concentration are increasing again on a level between the reference state and the reference experiment at 400 hours. Less than one fifth of the original catalyst amount was added to the reactor, but it results almost in the same performance of the reactor like for the non-deactivated catalyst. Since the methanation reaction in a fluidised bed is not restricted by kinetics, but



inter alia by heat transport at the given operational conditions, the main part of the catalyst is used to dissipate heat via heat exchanger, so that approximately isothermal conditions are reached. Now, the small amount of 150 g new catalyst is kinetically active enough to almost compensate the 800 g of partly deactivated old catalyst. Nevertheless, the catalyst material inside the reactor suffered slightly more, however not significant deactivation, until the operation conditions of the adapted gas cleaning section were optimised. Since then, activity stayed stable.

Normalised concentration profiles over the reactor height via lance measurements were derived at different points in time (Figure 23). Here, the dry molar fractions of the bulk components methane, hydrogen and carbon dioxide are illustrated. The norming of the concentrations to 100% was done in the same way like described for Figure 22. After 408 operational hours, the first lance measurement was conducted, where already a performance loss of the reactor occurred due to deactivation. Then directly before (630 h) and after the catalyst addition (640 h) the corresponding profiles are shown. In general, approximately two thirds of the total methane production is completed after 7cm of reactor height, which is about 12% of the total height. In the following 88% of reactor height, the remaining one third of total methane production is completed.

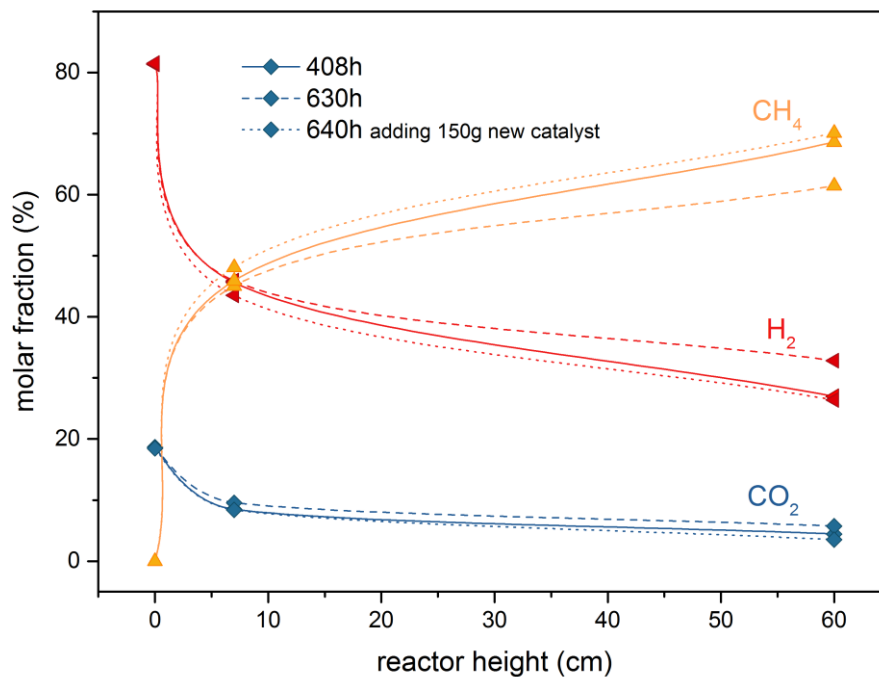


**Figure 23:** Normalised concentration profiles (dry) of bulk components over reactor height at different points in time at 350°C reactor temperature

Normalised concentration profiles are changing over time due to deactivation. After 408 hours of operation, signs of deactivation already occurred (see previous section). Then with further progressing in time until 630 hours, normalised concentration of methane decreases, hence hydrogen and carbon dioxide concentrations increase at the same time at lance height and the end of bed. With the catalyst addition after 640h, the methane content increases again. It was expected, that the difference in con-



concentrations for one component at different points in time would be more pronounced at lance height than at total height. Therefore, this method was supposed to give early warnings of deactivation. However, the measurements show that this is hardly the case. Mass transfer limitations from bubble to dense phase may influence the reaction in a way that the reaction course is not as fast as assumed, therefore deactivation of the catalyst cannot be seen so clearly at lance height via different concentrations of each component, because the local mass transfer overrules the effects of catalyst deactivation. Hence, the lance measurements are not easily suitable to give early warnings regarding catalyst deactivation.

#### Evaluation of Methanation Model with experimental Results from COSYMA and Optimisation of Operational Conditions

For maximising the methane content in the outlet gas, two parameters were considered: The hydrogen-to- $\text{CO}_2$  ratio at the inlet and the reactor temperature. Other parameters influencing the methanation reaction ( $\text{H}_2\text{O}/\text{CO}_2$ , catalyst stress and pressure) were kept constant within a range. The data for the analysis were taken from the regular operational hours. Therefore, like explained earlier the parameter water-to- $\text{CO}_2$  ratio is varying in a range from 0.51 to 0.67. The catalyst stress contains indirect the information about the carbon dioxide flow in the biogas entering COSYMA setup. Hence, also the entering carbon dioxide flow was kept constant within the mentioned range. The experimental data are compared to the results of the methanation model, for which an equilibrium model as well as a rate-based model is used.

The result of the variation of the parameter  $\text{H}_2/\text{CO}_2$  at the inlet is shown in Figure 24. Experimental data are compared with results from the equilibrium and rate-based model. Dry molar fractions of the bulk components methane, hydrogen and carbon dioxide downstream the reactor, are illustrated as a function of the inlet ratio of  $\text{H}_2/\text{CO}_2$ .

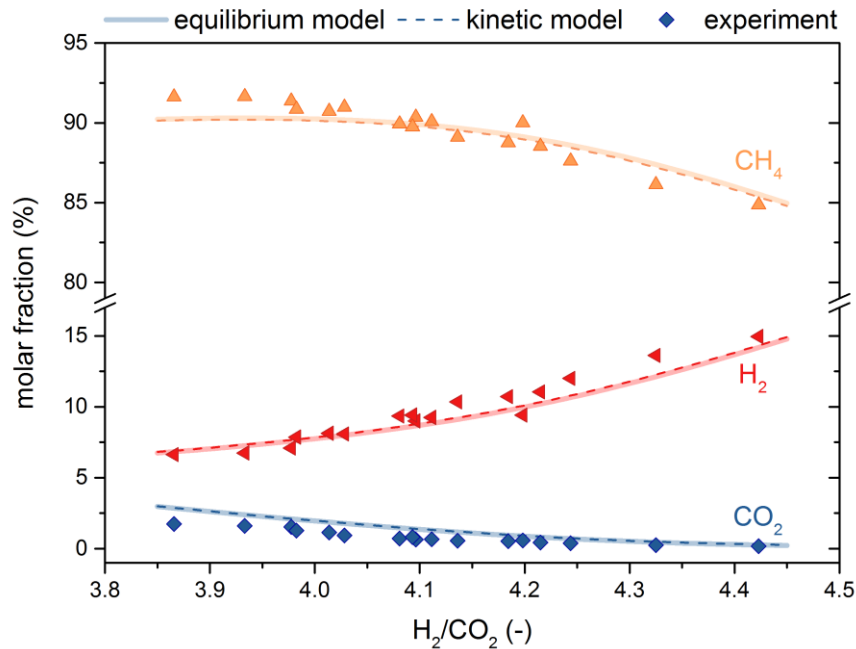


**Figure 24:** Dry molar fractions of bulk components after the reactor over different hydrogen-to- $\text{CO}_2$  inlet ratios derived via experiment, rate based model and equilibrium model at  $T=340^\circ\text{C}$ , average  $\text{H}_2\text{O}/\text{CO}_2 = 0.6$  and  $p=5.7$  barg

For high inlet ratios of  $\text{H}_2/\text{CO}_2$ , bigger amounts of hydrogen remain in the outlet stream, hence the hydrogen fraction is at maximum at high  $\text{H}_2/\text{CO}_2$  ratios and decreases with the  $\text{H}_2/\text{CO}_2$  ratio. The fraction of carbon dioxide behaves in the opposite way. For high  $\text{H}_2/\text{CO}_2$  ratios carbon dioxide fraction is very low, because bigger amounts of hydrogen enhance the reaction and therefore the conversion of  $\text{CO}_2$ . With decreasing hydrogen addition, the reaction becomes more restricted by the lack of hydrogen and less carbon dioxide converts, so more  $\text{CO}_2$  remains in the outlet stream of the reactor.

The methane fraction behaves different since a weak maximum is formed. For increased hydrogen addition, high conversion rates to methane are obtained, but also more hydrogen remains in the outlet flow. For decreased hydrogen addition, less hydrogen remains in the outlet flow, but the conversion to methane is inhibited. The interplay of these factors results in an optimum value of  $\text{H}_2/\text{CO}_2$ -ratio where conversion-rates to methane and low hydrogen addition is balanced. This optimum can be found at an  $\text{H}_2/\text{CO}_2$  -ratio of 3.9 in the model. However, sub-stoichiometric hydrogen addition may increase the risk of catalyst deactivation due to coking. The equilibrium model shows the same result as the rate-based model. This means that the reaction was not limited mass transfer within the whole reactor (which does not necessarily mean that there is no local mass transfer limitation, if the reactor is sufficiently large!) and could reach the maximum conversion rate, which is restricted by thermodynamics.

For lower  $\text{H}_2/\text{CO}_2$  -ratios, the conversion rates in the experiments seem to be even higher than the models predict, because higher methane concentrations and lower hydrogen and  $\text{CO}_2$  concentrations are obtained than in the model. Theoretically it is not possible to go beyond the thermodynamic limit shown by the equilibrium model, but in the experiment differences occurred in comparison to the model. First the water-to- $\text{CO}_2$  ratio was slightly decreased with 0.53 due to technical reasons for lower  $\text{H}_2/\text{CO}_2$  -ratios, therefore a slightly more beneficial thermodynamic equilibrium was established, where



higher conversion rates are possible. Whereas the fixed input parameter for the models was constant with an average water-to-CO<sub>2</sub> ratio of 0.6.

Secondly, the models are based on the assumption of isothermal conditions; therefore, they are calculating with a constant temperature over the height. However, temperature measurements have shown that the temperature varies over the bed height within a range of 5K to 10K depending on the achieved conversion rate, as shown in Figure 25. The gas inlet temperature was set to 260°C. Due to reaction heat, temperature is increasing very steeply in the first few centimetres. Then the temperature forms a plateau with approximately constant values. After 12 centimetres, the temperature is dropping. From lance measurements it is known that at this point more than two thirds of the total reaction rate is reached and hence, less reaction heat per volume is produced. Consequently, within the not perfectly mixed reactor the temperature drops. Nevertheless, temperature differences of maximum 10 K are very small in comparison to fixed bed behaviour with temperature differences of 300 K to 400 K [1, 2]. It seems that the formation of a moderate temperature profile even improves conversion rates. The higher temperatures at the beginning enhance the activity of the catalyst for increased conversion rates, and the lower temperatures in the middle and top part provide thermodynamically more beneficial conditions to convert even more CO<sub>2</sub> since the thermodynamic limit is shifted towards higher methane concentrations at lower temperatures.

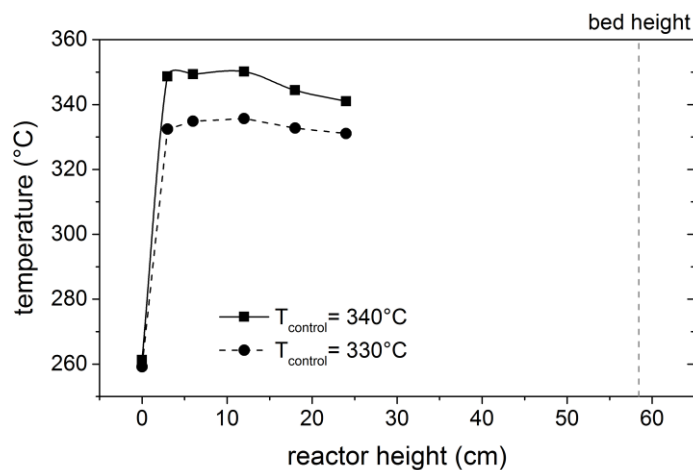


**Figure 25:** Temperature profiles over the height of COSYMA reactor for different outlet temperatures

The results of parameter variations regarding the reactor temperature are shown in Figure 26. Here again, experimental results are compared with results of the rate-based model for bubbling fluidised bed methanation. The experimental results show dry molar fractions of methane at the reactor outlet for different H<sub>2</sub>/CO<sub>2</sub> –inlet ratios over the reactor outlet temperature. Model results are illustrated with a normal and a dashed line as a maximum and minimum case.

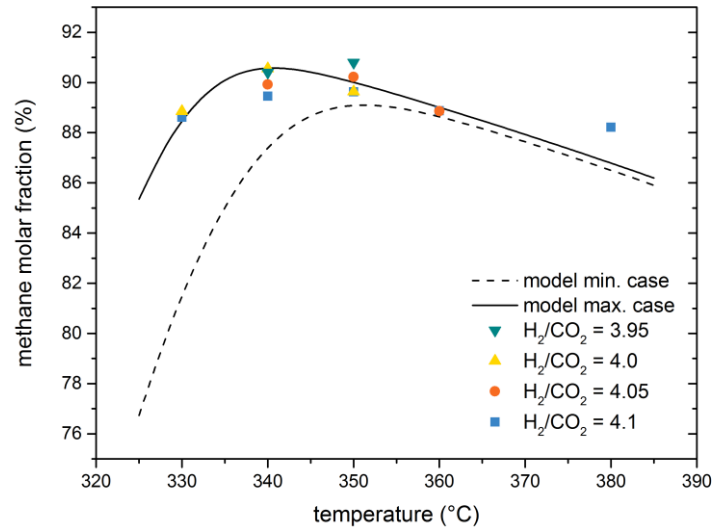


**Figure 26:** Dry molar fraction of methane after the reactor over reactor temperature at different hydrogen-to-CO<sub>2</sub> ratios derived via experiment and rated based model for a minimum and maximum case; average H<sub>2</sub>O/CO<sub>2</sub> = 0.5, average catalyst stress= 14.4 NI/(min kg) and p=5.7 barg for the experiments

Since in the experiment water-to-CO<sub>2</sub> inlet ratio and catalyst stress were varying in a certain range, experimental results are not directly comparable with model results. Therefore, model results are divided into the case where maximum methane concentrations are established after the reactor within the given experimental ranges of the two varying parameters and into a case for minimum methane concentration. The experimental results should be situated within the range given by the maximum and minimum case of the rate-based model. The input parameters of the two cases are listed in Table 8. For the case with maximum methane concentration at the outlet, within the given experimental operational conditions a low H<sub>2</sub>-to-CO<sub>2</sub> inlet ratio was chosen together with a lower water addition and a lower catalyst stress. At the beginning of this section it was already shown that sub-stoichiometric H<sub>2</sub>-to-CO<sub>2</sub> inlet ratios until 3.9 cause higher methane contents at the outlet than stoichiometric or hyper-stoichiometric hydrogen addition. Also, lower water addition influences the thermodynamic equilibrium beneficially towards higher methane concentration. A lower catalyst stress and, in general, a smaller inlet volume flow result in higher reaction performance and less mass transfer limitations. For the case with minimum methane concentrations at the outlet, vice versa a hyper-stoichiometric hydrogen addition was chosen, high water addition and a higher catalyst stress value. All parameters chosen in Table 8 were actual experimental conditions with corresponding experimental results shown in Figure 19.

**Table 8:** Input parameters corresponding to experimental conditions of the cases *maximum and minimum methane output concentrations* for the rated-based methanation model

Case	H <sub>2</sub> /CO <sub>2</sub> at inlet	H <sub>2</sub> O/CO <sub>2</sub> at inlet	V <sub>CH<sub>4</sub>,in</sub> , NI/min	V <sub>CO<sub>2</sub>,in</sub> , NI/min	Pressure, barg
Max	3.95	0.47	17.36	9.85	5.71
Min	4.10	0.51	24.94	14.15	5.71

Water addition to the reactor shifts the thermodynamic equilibrium towards less methane at the reactor outlet. On the other hand, water is supposed to protect the catalyst from deactivation by preventing coking of the catalyst. Still, water addition should be as low as possible, because it inhibits the methane production.

The target of the temperature variation is the identification of the optimum temperature at other given conditions where maximum methane concentration is reached. The optimum temperature is influenced by the kinetics of the catalyst and thermodynamics of methanation reaction. The experimental results illustrated in Figure 26 form a characteristic curve with a maximum for the methane concentration at a certain temperature. At lower temperatures, the catalyst is less active; therefore the reaction does not reach the thermodynamic limit. At higher temperatures, the thermodynamic limit for methane concentration is decreasing due to exothermic properties of the reaction. Hence, a maximum of methane concentration is formed, where the reaction limited by the kinetics hits the thermodynamic limit. For a higher hydrogen addition, the optimum temperature shifts towards higher temperatures in the model. For H<sub>2</sub>-to-CO<sub>2</sub> ratios of 4.0 to 4.1, experimental results are in accordance with the model results regarding the optimum temperature. For low H<sub>2</sub>-to-CO<sub>2</sub> ratios, the model predicts an optimal temperature of 340°C (maximum case) and for high ratios 350°C (minimum case). The optimal temperature of the experimental data for each H<sub>2</sub>-to-CO<sub>2</sub> ratio is in the range of the model predictions for ratios between 4.0 and 4.1. Except for the sub-stoichiometric ratio, optimal temperatures for the experiments shift towards higher temperatures for increased H<sub>2</sub>-to-CO<sub>2</sub> ratios like the model predicts. The kinetics used in the model were derived from experiments, where CO methanation was investigated and at operational conditions far away from this work (H<sub>2</sub>/CO = 5 to 6, p = 1barg) [3]. Nevertheless, experimental data are in good agreement with the rate-based model. For two experimental points, higher methane concentrations are reached than the model predicts for the maximum case. These two points refer to more advanced conditions (H<sub>2</sub>/CO<sub>2</sub>=3.95 or T=380°C), where the model may be not as accurate as for regular conditions.

### Summary of chapter

The COSYMA set-up, including the bubbling fluidised bed reactor for direct CO<sub>2</sub> methanation, was able to produce bio-methane continuously over 1'000 hours of operation. The produced bio-methane was injected into the gas grid at the biogas plant in Zurich-Werdhölzli as restricted injection. During the whole operation, methane yields of minimum 93% and maximum 99% were obtained with an average value of 95.3 %. In the bio-methane stream, the average concentration of methane was 87.2 vol-%, of hydrogen 10.4 vol-% and of carbon dioxide 1.3 vol-%. If helium is not considered in the outlet gas, the average methane content would go up to 88.2%. For unrestricted injection into the gas grid, further gas upgrading is necessary via a process unit which reduces the amount of hydrogen in the bio-methane stream down to a content of less than two mole-percent. Deactivation of the catalyst was



monitored and turned out to be small. Effects of deactivation could be reduced by the addition of 15% fresh catalyst and by measures for improving the gas cleaning unit. An optimisation procedure was carried out in order to maximise the methane content in the bio-methane stream during the first 200 hours. After this, the set-up was operated with the obtained optimised operational conditions for the following 700 hours. The evaluation of predictions from the fluidised bed methanation model with experimental data was successful. The results of both sensitivity analyses regarding hydrogen addition and reactor temperature variation could be verified by experimental data.

#### References for chapter “Operation of the Cosyma – Methanation”

- [1] Parlikkad NR, Chambrey S, Fongarland P, Fatah N, Khodakov A, Capela S, Guerrini O. Modeling of fixed bed methanation reactor for syngas production: Operating window and performance characteristics. *Fuel*. 2013; 107(0):254 – 260.
- [2] Schlereth D, Hinrichsen O. A fixed-bed reactor modeling study on the methanation of CO<sub>2</sub>. *Chemical Engineering Research and Design*. 2014; 92(4):702 – 712.
- [3] Kopyscinski J, Schildhauer TJ, Vogel F, Biollaz SMA, Wokaun A. Applying spatially resolved concentration and temperature measurements in a catalytic plate reactor for the kinetic study of CO methanation. *Journal of Catalysis*. 2010; 271(2):262 – 279.



## Sorbent based gas cleaning

### Introduction and review

The overall goal of the gas cleaning sub-project was to make recommendations on the choice of sorbent based gas cleaning process for the long-duration test in COSYMA, and subsequently for a scaled-up TRL 8 installation. There are multiple commercial sorption materials available for diverse applications. The challenge in this sub-project was therefore to select the right material and appropriate operation conditions in order to protect sufficiently the methanation catalyst over its lifetime.

One of the first steps in this activity was a review of expected contaminants and expected concentration levels in the biogas. In parallel, a review of the sensitivity of the key contaminants H<sub>2</sub>S and siloxane for different uses of the biogas was done and compared to the expected requirement for a methanation reactor concerning these contaminants. In order to get our own data, first measurements of the raw biogas quality at the specific site in Werdhölzli were done at the beginning of this project in 2015. These two boundary conditions – gas quality and converter sensitivity – are summarized in Figure 27.

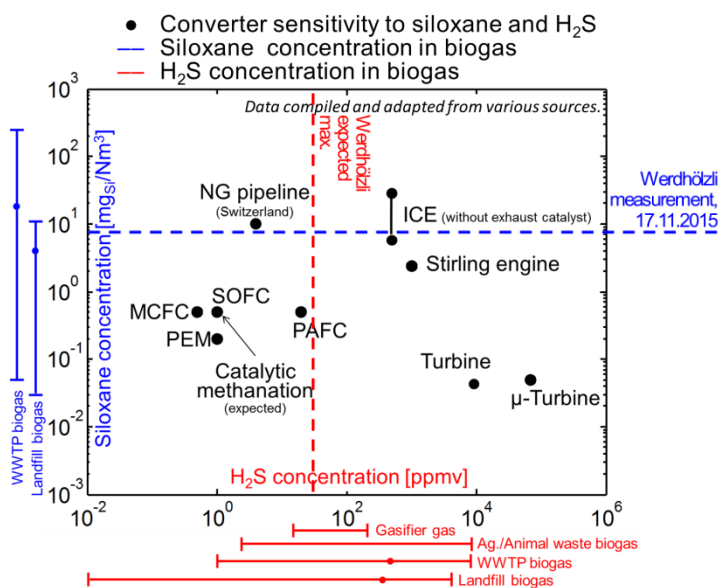


**Figure 27:** Sensitivity of various energy converters to H<sub>2</sub>S and siloxane in biogas [1-6]. Abbreviations: ICE = internal combustion engine; NG = natural gas; SOFC = solid oxide fuel cell; MCFC = molten carbonate fuel cell; PEM = proton exchange membrane fuel cell; PAFC = phosphoric acid fuel cell.

Thermochemical catalytic methanation is a process that is sensitive to several impurities in biogas, to a greater degree than for many “traditional” downstream processes such as internal combustion engines (ICE). Catalysts are especially sensitive to even low levels of sulphur compounds (~1 ppm), and may be sensitive to siloxanes as well. The presence of moisture and of other contaminants in the gas can also strongly affect the gas cleaning.

The selection of an appropriate sorbent based gas cleaning system for this Power-to-Gas application followed a multi-step approach:



1. The first step was the screening of potential sorbents based on published information and supplier information. This was the focus in fall 2015.
2. The second step was the screening of selected sorbents in the lab with a synthetic gas mixture. This gas mixture should demonstrate a degree of realism, especially concerning the gas matrix, in order to generate useful results. This was the focus in 2016.
3. The final step was the operation of a gas cleaning concept in the COSYMA installation that has to protect successfully the catalyst in the methanation reactor. Several sorbents or conditions were tested with real biogas on a kg scale. This was the focus in 2017.

### **Outcome of screening of potential sorbents**

Sorbent types and specific materials were pre-selected based on a survey of scientific literature, final reports of pilot projects for fuel cells operating on biogas, and based on the recommendation of suppliers. The focus was on selecting a first stage for H<sub>2</sub>S removal, and a second stage for sulphur polishing which includes both removal of trace H<sub>2</sub>S and of other sulphur compounds. Meanwhile, it had to be shown that at least one of the two steps would also remove siloxanes. The options considered and tested for these two steps are shown below.

#### *Potential sorbents for H<sub>2</sub>S removal:*

Activated carbons (Desorex K43Na and Solcarb KS3) and SulfaTrap R7 (a mixed transition metal oxide sorbent).

#### *Potential polishing sorbents for removal of organic sulphur:*

SulfaTrap R8 (an activated carbon with functionalized mixed transition metal oxides), SulfaTrap R2 (a mixed transition metal oxide dispersed on high surface area supports), ZnO preceded by a hydrodesulfurisation catalyst.

### **Sorbent testing in bench-scale tests**

The focus in 2016 was on accelerated sorbent testing in the lab with synthetic gas mixtures, and concurrently on the design and construction of the gas cleaning steps for the 1000 hour experiment in COSYMA. In the lab, sorbents were tested in a bench-scale experimental set-up using a synthetic gas mixture. The experimental set-up includes the ability to generate a gas mixture that contains CH<sub>4</sub>, CO<sub>2</sub>, N<sub>2</sub>, H<sub>2</sub>O, H<sub>2</sub>S, and siloxane D4 in specified concentrations. The real biogas in the long-duration test at Werdhölzli was expected to contain variable amounts of gas contaminants and water content, especially depending on the season.

Figure 28 shows the key results of these bench-scale tests. Tests for the removal of H<sub>2</sub>S were performed in a gas matrix of 55% CH<sub>4</sub> and 45% CO<sub>2</sub> by mole, moisture at a relative humidity (RH) of 50%. The contaminant used was either H<sub>2</sub>S alone, or H<sub>2</sub>S and siloxane D4. Figure 28 shows that different sorbents behaved differently in the presence of multiple contaminants. Activated carbons (Desorex K43Na and Solcarb KS3) showed a marked difference between the removal rate of H<sub>2</sub>S in “siloxane” and “no siloxane” environments. Meanwhile, SulfaTrap R7 (a mixed transition metal oxide sorbent) was robust to the addition of siloxane, with effectively no change in the adsorption behaviour for H<sub>2</sub>S.

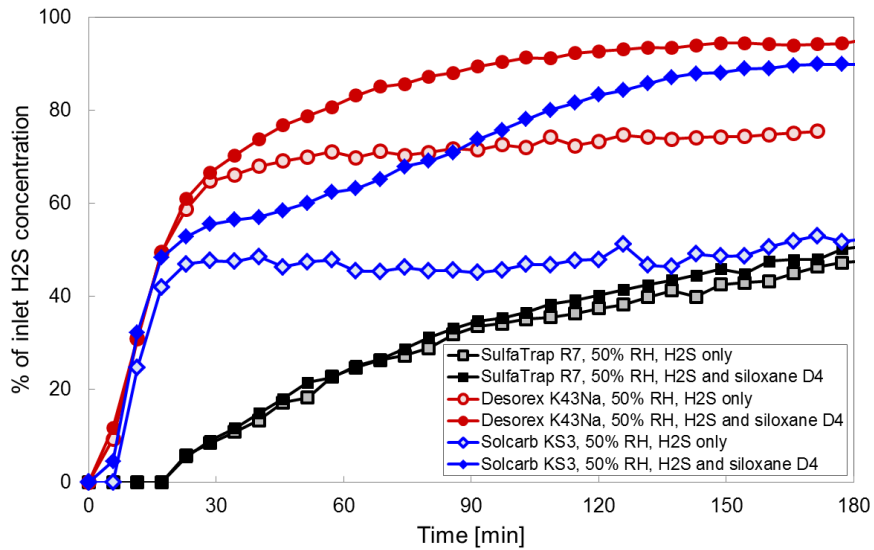


**Figure 28:** H<sub>2</sub>S breakthrough curves in several sorbents under single-contaminant (H<sub>2</sub>S only) and multiple-contaminants (H<sub>2</sub>S and siloxanes) conditions in lab, in both cases with 50% relative humidity (“RH”). Camilla Karlemo is gratefully acknowledged for experimental contributions to this figure.

Based on the lab scale tests, a two steps sorbent gas cleaning concept was selected for operation in the 1000 hour experiment, as shown in Figure 29:

1. Step: H<sub>2</sub>S removal step that is robust to the presence of other contaminants
2. Step: Polishing step that removes other sulphur compounds and siloxanes

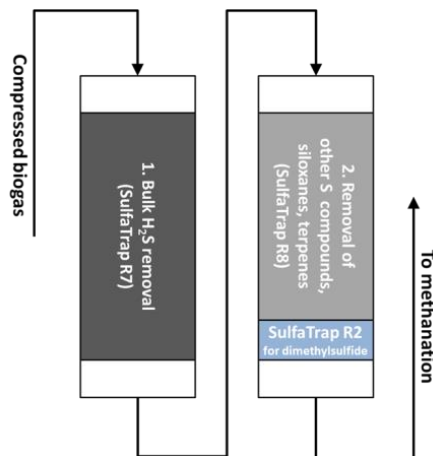


**Figure 29:** Overview of two step adsorption based gas cleaning finally chosen for the 1000-hour experiment in COSYMA.

Based on the robustness of the SulfaTrap R7 material to additional contaminants, and its better performance in both wet and dry environments relative to the other sorbents, it was chosen as the primary H<sub>2</sub>S removal sorbent for the long duration test in COSYMA.



SulfaTrap R8 was selected as a polishing step, because of its expected ability to remove trace sulphur compounds as well as siloxanes. This sorption material is an activated carbon with functionalized mixed transition metal oxides. Over the course of the 1000 hours experiment, it became clear that an alternative sorbent to R8 should be tested to remove dimethyl sulphide (DMS), a volatile organic sulphur compound. SulfaTrap R2 was suggested for this application by the R7/R8-supplier. This sorption material is a mixed transition metal oxide dispersed on high surface area supports.

### **1000-hr experiment: Behaviour in the first gas cleaning step (Bulk H<sub>2</sub>S removal)**

#### **Sorbents and gas conditions used**

SulfaTrap R7 (a mixed transition metal oxide sorbent) was used for the entirety of the 1000-hr experiment in the first gas cleaning step. It was operated at 35°C at the system pressure of 6.7 bara.

#### **Sampling and analytical devices used**

The first gas cleaning step is intended as the primary and bulk H<sub>2</sub>S removal step, and is it therefore this compound which is monitored continuously. The H<sub>2</sub>S concentration just before the first gas cleaning step and after this cleaning step are monitored online by use of a sulphur- $\mu$ GC. The sulphur- $\mu$ GC has a limit of detection (LOD) for H<sub>2</sub>S at 1-2 ppmv; therefore, Dräger indicators with limit of quantification (LOQ) of 0.2 ppmv are used to monitor H<sub>2</sub>S at sub-ppm concentrations. The transfer line from the “clean” gas sampling point to the S- $\mu$ GC was treated with Sulfinert by Restek.

The S- $\mu$ GC also monitors carbonylsulphid (COS) in the gas online, with a LOD of 1-2 ppmv. Other trace compounds are first sampled manually at the COSYMA by use of the Liquid Quench (LQ) sampling system. The solvent samples with quenched contaminants produced by the LQ sampling system are then analysed at PSI by GC-SCD (sulphur-containing compounds), GC-FID (carbon-containing compounds), and occasionally by GC-MS for compound identification.

#### **Behaviour of sulphur compounds**

##### **H<sub>2</sub>S behaviour**

Figure 30 shows the H<sub>2</sub>S before and after the first gas cleaning over the operation of the 1000 hour experiment, as monitored by Sulphur- $\mu$ GC.

As seen in Figure 30, H<sub>2</sub>S in the compressed raw biogas remained around 20 ppmv for the first 400 hrs of operation. The increase in H<sub>2</sub>S content after this time was due to changed operation conditions in the biowaste digester which is one of the two sources of the biogas fed to the COSYMA container. A temporary decrease in the dosing of iron hydroxide in this digester resulted in the increased H<sub>2</sub>S content in the biogas. This dosing was rectified, leading to the stabilization around 20 ppmv again just after 800 hrs of operation. The cause of the renewed increase in H<sub>2</sub>S content observed after 800 hrs of operation has not yet been confirmed with the operators of the digester, but it is assumed that the iron hydroxide dosing was again the reason.

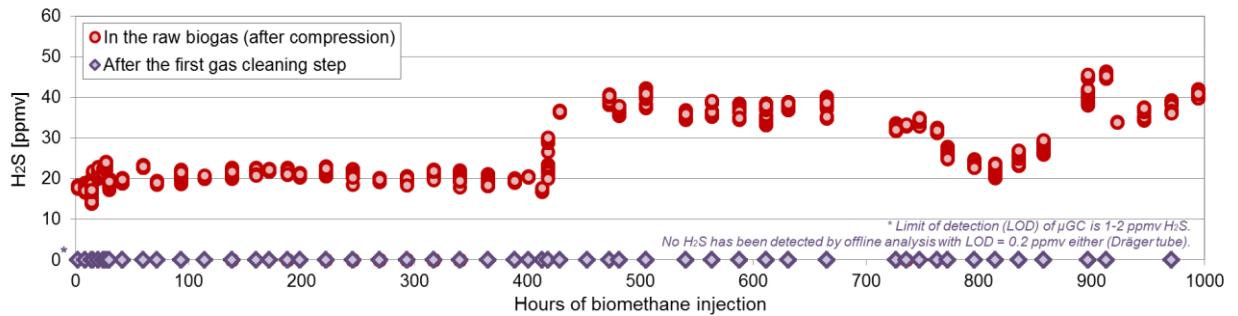


**Figure 30:** H<sub>2</sub>S concentration in the raw biogas (after compression) and after the first gas cleaning step measured with the S-μGC.

Figure shows that the H<sub>2</sub>S in the biogas is still being removed by the first sorbent step to below the limit of detection of the S-μGC (1-2 ppmv) and of offline Dräger indicators (limit of quantification, LOQ = 0.2 ppmv). Representative photographs of Dräger indicators are shown in Figure 31 after sampling raw biogas (top) and clean biogas (bottom). The SulfaTrap R7 sorbent has therefore successfully protected the downstream process from H<sub>2</sub>S even in the presence of many other impurities and moisture in the biogas, as expected from the lab tests.

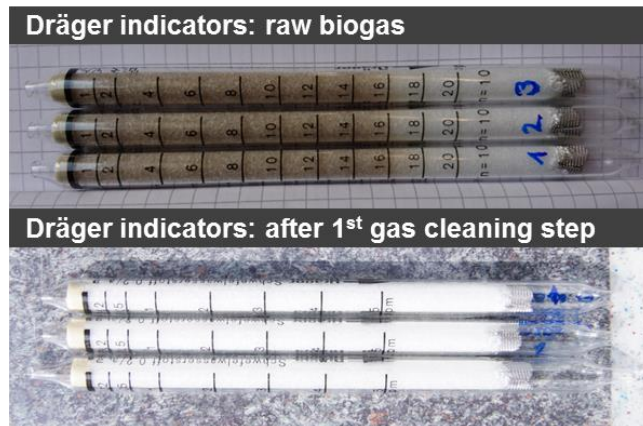


**Figure 31:** Dräger indicators for H<sub>2</sub>S, shown after sampling raw biogas (16-18 ppmv H<sub>2</sub>S here) and after the first gas cleaning step (<0.2 ppmv H<sub>2</sub>S).

#### Non-H<sub>2</sub>S sulphur-containing compounds

Other sulphur-containing compounds than H<sub>2</sub>S exist in biogas, as shown in Figure. Some are highly volatile (H<sub>2</sub>S, COS), while some have high boiling points and are readily condensable (e.g., dimethyl trisulphide), and others still have boiling points in intermediate temperature ranges (methyl mercaptan, and to some extent dimethyl sulphide and carbon disulphide). These widely varying volatilities have an influence on the ability to sample these compounds and analyse them in the lab at PSI.

Compounds with high boiling points are readily captured by the Liquid Quench sampling system, which concentrates these contaminants at a quench point of -10°C or -20°C into a liquid solvent solution, samples of which can be analysed off-line. Compounds with very low boiling points (H<sub>2</sub>S, COS) are monitored online by S-μGC. However, compounds with intermediate boiling points are expected to be captured only partly into the LQ solvent. Therefore, methyl mercaptan was not quantified in the LQ



samples taken, and DMS and CS<sub>2</sub> quantification would only provide a minimum value. The gas would then contain *at least* as much DMS or CS<sub>2</sub> as is found in the LQ solvent samples.

An alternative sampling technique for these intermediate volatility compounds is needed such as gas tank treated with Sulfinert or other sulphur-resistant coating. Such samples were not taken in the 1000 hours experiment for two reasons: (1) the GC-SCD which would be needed to analyse the gas samples was configured for liquid solvent samples, not gas samples; and (2) the stability of sulphur compounds in real biogas can be quite short in gas tanks, especially in the presence of moisture [7]. By contrast, LQ samples have shown reasonable stability, with <20% change in analysed concentration over the course of two weeks in a repeated analysis of a solvent sample performed during this project.

#### Some possible S compounds in biogas:

Compound		Boiling Point (°C)
Hydrogen sulfide (H <sub>2</sub> S)		-60
Carbonyl sulfide (COS)		-50
Methyl mercaptan (MM)		6
Dimethyl sulfide (DMS)		38
Carbon disulfide (CS <sub>2</sub> )		46
Methyl ethyl sulfide (MES)		67
Diethyl sulfide (DES)		92
Dimethyl disulfide (DMDS)		110
Diethyl disulfide (DEDS)		152
Dimethyl trisulfide (DMTS)		170
<b>Others</b>		?

**Figure 32:** Boiling points of some sulphur compounds which may be found in biogas.

The non-H<sub>2</sub>S sulphur compounds observed in the biogas prior to cleaning in COSYMA were mainly higher volatility ones, including DMS in particular. However, the non-H<sub>2</sub>S sulphur compounds observed after the first bed include larger compounds such as DMDS and DMTS. This is seen in Figure , which shows significantly larger peaks at longer retention times (farther to the right) in the GC-SCD chromatogram for “cleaned” biogas than for raw biogas. Similarly, Figure shows this effect over time.

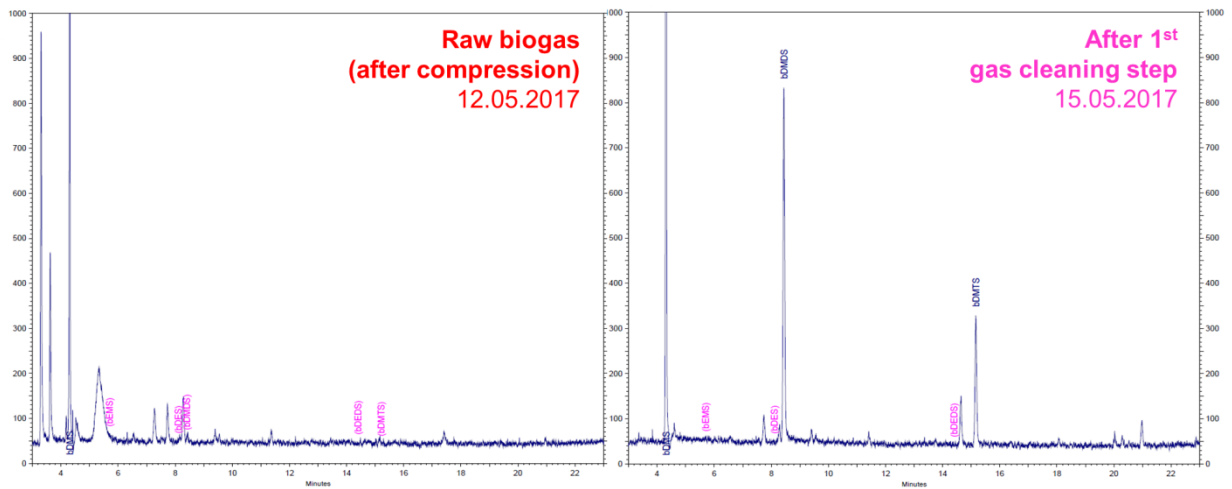


**Figure 33:** GC-SCD chromatograms before and after the SulfaTrap R7 sorbent. The increased peaks on the right side of the "after" gas suggest that larger sulphur compounds (DMDS, DMTS, others) were formed in the R7 bed.

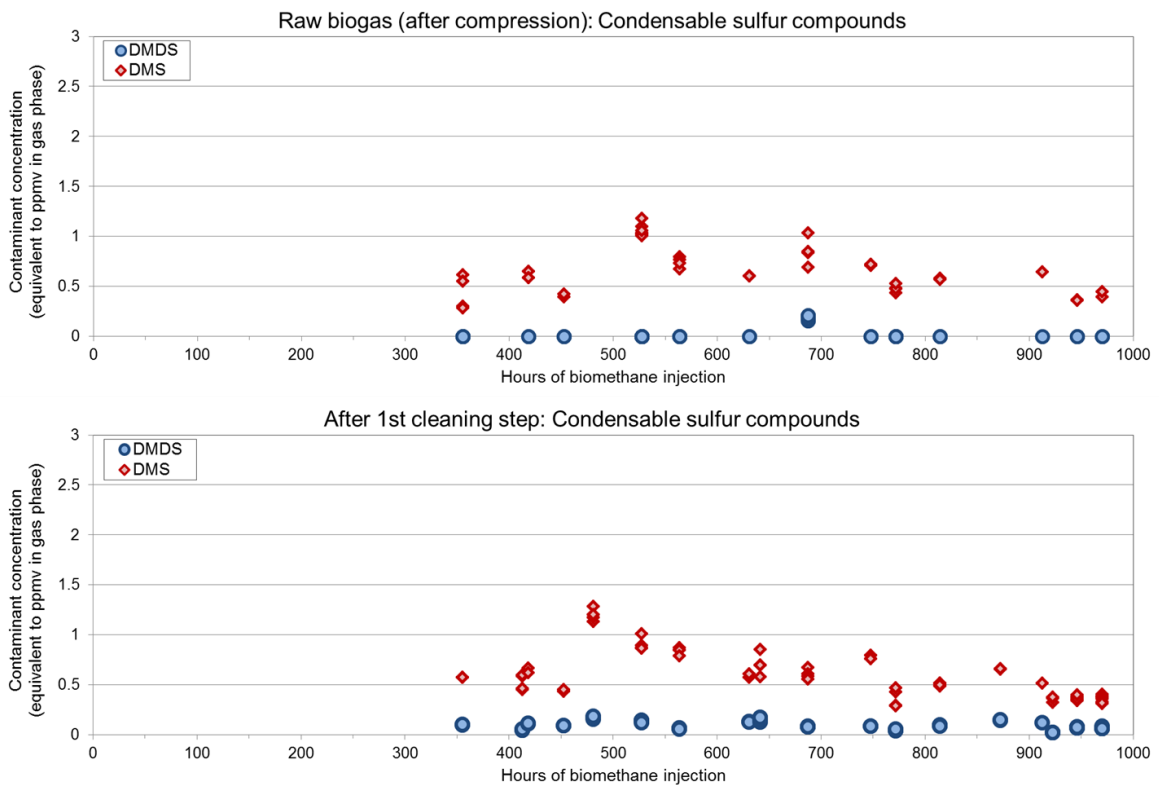


**Figure 34:** Behaviour of 2 key sulphur contaminants (DMS, DMDS) in the first gas cleaning step. The "after" data show more DMDS, a larger compound, than the "raw biogas" data. Data are from LQ samples analysed in GC-SCD.

This indicates that the SulfaTrap R7 sorbent, in addition to removing H<sub>2</sub>S from the biogas, is also causing the formation of larger sulphur-containing molecules from existing sulphur molecules. For example, DMS could be dimerized to DMDS. This is not necessarily an undesired effect, as long as a



second gas cleaning step exists. In a second gas cleaning step, any adsorption process based on physisorption should be facilitated for larger, less volatile molecules relative to higher volatility ones.

#### Behaviour of non-sulphur compounds

Other contaminants also exist in the biogas. Due to the biowaste digester source of part of the biogas, these are mainly terpenes, with some siloxane from the wastewater treatment plant. In an initial step, the primary non-sulphur compounds in the biogas were identified by taking Liquid Quench samples followed by an analysis by GC-MS. These results are shown in Figure .

During the long duration experiment a few key compounds (limonene, p-cymene, and siloxane D5) are monitored over several hundred hours of operation to observe any changes. These results are shown in Figure and demonstrate that non-sulphur compounds are not substantially removed in the first gas cleaning step by the SulfaTrap R7 sorbent. This is good, as these results confirm the expected selectivity of R7.

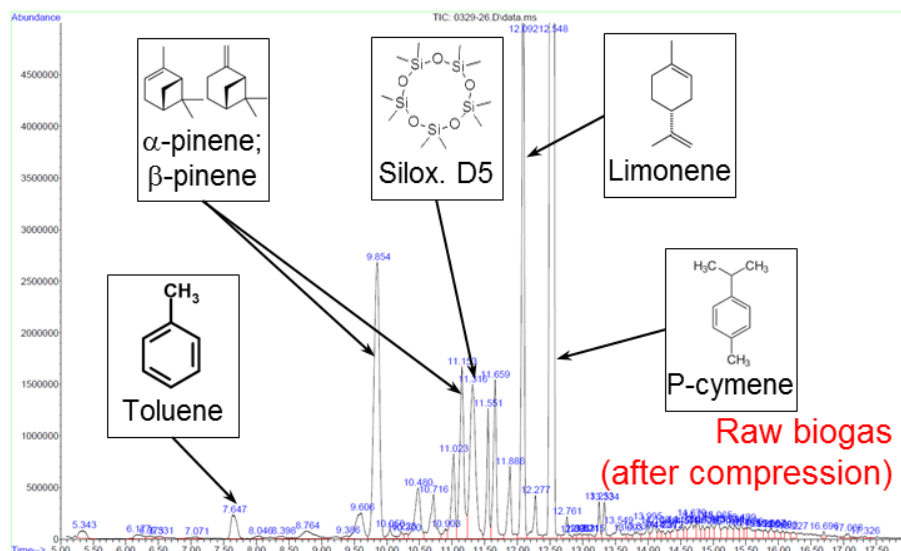


**Figure 35:** GC-MS chromatogram used to identify several key impurities in the raw biogas. As seen here, others exist but are not specifically identified or quantified. Data are from LQ samples analysed in GC-MS.

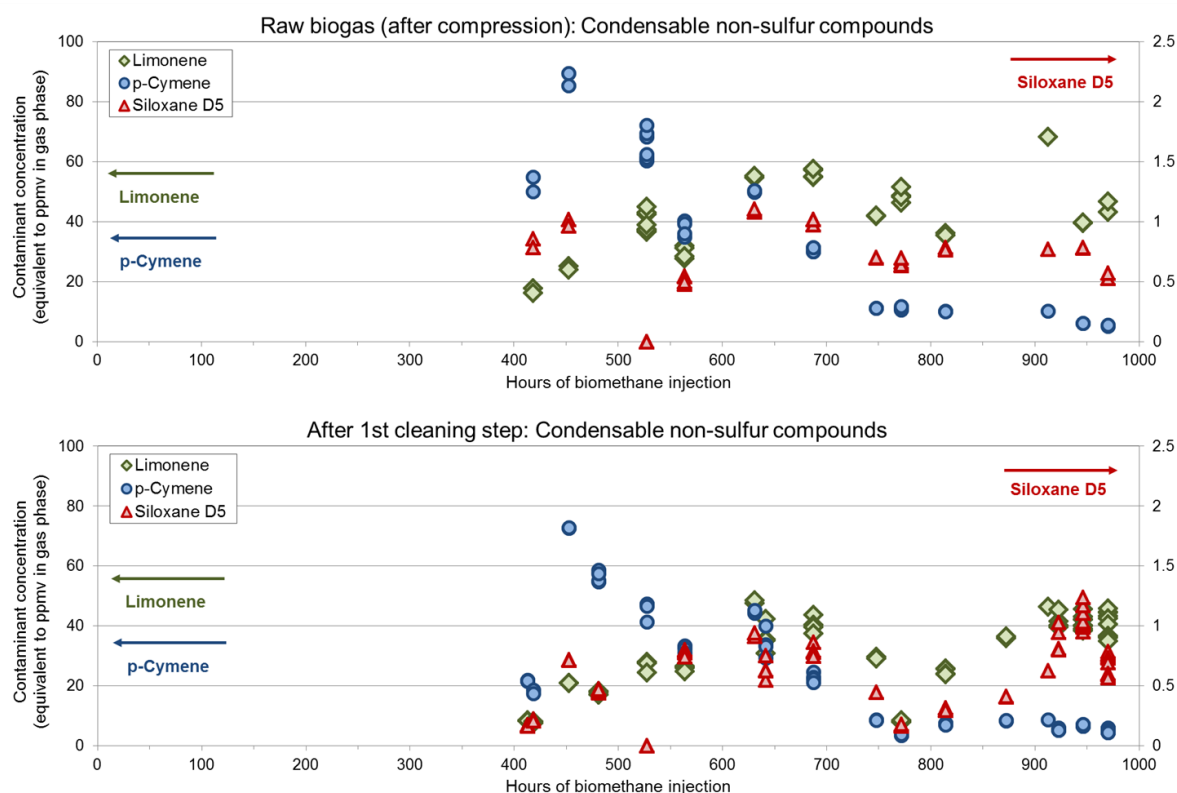


**Figure 36:** Behaviour of three key selected non-sulphur contaminants in the first gas cleaning step. As seen here, non-sulphur compounds are not substantially removed in this step. Data are from LQ samples analysed in GC-FID.

### 1000-hr experiment: Behaviour in the second gas cleaning step

#### Sorbents and gas conditions used

Several sorbents, sorbent combinations, and gas conditions were tested for this second gas cleaning step. While the first gas cleaning step had the clear and narrow aim of removing H<sub>2</sub>S robustly, the goal of the second step was more broadly defined as a polishing step for all other remaining sulphur compounds and other harmful compounds.

The difficulties with this broad aim include the fact that non-H<sub>2</sub>S contaminants are generally present at much lower concentrations than H<sub>2</sub>S (for non-H<sub>2</sub>S sulphur compounds, this was on the order of < 3 ppm, as seen in Figure 34). This means that these compounds are often difficult to sample and analyse. Moreover, these compounds are quite varied: as was already shown in Figure 33 and Figure 34 and will be seen again in this section, the sulphur compounds include highly volatile compounds and larger compounds, and the non-sulphur compounds include terpenes, siloxane D5, toluene, and others. Sorbents often interact differently with different compounds, such that a general goal of “removing **all** other sulphur compounds” can be, in reality, quite a difficult task.

The two sorbent materials tested in this second gas cleaning step were SulfaTrap R8 (an activated carbon with functionalized mixed transition metal oxides) and SulfaTrap R2 (a mixed transition metal oxide dispersed on high surface area supports). The SulfaTrap R8 was recommended as a material to use as a polishing bed for non-H<sub>2</sub>S sulphur compounds, which had also been previously shown to remove siloxanes successfully, while SulfaTrap R7 in the first gas cleaning step did not. However,



upon finding that we had significant ( $> 0.5$  ppmv) amounts of dimethyl sulphide (DMS) in the gas, the supplier of the SulfaTrap R8 recommended that SulfaTrap R2 be used as a final step, as SulfaTrap R8 was not intended to remove DMS for extended periods of time.

Therefore, several operation stages were used in the second gas cleaning step as follows. These stages are also represented in Figure .

- From 0 – 408 hrs of biomethane injection, only SulfaTrap R8 was used (1.8 kg of material).
- From 408 – 635 hrs of biomethane injection, the bed was filled with 80%v SulfaTrap R8 (1.4 kg) on top and 20%v SulfaTrap R2 (0.4 kg) on the bottom as a final stage.
- From 635 – 912 hrs of biomethane injection, the bed was filled with 35%v SulfaTrap R8 (0.6 kg) on top and 65%v SulfaTrap R2 (1.2 kg) on the bottom as a final stage. At 735 hrs, the sorbent was heated to between 80-100°C overnight in a flow of N<sub>2</sub>, and simultaneously a chiller was added after the biogas compression. Both of these were done in an attempt to remove more moisture from the system, both from the sorbent (heating and purging) and from the biogas (chiller addition). This was done in an attempt to extend the lifetime of the SulfaTrap R2, whose capacity was seen to be quite sensitive to moisture.
- From 912 – 1000 hrs of biomethane injection, the bed was once again filled with fresh SulfaTrap R8 only (1.7 kg of material) to observe the early stages of breakthrough, which had not been monitored in the first 300 hrs of operation.

This second gas cleaning step was operated with a temperature setpoint of 25°C, although in practice the temperature was often higher due to weather conditions, with temperatures reaching up to 40°C in the COSYMA container and in the sorbent beds. The gas cleaning step was operated at the system pressure of 6.7 bara.

#### Sampling and analytical devices used

Trace compounds are first sampled manually at the COSYMA by use of the Liquid Quench (LQ) sampling system. The solvent samples with quenched contaminants produced by the LQ sampling system are then analysed at PSI by GC-SCD (sulphur-containing compounds), GC-FID (carbon-containing compounds), and occasionally by GC-MS for compound identification.

#### Behaviour of sulphur compounds

H<sub>2</sub>S behaviour in this gas cleaning step is not shown, as the first gas cleaning step successfully prevented a breakthrough of H<sub>2</sub>S.

The behaviour of non-H<sub>2</sub>S sulphur compounds, as monitored by sampling by LQ and subsequent analysis in GC-SCD, is shown in Figure along with a summary of the sorbent(s) used. The first result to be observed here is that the combination of SulfaTrap R8 and SulfaTrap R2 is successfully able to remove all sulphur compounds including dimethyl sulphide during some period of time (see the stretch from 408 hrs to ~520 hrs, or the stretch from 735 hrs to 912 hrs).

The second observation, however, is that breakthrough of certain sulphur compounds did occur over the course of the 1000 hours operation. Dimethyl sulphide, which is the lightest sulphur compound to be captured to a significant extent by the LQ sampling system, was always the first compound to break through. Larger compounds (DMDS for example) broke through later. For example, the time period from ~300 to 400 hrs shows the occurrence of a DMDS breakthrough, as does the time period from ~560 to 630 hrs. In both cases, the DMS breakthrough occurred earlier.



Additionally, the concentrations of DMS and DMDS observed after the breakthrough were higher than those observed after the 1<sup>st</sup> gas cleaning step as seen in Figure 34. This is assumed to be due to a phenomenon known as concentration roll-up, which describes the increase in outlet concentration observed of adsorbed compounds in a multi-compound adsorption situation. In effect, the more weakly adsorbed compounds (DMS in this case) are displaced forward by more strongly adsorbed compounds as time progresses. This moves the zone of DMS adsorption forward in the sorbent, and when the front leaves the bed, the DMS has been concentrated by this mechanism.

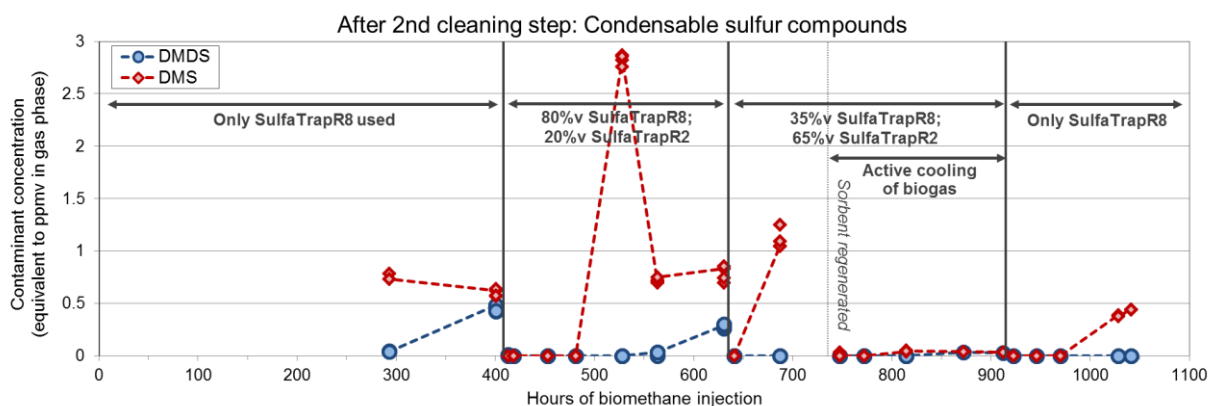


**Figure 37:** Behaviour of two key sulphur contaminants in the second gas cleaning step. The sorbent(s) used during each time interval are shown, along with any changes in gas operating conditions. Data are from LQ samples analysed in GC-SCD.

The unexpectedly fast breakthrough observed in this bed, as well as the concentration roll-up effect, are both assumed to be made worse by the presence of other non-sulphur contaminants in the gas. Water and non-sulphur contaminants will compete for physisorption sites in these high surface area sorbents, as was already observed in the lab tests reported in the 2016 report.

It was originally assumed that the very low concentration of non-H<sub>2</sub>S sulphur compounds would mean that the large capacity of the second bed would be enough even in the presence of other contaminants. Additionally, it was assumed that the compression of the raw biogas to 6.7 bara and subsequent passive cooling to room temperature would result in sufficient moisture removal from the biogas. However, the months of May and June were particularly warm, with temperatures reaching up to 40°C in the COSYMA container, such that significant moisture remained in the biogas.

The effect of moisture in competitive adsorption with sulphur compounds can be clearly seen in Figure 37 between in the time period 635 – 912 hrs. During the first 100 hrs of operation of this bed, which was comprised of 35%v SulfaTrap R8 followed by 65%v SulfaTrap R2, breakthrough of DMS occurred nearly immediately. At 735 hrs, the biogas flow was stopped and the sorbent bed was heated to 80-100°C overnight in a flow of N<sub>2</sub>. Simultaneously, a cooling system was added after the biogas compression, which cooled the biogas to 17°C. The effect of these two drying processes extended the time to breakthrough by a factor of more than 3.

In conclusion, the adsorption and removal of non-H<sub>2</sub>S sulphur compounds has been seen to be possible, but care must be taken in several aspects to prolong the time to breakthrough. First, non-DMS compounds were removed by SulfaTrap R8, but in cases where DMS exists in non-negligible amounts, SulfaTrap R2 should also be used. However, this sorbent is much more sensitive to moisture than SulfaTrap R8 is. The supplier lists standard tests conditions as 2.2% moisture for SulfaTrap R8,



and 4000 ppm (0.4%) for SulfaTrap R2. The maximal moisture content contained in the biogas can be estimated by assuming a saturated vapour in a 6.7 bar environment at a maximum temperature of 40°C, resulting in a moisture content of 1.1%, which is fine for R8 but not R2. Therefore, the biogas should be dehumidified to the greatest extent possible prior to this gas cleaning step for the use of R2 to remove DMS.

#### Behaviour of non-sulphur compounds

The compounds limonene, p-cymene, and siloxane D5 seen in Figure 36 were also monitored at the outlet of the second gas cleaning step, with the results shown in Figure 38. Noting that the y-axis scale is reduced in Figure 38 relative to Figure 36, we see that these contaminants, which were not removed in the first gas cleaning step, are now removed to a large extent in the second gas cleaning step.

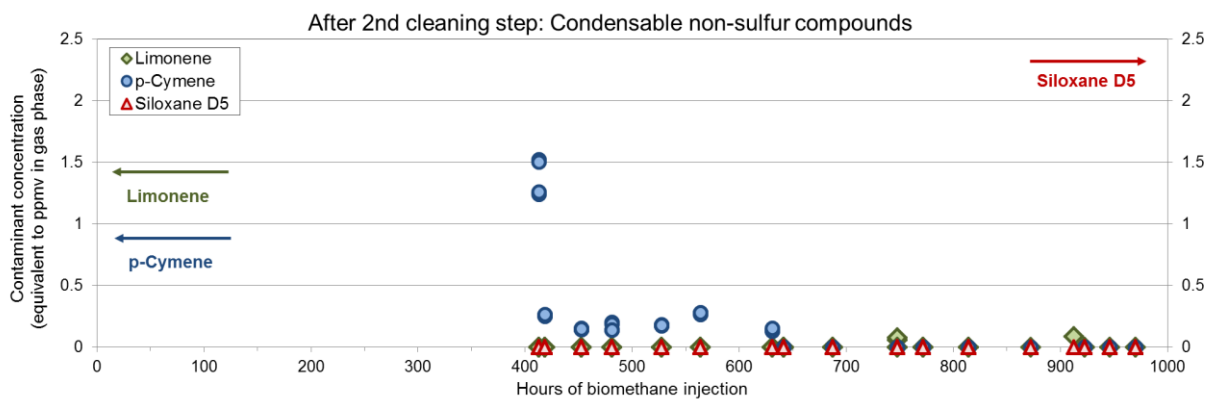


**Figure 38:** Behaviour of three key selected non-sulphur contaminants in the second gas cleaning step. As seen here, non-sulphur compounds are primarily removed in this step. Note the changed y-axis scale relative to Figure. Data are from LQ samples analysed in GC-FID.

On one hand, this is a welcome effect: it means that the methanation reactor was protected from siloxanes which may cause deposits of silica, similar to the effect observed in high-temperature fuel cells [8]. On the other hand, these other compounds compete for adsorption sites with the non-H<sub>2</sub>S sulphur compounds, which must also be removed in this gas cleaning step. Management strategies which reduce moisture in the gas, such as biogas cooling, could also reduce the presence of these contaminants prior to the second gas cleaning step.

#### Recommendations for gas cleaning and monitoring

We can first state some conclusions and recommendations which apply specifically to this project and could be applied to similar projects in future:

- The SulfaTrap R7 sorbent has successfully protected the downstream process from H<sub>2</sub>S even in the presence of many other impurities and moisture in the biogas, over the full 1000 hours of operation. H<sub>2</sub>S was never detected downstream of the first large sorbent bed, even with instruments which would be sensitive to 0.2 ppmv H<sub>2</sub>S.
- Management of non-H<sub>2</sub>S sulphur compounds proved more difficult, especially due to the moisture in the biogas and to the significant presence of the volatile compound DMS. However, by careful rearrangement of the second stage of gas cleaning, it was possible to limit the catalyst deactivation to a tolerable degree. An additional sorbent was added for DMS removal, and increased moisture removal was shown to allow the successful operation of the sorbents.



- During this 1000 hr experiment, a S- $\mu$ GC and Dräger indicators were used to monitor H<sub>2</sub>S. Sampling lines for clean gas samples (after the first gas cleaning step, after the second gas cleaning step) were treated with Sulfinert to prevent accumulation of sulphur compounds on the lines. Meanwhile, a Liquid Quench sampling system was successfully used to sample other contaminants prior to their analysis in GC-SCD, GC-FID, or GC-MS.

Based on our experience we make more general recommendations about sorbent evaluation, usage, and gas quality monitoring:

- Sorbent tests performed in lab (synthetic) conditions should, to the greatest degree possible, include realistic gas compositions. In particular, the behaviour of sorbents often changes drastically in humid gases relative to dry gases, so moisture addition must always be included.
- However, it is unlikely that any test in synthetic mixtures can ever capture fully the complexity of real gases. In the case of COSYMA, the long-term operation in real gas revealed in particular two important effects which had not been observed in lab tests: (1) the creation of larger sulphur-containing compounds in the first adsorbent bed; and (2) the difficulties caused by higher moisture levels than expected in the second adsorbent bed. Tests of sorbents in real gas are therefore strongly recommended when possible.
- Furthermore, several effects of the real gas on the gas cleaning process were observed over quite long time scales (100-300 hrs). This includes observing the breakthrough profiles of DMS and DMDS, allowing the understanding of the behaviour of the second sorbent bed. It is therefore recommended that, in a pilot project such as COSYMA, gas cleaning tests be performed for a minimum of 300 hours to verify operation of sorbents.
- For commercial plants, sufficient attention to the amounts and type of impurity compounds should be paid by applying appropriate and sufficiently sensitive analytics before design of the gas cleaning. However, during operation, using commercially available total sulphur indicators online is recommended rather than the manual offline sampling used in COSYMA.

## Summary of chapter

Sorbent based gas cleaning was reviewed. Promising sorbent materials were selected and tested in the laboratory and integrated into the pilot plant COSYMA. For the continuous documentation and monitoring of the long-duration test with the pilot plant, improved gas diagnostic systems were successfully used (mGC, liquid quench system). This way, it could be detected at an early stage if impurities such as H<sub>2</sub>S, dimethylsulphide (DMS) or siloxanes were no longer sufficiently protected by the gas purification.

## References for chapter “Gas Cleaning”

- [1] Thimsen, D., *Assessment of Fuel Gas Cleanup Systems for Waste Gas Fueled Power Generation*, EPRI Technical Update 1012763; 2006.
- [2] De Arespacochaga, N., S. Gutiérrez, A. Hornero, *LIFE-Biocell Deliverable D11: Fuel cells on WWTP: General Guidelines*, BIOCELL LIFE07 / ENV / E / 000847; 2012.
- [3] Allegue, L. B. and J. Hinge, *Report: Biogas and Bio-syngas upgrading*, Danish Technological Institute; 2012.
- [4] SVGW/SSIGE G13f, *Directive pour l'injection de biogaz*; 2014.
- [5] Torres, W., S. S. Pansare, J. G. Goodwin Jr., “Hot Gas Removal of Tars, Ammonia, and Hydrogen Sulfide from Biomass Gasification Gas”, *Catalysis Reviews* 49: 407-456; 2007.
- [6] Papadias D. D., S. Ahmed, *Database of trace contaminants in LFG and ADG*. Argonne National Laboratory. Excel files available for download at: [http://www.cse.anl.gov/FCs\\_on\\_biogas](http://www.cse.anl.gov/FCs_on_biogas); 2012.



- [7] Brown, A. S. et al., "Sampling of gaseous sulphur-containing compounds at low concentrations with a review of best-practice methods for biogas and natural gas applications", *TrAC Trends in Analytical Chemistry* 64: 42-52; 2015.
- [8] Madi, H. et al., "Solid oxide fuel cell anode degradation by the effect of siloxanes", *Journal of Power Sources* 279: 460-471; 2015.



## Technical learnings for scale-up to 200 m<sup>3</sup>/h biogas plant

One of the goals of this project was to demonstrate the technical feasibility of the direct methanation of biogas in catalytic fluidized bed reactors and to evaluate the process economics. This object was fully met as it could be shown that the methanation runs stable and allows increasing the biomethane yield from raw biogas by around 60%.

As expected from modelling/simulation, the reactor temperature and the ratio of hydrogen to CO<sub>2</sub> turned out to be the most sensitive operation parameters. Further, it was shown that the reactor is able to reach the thermodynamic limit at the chosen optimised operation conditions with close to stoichiometric H<sub>2</sub>/CO<sub>2</sub> ratios. As there is already significant technical experience for fluidised bed methanation on an industrial scale [1, 2] the generated insights on direct methanation of biogas in catalytic fluidized beds can be up-scaled to around 1 MW<sub>SNG</sub> which is the necessary size for 200 m<sup>3</sup>/h biogas flow.

For a 200 m<sup>3</sup>/h biogas plant, design calculation shows that a fluidised bed reactor of 60 cm diameter and around 2 m bed height is necessary. The bed height is chosen for the heat transfer via heat exchanger, while already 60 cm bed height is sufficient to reach the thermodynamic limit as shown in the long duration experiment with COSYMA. The additional bed height comprises activity reserve in case of slow catalyst deactivation. Even with the reserve, the reactor is significantly smaller than a cooled fixed bed reactor (2-3 times more volume) or a biological methanation (9 m high reactor at 70 cm diameter for the electrochaeta plant within the Biocat project [3]). A more detailed comparison between the different methanation technologies is presented in the Annex.

Start-up time from warm stand-by to injection was less than 15 min in COSYMA. Experiences from the 1 MW<sub>SNG</sub> plant in Güssing are similar. Experiments on PSI's pilot scale plant GanyMeth (160 kW<sub>SNG</sub> nominal capacity, TRL 6) will provide better insights into the dynamics of a fluidised bed reactor with biogas as GanyMeth comprises the same cooling coils and thermos-oil system as an industrial plant. Further, the GanyMeth experiments will be used to obtain better understanding of heat transfer performance and to validate the reactor model in more detail by predicting the measured concentration profiles with the simulation.

Biological methanation reactors can produce injectable biomethane (> 96% CH<sub>4</sub>, < 2% H<sub>2</sub>) in one step as the methanation process is operated at temperatures around 40-70°C. In catalytic methanation reactors, which run minimum at 250-400°C are limited by thermodynamics at methane contents of around 90% and H<sub>2</sub> fractions of >8%. Operation at the higher temperature level of catalytic methanation reactors allows recovering more than 120 kW<sub>th</sub> high temperature heat from each reactor cooling (> 250°C) and water condensation (> 120°C).

The incomplete conversion of H<sub>2</sub> and CO<sub>2</sub> in catalytic methanation reactors, asks for a further upgrading step to reach the grid injection specifications by either a 2<sup>nd</sup> methanation or a membrane, which allows the separation and recycling of hydrogen, CO<sub>2</sub> and humidity from the biomethane. Detailed knowledge on commercially available membranes is scarce while process optimization results strongly depend on the assumed membrane properties. Therefore, experiments with an industrial membrane are needed in order to have the necessary basis for a basic engineering study which will also develop the concept for the process automatization.

Process chain analysis shows that the electricity consumption for the hydrogen recycling into the catalytic methanation is lower than the published values for electricity consumption of the stirring devices in biological methanation. As the biomethane costs are dominated by the electrolysis (both with re-



spect to CAPEX and OPEX), the membrane costs are therefore not significant. A detailed engineering study is necessary to exactly determine the costs differences for a specific site.

With respect to gas cleaning, the project showed the importance of appropriate gas sampling, both with respect to sampling points and species to be detected. Within the 1'000 h campaign, a surprisingly large number of sulphur compounds and even one before not expected was found (di-methylsulphide) which is a challenge for many sorbent materials. By careful rearrangement of the sorbent based gas cleaning section, it was possible to limit the catalyst deactivation to a tolerable degree. For commercial plant, sufficiently attention to the amounts and type of impurity compounds should be paid by applying appropriate and sufficiently sensitive analytics before design of the gas cleaning, while using commercially available low cost total sulphur indicators during operation. With known impurity concentrations, it will be possible to design a gas cleaning with available sorbent materials. Again, the economic calculations show that the contribution of the gas cleaning to the overall costs is small.

The economic analysis of the direct methanation of biogas shows the dominant impact of the electrolysis capital costs and especially of its electricity consumption. Therefore, on the one hand, cost differences between the different methanation technologies may become insignificant and aspects such as quality of the recovered heat and dynamics/flexibility of the methanation gain importance. On the other hand, electricity costs below 5 Rp/kWh are necessary which does not allow the payment of the electricity grid use fee. Under the given legal boundary conditions (only pumped hydropower plants are excluded from grid use fee payment), this asks for sites where the electricity production is geographically sufficiently close to the biogas production sites such that the electrolysis can be placed at the power plant while hydrogen and/or raw biogas can be transported in pipelines to the methanation and up-grading plant.

References for chapter "Technical learnings for scale-up to 200 m<sup>3</sup>/h biogas plant"

- [1] 1 MW<sub>SNG</sub> from wood gasification gas in Güssing, Austria; cf. to: Kopyscinski J, Schildhauer TJ, Biollaz SMA. Production of synthetic natural gas (SNG) from coal and dry biomass - A technology review from 1950 to 2009. *Fuel*. 2010; 89(8):1763 – 1783.
- [2] 20 MW<sub>SNG</sub> from coal gasification gas, Hüls/Germany; cf. to: Friedrichs G, Proplesch P, Wismann G, Lommerzheim W. Methanisierung von Kohlenvergasungsgasen im Wirbelbett Pilot Entwicklungsstufe, *Technologische Forschung und Entwicklung - Nichtnukleare Energietechnik*. Thysengas GmbH prepared for Bundesministerium fuer Forschung und Technologie; 1985.
- [3] Presentation of D. Hafenbradl (electrochaea) and subsequent discussion during Regatec Conference 2017



## National collaborations

### *SCCER (BIOSWEET, STORAGE)*

The project “direct methanation of biogas” is an important contribution to the investigations on Power-to-Gas conducted within SCCER BIOSWEET in collaboration with SCCER STORAGE. Here, the long duration test with biogas at TRL 5 covers research questions which are not covered by other groups or projects. Especially, this project is complementary to the work within the underlying projects RENERG2 (CCEM) and Future Mobility Demonstrator (BfE/FOGA), where pilot scale methanation experiments at TRL 6 are in the focus.

### *BAFU PtX-Study*

The aim of the BAFU Study on PtX (EMPA, in collaboration with PSI) is to consider the potential of PtX to replace fossil fuels in mobility. As (bio-)methane is an established fuel with existing infrastructure, the increase of biomethane production by PtG/direct methanation of biogas is the pathway with the lowest economic hurdle in this direction. This project “direct methanation of biogas” delivers therefore technical information and economic data, which both are important input for the BAFU PtX-study.

### *ESI Swissgrid Study*

Within the framework of the Energy System Integration platform (ESI), several groups within PSI investigate the potential of PtG (both, to H<sub>2</sub> and to CH<sub>4</sub>) for stabilizing the electricity grid when challenged by integrating photovoltaic and wind electricity production. Again this study covers one important aspect of biomass based power to methane. By close collaboration of the three studies (this study, BAFU PtX-study and ESI/Swissgrid study) it is secured, that consistent and realistic set of cost data (investment, operation, etc.) is used for the considered technologies.

### *SCCER (BIOSWEET, STORAGE) Phase II*

The project “direct methanation of biogas” is well integrated within SCCER Phase II (2017 – 2020). The ongoing project will show the potential of biogas PtG applying fluidized bed methanation with membrane based gas upgrading after the methanation. While the robustness of gas cleaning and methanation will be experimentally proven in this project, the potential of the membrane upgrading is estimated based on literature data and computer simulation. Therefore integration of a hydrogen separation membrane module into the COSYMA plant is the next logic experimental step. Such a follow-up project allows showing the robustness of the suggested technology combination in direct methanation of biogas especially for sources with fast changing CO<sub>2</sub> content. Such fast changes can take place in digester plants digesting green waste. CO<sub>2</sub> concentration can change from 40 to 50% within hours.

Within SCCER BIOSWEET Phase II a techno-economic comparison of all relevant biomethane production technology is updated. Focus is on PtG technologies (catalytically and biological methanation). The analysis includes also conventional biomethane processes as well as agriculture feedstock (manure), which can also be used as a feedstock for biomethane production.



*Coherent Energy Demonstrator Assessment (CEDA), PtX Whitepaper*

Within several SCCERs processes are investigated and tested on TRL 5 and TRL 6. In order to further facilitate the information and knowledge exchange between multiple research groups two joint activities have been defined for the coming years and are financially supported by CTI. CEDA and PtX-Whitepaper aim at making information on technical, social and economic aspects of PtX technologies consistently available for other research groups and the public. The project “direct methanation of biogas” aims at delivering very important input to CEDA and the PtX Whitepaper and even at setting a best practice in technology evaluation.



## Annex: Communication

Kommunikation, Event	
Tag der Offenen Tür: ESI Plattform PSI (Poster / Flyer)	18.10.2015
Artikel Konzept / Zusammenarbeit - Fenster der Forschung PSI - Online Magazin Energie 360° <u>Vielleicht bauen wir künftig Solarparks, um erneuerbares Gas zu produzieren</u> - Online Magazin Energie 360° <u>Energie aus fossilen Quellen mit besseren Konzepten ablösen</u> - Website VSG <u>Mehr Biogas dank Power to Gas</u> - Online Magazin Energie 360° <u>Reportage Wissenschaft / Bau der Cosyma</u>	Heft1/2016 15.3.2016 16.4.2016 17.5.2016 26.10.2016
Medienmitteilung Zusammenarbeit PSI –Energie 360° - Basellandzeitung: <u>PSI und Energie 360° testen die Power-to-Gas-Technologie</u> - Limmattalerzeitung: <u>Biogas-Anlage Werdhölzli wird zum Versuchslabor</u> - Aargauerzeitung: <u>PSI und Energie 360° testen die Power-to-Gas-Technologie</u>	16.3.2016
Erlebnistag Biogas Biogasanlage Werdhölzli -Stand, Präsentation PtG Projekt, Podiumsgespräch PtG (P.Dietiker, P.Jansohn, Ch.Bach)	16.4.2016
Fachartikel: Methanisierung von Biogas - Aqua&Gas, Direkte Methanisierung von Biogas (Heft Juli / August) - Magazin Umwelt Perspektiven (25.4.2016) - Bericht in Energiefachbuch 2017	05.07.2016 25.04.2016 Sept 2016
Kommunikation, Event	
Präsentation: Projekt / Konzept an Branchenveranstaltungen - FOGA Anlass (Forschungstag der Schweizer Gaswirtschaft) 6.7.2016 - Poster (Biogas cleaning) Biomass for Swiss Energy Future (Biosweet) - ESI Plattform: Vernetzte Energieforschung Schweiz (22.09.2016) - Conference, European Biogas Association, Gent Belgium	06.07.2016 07.09.2016 22.09.2016 27/29.9.2016
Artikel: Aufstellung in Werdhölzli - PSI Website <u>Höhere Methan-Ausbeute aus Bioabfällen</u> - Online Magazin Energie 360° <u>Mehr erneuerbares Gas dank Power-to-Gas</u> - my Sience <u>Höhere Methan-Ausbeute aus Bioabfällen</u> - Schweizerbauer <u>Bioabfälle: Grosses Energiepotential</u>	23.01.2017 23.01.2017
Artikel: Test in Werdhölzli / Erkenntnisse - NZZ Reportage <u>Überschüssiger Strom produziert Gas</u> - BFE Blog (Feb 2017) - Aqua & Gas <u>Beitrag ausgehend von Artikel PSI Website</u>	3.02.2017 27.02.2017 März 2017
Besichtigungsevent : Testanlage in Werdhölzli - Behörde / Verbände / Institute / Partner : VSG, SVGW, BFE, Swissgrid, ZHAW, HSR, EMPA, ETH	5.04.2017

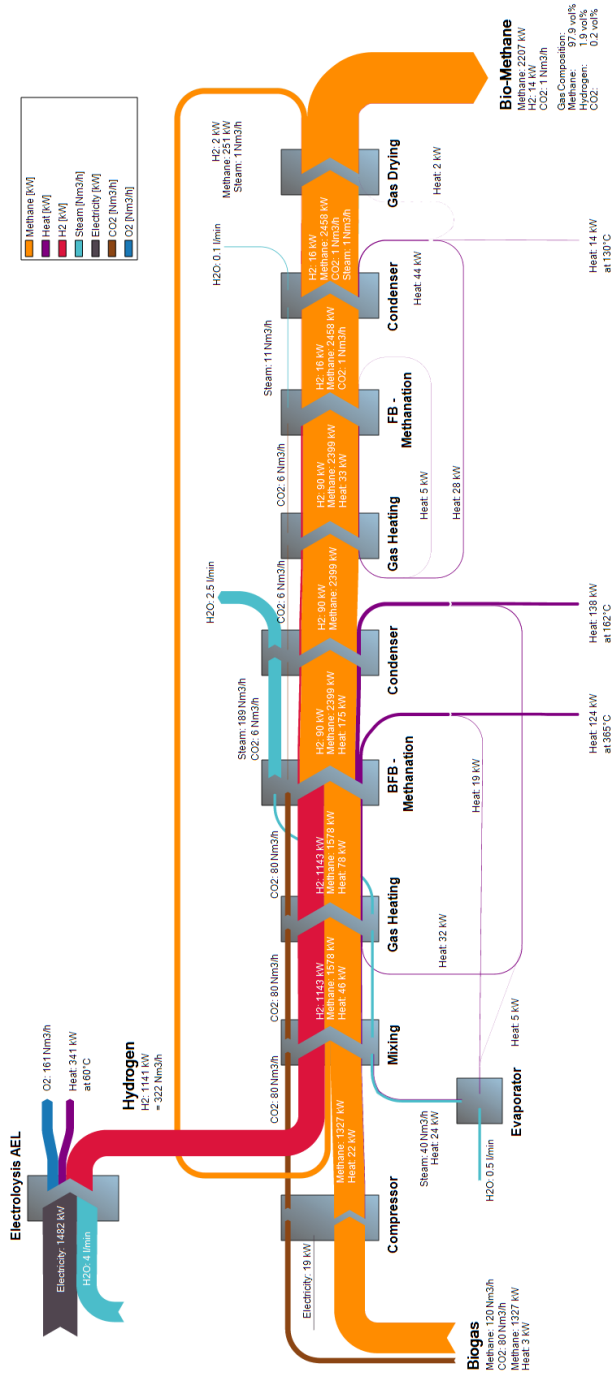


Kommunikation, Event	
Medienmitteilung Besuchs Event Werdhölzli <small>Mehr erneuerbares Gas dank neuer Power-to-Gas- Technologie</small>	05.04.2017
Besichtigung Testanlage Werdhölzli für spezifische Interessengruppen - Energie 360°: MA, GL, VR - Behörde / Verbände / Institute: (eingeladen zu Besichtigungstag) - HSR: Power to Gas Expertengruppe - PSI: MA ESI Plattform; künftige Projektinteressenten	Jan - Juni 2017
TV Beitrag: Power to Gas - TV SRF Einstein: <small>Transfer Cosima von PSI ins Werdhölzli Teil von Einstein Sendung 23.2.2017</small>	23.02.2017
Fachartikel: Biogas PtG im Pilotmasstab - VSG Aqua&Gas (Heft Sept 2017) - VSE Bulletin (Heft Okt 2017) - Artikel BFE - BFE Website August - Energy now (Beilage von ‚Swiss Engineering STZ‘) 8.Aug2017 - Erneuerbare Energien (deutsch/französisch) 11.August - Effience 21 (französisch) Oktober	
Kommunikation, Event	
Artikel Projekt Erkenntnis: eigene Webseiten/Hauszeitungen - Online Magazin Energie 360° (April 2017) - Online Magazin Energie 360° (Abschluss 1'000 h Versuch) - PSI und Online Magazin Energie 360° (Abschluss Projekt, Veröffentlichung Bericht BfE homepage)	20.04.2017 25.07.2017 x.09.2017
Präsentation Projekt, Erkenntnisse an Branchenveranstaltungen - HSR Expertengespräch (2017) - Zukunftsforum Biogas an der EMPA, 3. Mai 2017 (2017 Q2) - Forschungstagung Bioenergie 2017 des BFE - Regatec 2017: 2 Poster (Biogas cleaning, Erfahrung Methanisierung) - BFE Lunch Session, 7.6.2017 - SCCER BIOSWEET Konferenz, 5.9.2017 - FOGA Abschlusspräsentation, 6.9.2017 - Power-to-Methane Joint Workshop, Brüssel, 6.9.2017	12.01.2017 03.05.2017 10.05.2017 22.05.2017 07.06.2017 05.09.2017 06.09.2017 06.09.2017
Innovationspreis	
- Anmeldung zu Watt d'Or 2018	



## Annex: Sankey diagrams

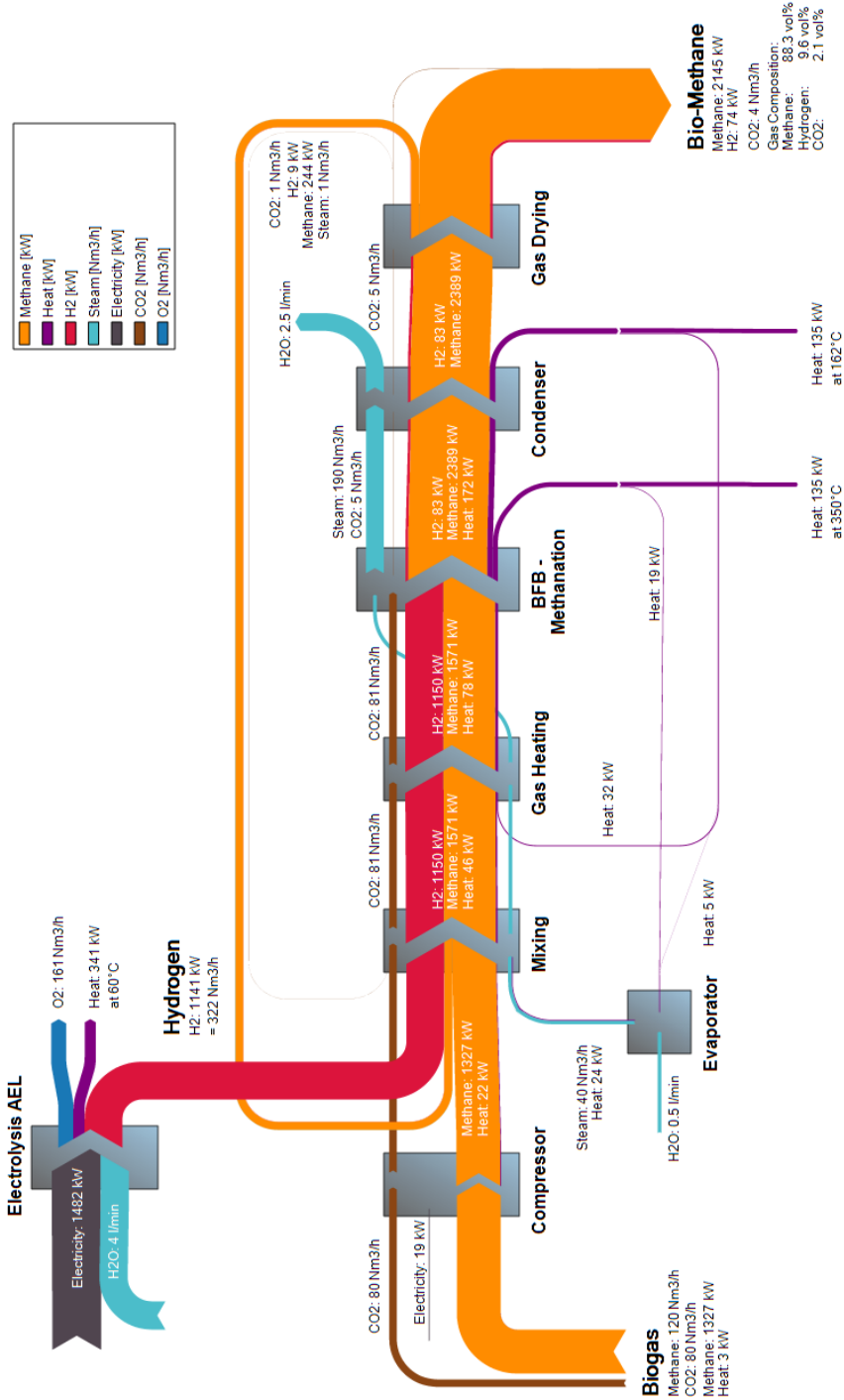
### Two stage methanation



Flow diagram for energy flows and mass flows for process concept II (BFB-FB) with two stage methanation at 7 bara, applying isothermal fluidised bed methanation for the main reactor and cooled fixed bed methanation for the upgrading reactor.



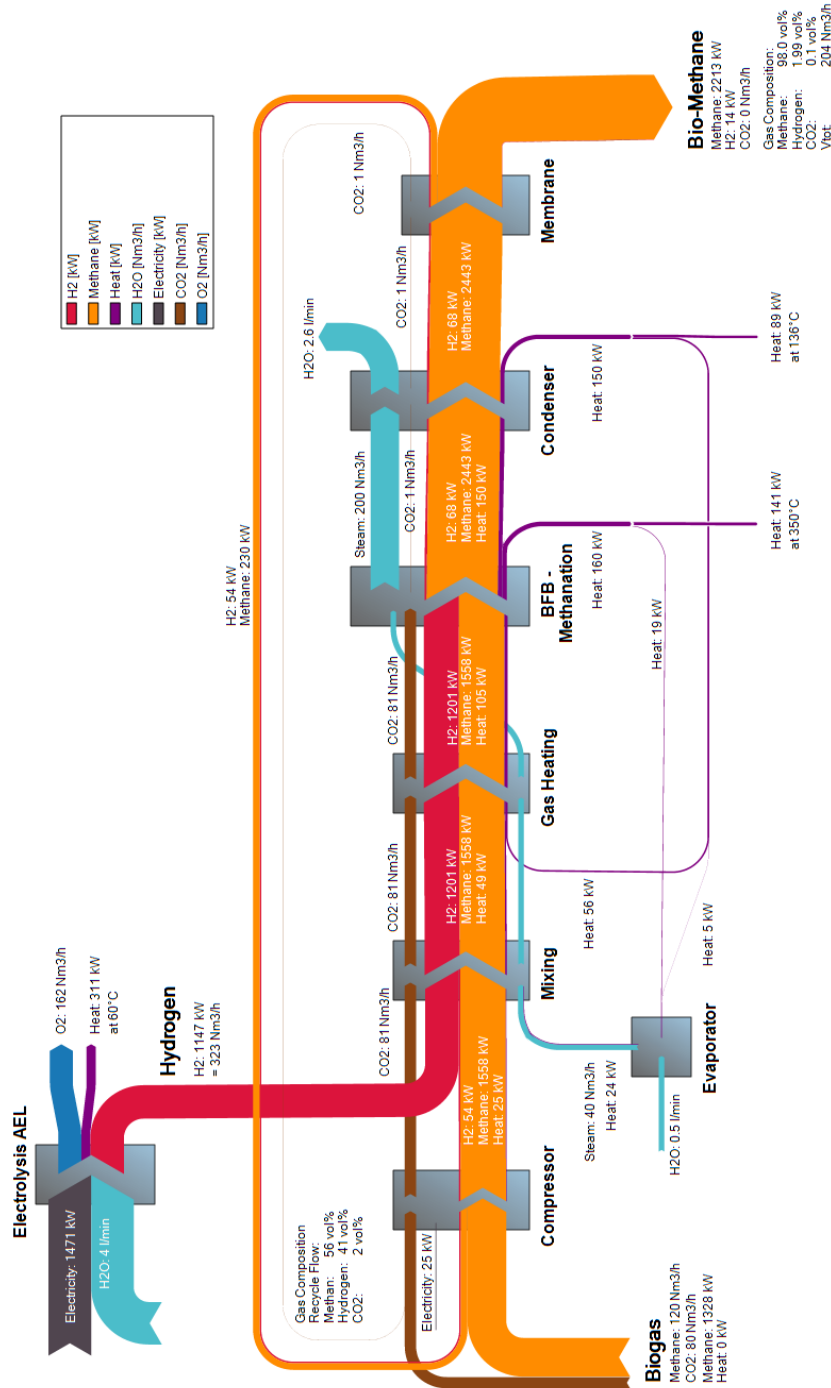
### Single stage methanation



Flow diagram for energy flows and mass flows for single stage methanation at 7 bara (Process concept I, BFB only), applying isothermal fluidised bed methanation and only drying for gas upgrading



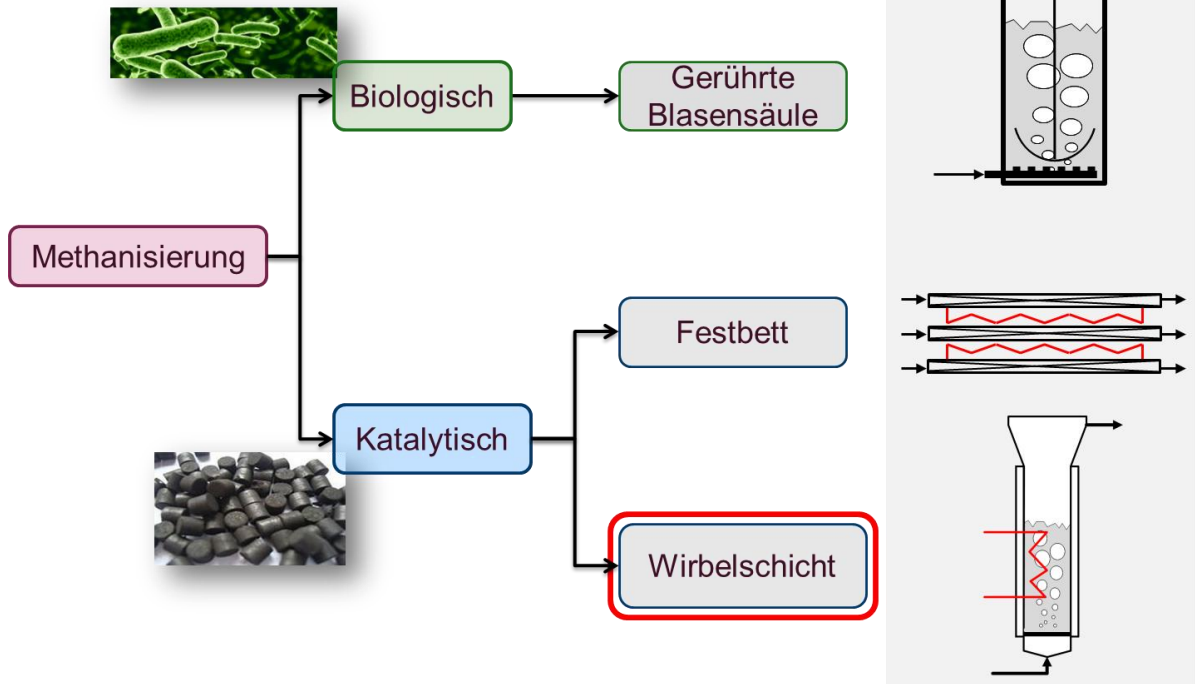
### Single stage methanation and membrane upgrading



Flow diagram for energy flows and estimated mass flows for single stage methanation and membrane upgrading at 7 bara (process concepts III and IV, BFB-Memb and FB-Memb); As both methanation reactors (BFB and FB) are limited by thermodynamics, no significant differences are visible in the energy and mass flow diagram.



Annex: Comparison of methanation technologies





## Vergleich zwischen katalytischer (Wirbelschicht und Festbett) sowie biologischer Methanisierungsverfahren

In der Tabelle ist ein Vergleich der wichtigsten Parameter der katalytische Wirbelschicht- und Festbett-Methanisierungstechnologie sowie dem biologischen Rührkesselverfahren dargestellt. Die Stärken und Schwächen der Wirbelschicht Technologie sind im Vergleich zur biologischen Rührkessel-Methanisierung aufgeführt

	Methanisierungs-Technologie Vergleich			Stärken / Schwächen	
	Katalytisch		Biologisch	Wirbelschicht vs. biologische Verfahren	
Reaktorbauweise	Wirbelschicht	Festbett	Rührkessel	Vorteile der Wirbelschicht	Nachteile der Wirbelschicht
<b>Katalysator</b>	Nickel Katalysator	Nickel Katalysator	Mikroorganismen		
<b>CH<sub>4</sub> Gehalt in Produkt Gas (ohne Postprozessing Unit, nur Trocknung)</b>	90-92%	90-92%	>98%		(>96% nur mit Postprocessing Unit oder zweistufiger Reaktorschaltung möglich)
<b>H<sub>2</sub> Gehalt in Produktgas (ohne Postprozessing Unit, nur Trocknung)</b>	>8%	>8%	<2%		(<2% nur mit Postprocessing Unit oder zweistufiger Reaktorschaltung möglich)
<b>Temperatur</b>	300-400°C	250-650° (je nach Verfahrens-Variante)	35 - 70°C	Abwärme auf hohem Temperaturniveau (Reaktionswärme und Kondensationswärme)	In Standby hohe Betriebstemperatur, die auch benötigt wird um die Reaktion zu starten (Energiebedarf in Standby, um Wärmeverluste auszugleichen)



	Met hanisierungs-Technologie Vergleich			Stärken / Schwächen	
	Katalytisch		Biologisch	Wirbelschicht vs. biologische Verfahren	
Reaktorbauweise	Wirbelschicht	Festbett	Rührkessel	Vorteile der Wirbelschicht	Nachteile der Wirbelschicht
<b>Nutzung der Reaktionswärme</b>	Sehr Gut	Sehr gut	bedingt möglich	Intensiver Wärmeaustausch, dadurch nahezu isothermer Betrieb; Abwärme auf hohem Temperaturniveau	
<b>Druck</b>	> 6 bar	> 10 bar	> 1 bar		
<b>Gas hourly space velocity (GHSV): Reactant Gas Flow Rate / Reactor Vol.)</b>	> 2000	2000 - 5'000	< 100	Reaktorvolumen mindestens 2 mal kleiner als Festbett und mindestens 5 mal kleiner als Biologische Methanisierung	
<b>Limitierung der Reaktionsrate</b>	Gleichgewicht (Kinetik, Thermodynamik)	Gleichgewicht (Kinetik, Thermodynamik)	Stofftransport (Gas-Flüssigkeit)		
<b>Toleranz gegenüber Spurenstoffen wie Schwefelverbindungen</b>	gering	Gering	Hoch (benötigt geringe Mengen S als Spurenelement)	Gasreinigung nach Methanisierung entfällt.	Bei Anwendung mit Rohbiogas genügend effektive Gasreinigung nötig. Katalysator ist anfällig gegen bereits kleine Verunreinigungen des Gases mit Schwefel (ca. 1 ppm).



	Methanisierungs-Technologie Vergleich			Stärken / Schwächen	
	Katalytisch		Biologisch	Wirbelschicht vs. biologische Verfahren	
Reaktorbauweise	Wirbelschicht	Festbett	Rührkessel	Vorteile der Wirbelschicht	Nachteile der Wirbelschicht
<b>Umsetzung von Gasen mit Olefinen und Aromaten (Typisch für Holzvergasung)</b>	Möglich (gezeigt mittels 1000h Experiment und Hochskalierung auf 1 MW)	nein	Nein	Einziges Reaktortyp, der solche Gaskomponenten verarbeiten kann	
<b>Lastwechselverhalten (Turndown ratio)</b>	Flexibel (30%-120% d. Nominalkapazität gezeigt in Güssing)	mässig flexibel	sehr flexibel	Dank Isothermie auch zeitlich dynamisch flexibel	
<b>Anfahrzeit (Einspeisung ab Start aus warmem Stand-by)</b>	15 min	15 min	sehr schnelle Anfahrzeit im Bereich von einigen Minuten		
<b>Strombedarf Methanisierung [kWh/m<sup>3</sup><sub>Biogas</sub>]</b>	0.1–0.2 kWh/m <sup>3</sup> <sub>Biogas</sub> ; Kompressorleistung entspricht < 1.6% der Elektrolyseleistung	Etwas höher als bei Wirbelschicht, da meist bei höherem Druck betrieben und grösserer Druckabfall durch den Reaktor.	Für Microbenergy und Electrochaeta: Der Verbrauch des Rührsystems entspricht etwa 1-2 % der Elektrolyseleistung; der Stromverbrauch für den Kompressor kommt noch dazu.	Tiefer spezifischer Stromverbrauch, da tieferer Druckabfall als bei Festbett und kein Rührwerk nötig. Spezifischer Stromverbrauch ändert sich nicht bei der Hochskalierung (anders als bei Rührwerken).	
<b>Hilfsstoffe und Verbrauchsmaterial</b>	Katalysator	Katalysator	Nährstoffe/ Pufferlösung		Preiswerter Katalysator, der max. einmal pro Jahr ausgetauscht werden muss



	Met hanisierungs-Technologie Vergleich			Stärken / Schwächen	
	Katalytisch		Biologisch	Wirbelschicht vs. biologische Verfahren	
Reaktorbauweise	Wirbelschicht	Festbett	Rührkessel	Vorteile der Wirbelschicht	Nachteile der Wirbelschicht
<b>Komplexität Reaktor (Möglichkeit Hochskalierung)</b>	Vertikale Wärmetauscherrohre strukturieren den Reaktor; Scale-up durch grösseren Reaktordurchmesser und numbering-up der WT-Rohre	Einfacher Scale-up durch numbering-up der Katalysatorgefüllten Rohre	Rührwerk, komplexe 3-Phasenströmung, bei der Stoffübergang limitiert	Keine Rotierenden Teile (Rührwerk); Hochskalierung ab Pilotmassstab (GanyMeth) unproblematisch	
<b>Technologie Reifestufe</b>	5 (Cosyma in Zürich) 7 (PDU Güssing) 8 (Comflux-Anlage)	8-9 (Werlte)	5-7 (Stadtallendorf, Foulum)		
<b>Hersteller am Markt vorhanden</b>	Industriepartner von PSI (ongoing)	HZI	Electrochaea Viessmann		
<b>Demo-/ Kommerzielle Anlagen</b>	PDU Güssing: 1 MW, 2008-2009; Comflux-Anlage: 20 MW, 1980er Jahre	Werlte; 3 MW <sub>SNG</sub> Audi, Deutschland	Bio-Cat; 0.5 MW <sub>SNG</sub> Electrochaea, Dänemark Allendorf: 300kW <sub>el</sub> Viessmann, Deutschland 1-2 MW geplant in Solothurn u. Dietikon		



Quellen:

- Vergleich der Vor- und Nachteile der biologischen und katalytischen Methanisierung; (Graf et al., 2014)
- Methanogenese als mikrobiologische Alternative zur Katalytischen Methanisierung; (Krautwald et al. 2016 Aqua&Gas N°7/8,
- PSI-Betrachtung/ Berechnung
- Angaben von Vertretern Micobenergy und electrochaea bei den REGATEC-Konferenzen 2016 und 2017